University of Nottingham
UK | CHINA | MALAYSIA

Mathematical Modelling of Antimicrobial and Heavy Metal Resistance in Bacterial Populations Within the Flow of Agricultural Slurry in a UK Dairy Farm

Henry Todman

School of Biosciences

University of Nottingham

Supervisors: Dov Stekel, Theo Kypraios & Michelle Baker

Contents

Declaration

I have read and understood the School and University guidelines on plagiarism. I confirm that the work presented herein is the result of my own research completed during the period of study, with the exception of the acknowledged references. Any experimental work not completed by myself has been acknowledged and appropriately referenced.

Acknowledgements

The course of my studies has been an incredibly difficult and mentally strenuous process, and I owe a significant amount of gratitude to numerous individuals for helping me get to this stage.

Thank you to my supervisors Professor Dov Stekel, Professor Theo Kypraios and Dr Michelle Baker for their input, guidance and support throughout the course of my studies. In particular, a significant thanks to Dov for his enormous degrees of support and patience during my ongoing mental health troubles during my period of study

Thank you to the University of Nottingham, the School of Biosciences and the School of Mathematics for funding my research.

Thank you to the other members of our research group: Sankalp Arya, Hokin Chio, Anastasia Kadochnikova and Jennifer Brazier, for your help and support over the course of my research.

I would also like to thank all the many members of the EVAL-FARMS research project (funded by NERC) with whom I collaborated, learnt so much from and provided me with the experimental data necessary to conduct my studies: Richard Helliwell, Jon Hobman, Elizabeth King, Tom Dodsworth, Charlotte Gray-Hammerton, Alex Williams, Steve Hooton, Christine Dodds, Jan-Ulrich Kreft, Sujatha Raman, Carol Morris, Helen West, Rosa Baena-Nogueras, Mike Jones, Chris Hudson, Steve Ramsden, and Rachel Gomes.

Thank you also to the Medical Research Foundation for including me as part of their National PhD Training Programme in Antimicrobial Resistance Research, allowing me to attend annual conferences and residential training camps to learn about the wide array of interdisciplinary research being conducted in the field of AMR.

I would also like to issue my enormous gratitude to my partner, Emily, who has been forever supportive of me and helped me through of all of my struggles during the course of my studies. I would also like to thank my parents and sister - Kevin, Sandra and Amy - for similarly showing me such support - especially my father who is always eager to read through any draft that I may have written.

Finally, thank you to my friends for keeping me sane and distracting me - particularly my old friends from the Warwick University Climbing Club who provided me with much needed trips away to help with my mental state.

Thesis Abstract

Antimicrobial resistance (AMR) is a one of the most important global public health problems facing the modern era. Dairy cattle represents one of the largest agricultural industries, with approximately 265 million dairy cows across the globe. These are estimated to produce 3 billion tonnes of manure each year. Dairy slurry represents a major source for environmental contaminations of antimicrobial resistance genes (ARG). The management and storage systems of dairy slurry provide a setting in which bacteria, antibiotic residues, metals and chemicals to mix and may be a locus for selection of AMR. Mathematical modelling offers a powerful tool to explore the impact that changes to farm management practices may have on AMR dynamics, where it would be impossible to empirically explore such changes on a working farm.

We present a mathematical model describing the dynamics of AMR and waste within the slurry management system of a UK dairy farm, and explore the impact that different farm policies have on the selection of AMR within this system. This model is built on a volumetric flow model for the farm based on ethnographic observations of the farm and has been calibrated against metal concentrations in the slurry tank from a longitudinal study of the farm using Bayesian inference methods. We then coupled this model with a bacterial growth and gene transfer model to develop a multiscale, discrete-continuous, compartmental ODE model for the flow of slurry, bacteria, antibiotic residues and metals around the farm. The model found that footbath emptying practices lead to a significant bacteriocidal input in the slurry flow leading to large fluctuations in resistance levels on the farm. Furthermore, adjusting the model suggested that cephalosporin resistance is more observable when cephalosporin resistance is chromosomally-encoded (rather than on plasmids) - this observation is consistent with studies of a chromosomally encoded ISEcp1 element found on the farm. This work concludes that farm management practices can have a material impact on AMR in dairy slurry, and offers opportunities for farm-specific policies to mitigate the drive and spread of AMR, beyond reduction in antibiotic (Ab) usage.

The farm flow model details the beginnings of a possible pathway for environmental AMR contamination which may affect food crops - It is also important to consider the risk of dietary exposure to ARG/ARBs. The lifelong acquisition (through ARGs in food intake) and persistence of resistance genes in the gut resistome may lead to resistance in endogenous infections (e.g. urinary tract infections), particularly in individuals of older-age. Chapter 4 of this work presents a probabilistic model for the acquisition and persistence of ARGs over an individual's lifespan. We consider potential strategies to reduce the overall resistance load in the microbiome, and the effectiveness of these strategies in countries of different Ab usage. This work surmises that policies considering the ARGs in food intake would be more effective in reducing ARG accumulation than polices that solely consider reducing Ab usage.

Chapter 1

Introduction - A background to antimicrobial resistance and the use of mathematical modelling to study AMR

1.1 Introduction

Antimicrobial resistance (AMR) is an enormous global health concern and an area of extreme interest in research. In this chapter, we will provide a brief overview of the history of and research into AMR, as well as discuss the role that mathematical modelling has previously played in this field, We shall also discuss existing research gaps in the area and provide a summary of the work presented in later chapters and discuss how it seeks to fill some of the research gaps.

1.2 Antimicrobial Resistance

The problem of antimicrobial resistance is widely acknowledged as one of the most pressing global health concerns facing us in the modern era. Currently there are over 700,000 deaths associated with AMR each year. The problem of AMR carries not only a great cost in human life but also exerts a significant economic burden as well, costing over $50 billion a year in the USA alone. [24, 30]. It is estimated that there will be up to 10 million deaths each year due to AMR by 2050 if action is not taken to face this issue [24].

The discovery and development of antibiotics, following Alexander Fleming's discovery of Penicillin in 1928 alongside the clinical availability of sulphonamides in the 1930s, has often been hailed as one of the scientific triumphs of the 20th century. Throughout the 1950s and 1960s, the world saw a golden age of antibiotics drug development which has formed the basis of modern healthcare around the world: aminoglycoside, chloramphenicol, tetracycline, macrolides, vancomycin, and quinolones were among just a few of the new antimicrobials developed during this period [9, 10, 28]. This is perhaps epitomised by the famous statement of the US Surgeon General, William Stewart in 1969: "the war against diseases has been won" [30]. However, despite the assertions of Stewart, infectious diseases continue to attack humans and the past 20-30 years have seen a great slow down in the development of new antimicrobials. Since the 1990s, only four new classes of antimicrobials have been developed and released for clinical use: oxazolidinones in 2000, lipopeptides in 2003, pleuromutilins in 2007 and macrolactones in 2011 [18]. However, these newly developed classes do not in fact truly present any novel discoveries as they are largely based on previous developments in the 1970s and 1980s. Furthermore pharmaceutical companies have largely divested from research and development into new antimicrobials, often in favour of research into non-communicable diseases: a study in 2013 found only 4 large multinational pharmaceutical companies currently engaged in research and development of new antimicrobials [13, 18].

Resistance can be transmitted through bacterial populations by either vertical or horizontal transfer. Vertical transfer is where bacteria develop resistance through spontaneous chromosomal mutation, which may then passed onto daughter cells as the bacteria divides via binary fission. Horizontal evolution is

where bacteria acquire genetic material from other resistant organisms; this can occur by conjugation, transformation or transduction [1, 20].

Conjugation is where AMR is spread by the transfer of a plasmid - a circular segment of genetic material that can replicate independently of the chromosome. The plasmid can be passed to other bacterial cells when a pilus forms between neighbouring cells. Conjugation is the most commonly observed method of horizontal transfer of resistance.

Resistance can also be spread by transformation, where free genetic material of a cell that has been broken down, becomes integrated into the chromosome of a nearby bacterial cell.

The final method of horizontal transfer is by transduction where resistance transfer between bacterium is mediated by viruses called bacteriophage. Gene segments encoding resistance may be picked up by the phage as it infects resistant bacterium, and this genetic material can then be disseminated through a bacterial community as the phage infect new cells.

While much research into AMR has been focussed on human health, resistance in agriculture and the environment also poses a great concern [15, 19, 21, 32]. It is widely acknowledged among the scientific community that a One-Health approach is required to tackle the crisis of antimicrobial resistance. Figure 1.1 shows a simplified diagram showing possible ways in which AMR can be transmitted between humans, animals and the environment, highlighting the need for a One Health view of the AMR problem.

Antimicrobial Resistance in Agriculture

Agriculture accounted for 33% of total UK antibiotic sales in 2016 [7] and over 70% of overall antibiotic use in the USA [23]. Sustained, low dose uses of antimicrobials such as those we observe in most farms around the world provide an ideal selection environment for the propagation of resistance among bacterial populations: indeed we have observed increased levels of resistance found in farm animals, manures, slurries and soil.

The emergence and selection of AMR on farms then presents numerous potential risks for transfer to humans and animals by commensal or pathogenic bacteria either through directly on the farm, or indirectly through the food chain or spreading of manure and slurries on fields.

In 1998 in Nebraska, USA, a child contracted a salmonella infection resistant to ceftriaxone (a first generation cephalosporin). The resistant isolates were found to be the same strain as samples taken from faecal matter cattle on the child's family ranch following an outbreak of salmonellosis [2].

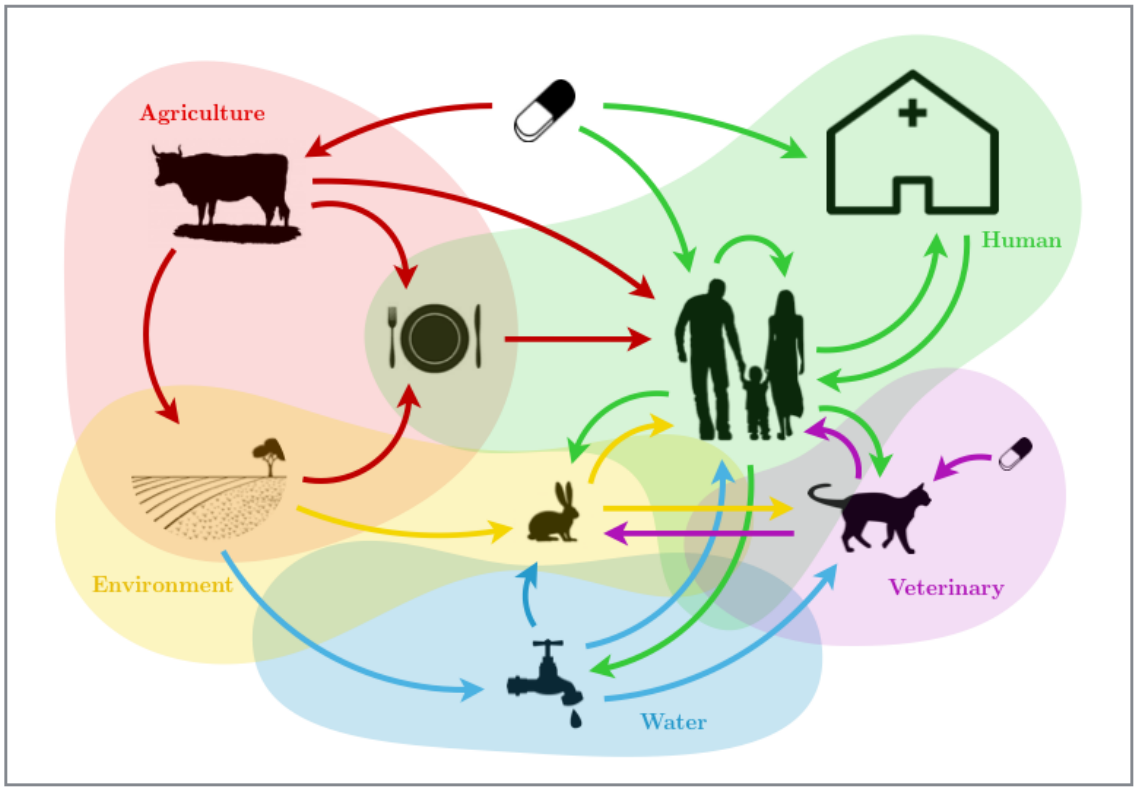

Figure 1.1: This diagram gives a simplified view of the One Health perspective of AMR and illustrates some of the possible methods that AMR can be transmitted across the human, agricultural, environmental, veterinary and water sectors. (1) Resistance can be acquired and selected for within hospitals putting humans at risk of nosocomial infections. (2) Humans may be prescribed antibiotics by a GP which can allow for the selection of resistant bacteria within the community. (3) Veterinarians may prescribe antimicrobials for pets. This allows for direct transmission of resistance through direct contact between pets and their owners. (4) Antibiotics are used on farms for therapeutic use and, in some countries, for nontherapeutic such as for growth promotion. AMR can then be transmitted either directly to farmers or indirectly through the food chain. (5) Resistance can also be spread into the environment from farms as manure and slurry from food producing animals is often spread on fields to help grow crops. These crops may then transmit resistance through the food chain. (6) Resistant bacteria in the environment can be carried by wild animals or insects, who may then spread AMR through interaction with humans or pets. (7) Waste water treatment plants do not fully eliminate resistant bacteria before releasing water back into the environment. Water run-off from fields can carry resistance to large sources of water such as the sea. Once resistance emerges in water reserves it can be easily distributed as humans and animals use water for drinking or washing.

The 1986 study of Hummel et al [17] following the spread of nourseothricin resistance is a clear

example of how resistance can spread from the use of antimicrobials in agriculture. Nourseothricin is a streptothricin antibiotic that was exclusively used as a growth promoter for pigs in East Germany between 1980 and 1990, and had no other applications to humans or animals. Prior to use in animal husbandry, resistance to nourseothricin was rarely observed and was never mediated by plasmids. Within two years of use as a growth promoter, resistance plasmids encoding streptothricin resistance in E.coli were found in 33% of strains from pigs fed nourseothricin as a growth promoter and also in manure and local rivers. Furthermore resistance was found in the local environment (on fields spread with swine manure and in the local rivers) and in the faecal matter of humans: both those having direct contact with the pigs (i.e. farmers working on the farm), and those who have obtained resistant strains indirectly: family of the farmers, and outpatients in nearby towns (including those with urinary tract infections) [17]. The plasmids encoding resistance to streptothricins were later found in pathogenic strains of salmonella and shigella of human diarrhea between 1987 and 1989 [33]. While nourseothricin had no human applications, this case illustrates how the use of antimicrobials in agriculture can quickly spread resistance across to humans. The use of antibiotics for non-therapeutic use (e.g. for use as a growth promoter) has since been forbidden in the Europe Union, however, this practice still remains in many countries, especially in the developing world where regulation of antibiotic use in agriculture is nearly non-existent.

In 1969, the Swann Report concluded antimicrobials used as growth promoters contributed to the rise of MDR resistant infections - recommended growth promoters using antimicrobials used in human therapy should be banned [31]. Initially the UK (and other countries in Europe) banned growth promotion with antimicrobials used in human therapy. However, antimicrobials not used in human therapy were still used and similarities existed in the structure between some of the non-therapeutic agricultural antimicrobials and antibiotics used in human medicine. This means that there are still transmission pathways for bacterial strains to obtain resistance to human antibiotics.

By 2006, the European Union and several other countries (such as Canada and Scandinavia) had banned the use of antimicrobials for non-therapeutic use in agriculture. However, the practice of non-therapeutic antimicrobial use continues in many countries around the world especially in developing nations. Although more and more countries are beginning to recognise the need to address this issue: in 2017 the USA banned non-therapeutic use of antimicrobials in agriculture [11], and China implemented a ban on the use of colistin as a feed additive in animal husbandry in response to the discovery of the MCR-1 mobile genes encoding colistin resistance on plasmids in *E. coli* on a pig farm [38].

The World Health Organisation completed a global surveillance of antimicrobial resistance in 2014 which highlighted significant knowledge gaps on the impact of AMR in foodborne bacteria and the significance this could have on animal and human health [39].

Metal Resistance and Co-Selection of Antimicrobial Resistance

A potentially significant concern in the study of antimicrobial resistance is observed cases of co-resistance and co-selection of AMR [25].

While bacteria require metals (such as cadmium, copper, silver and zinc) as essential nutrients for growth, in high enough concentrations heavy metals can have toxic effects on bacteria, and these have historically been used as antimicrobials. However, in a similar way to antibiotic resistance, bacteria can develop tolerances to the antimicrobial effects of heavy metals [16,29]. A strong link has been established between resistances to metals and antibiotics. Co-resistance between metal and antibiotic resistance was first observed when mercury and penicillin resistances were found on plasmids in *Staphylococcus aureus* in the 1960s [27]. Since then, resistances to multiple drugs and heavy metals have been observed to co-occur on the same mobile genetic elements (MGEs). Co-resistance between metal and antibiotic resistances raises the significant issue of co-selection where we see resistant bacterial populations persist and selected for in the absence of antibiotics. [5,6,16,25,26,40]

Heavy metal use is also prevalent on farms as large amounts of elements such as copper and zinc are used in feed as growth promoters, and the majority of these metals are not absorbed within the animal and are passed through in the animal faeces, entering the farm slurry system. In addition to metals used in feed, heavy metal footbaths are often used to prevent hoof infections on dairy and swine farms. The heavy use of metals can lead to selection of MRGs and also brings the increased risk of co-selection of antimicrobial resistance. Faecal bacteria in swine slurry was found to be significantly more likely to carry genes for Cu^{2+}-resistance compared to bacteria found in the swine feed, along with a "strong association between heavy metal tolerance and antimicrobial resistance" between bacteria in swine slurry [22].

1.3 Mathematical Modelling in AMR

Mathematical modelling is a powerful tool in the study of AMR in the environment and agriculture and provides a valuable approach to answering questions for given a hypothetical parameter set, that cannot be predicted by experiments or observed. For example we can use mathematical models to estimate the effect of antimicrobials in an environment have on a bacterial population and predict the impact it may or may not have on the emergence of AMR in the population [3,36], or we can model the effects of potential control strategies for AMR within the environment, such as reducing the use of antimicrobials [34], or increasing withdrawal periods of animals subjected to antibiotic treatment [8].

Different methods of mathematical modelling have been used to model the spread of AMR in the environment. Most studies of antibiotic resistance evolution assume that it happens in a well-mixed, spatially homogeneous environment and use (relatively) simple deterministic ODE models to represent

the bacterial population dynamics and antibiotic concentrations [3, 4, 8, 35–37].

Some studies have also developed simple spatial mathematical models to model the spread of AMR within bacterial populations: Zhang et al developed a simple spatial model for the competition of antibiotic-susceptible and antibiotic-resistant bacterial populations in a heterogeneous environment made up of microhabitats [41]. This model uses a system of coupled equations on a 2D lattice to model the heterogeneity of a larger environment consisting of different smaller homogeneous microhabitats, and has been used as the basis to apply an antibiotic concentration gradient across an environment in other models for the spread of AMR [12, 14].

Two mathematical models of particular interest to the research presented herein would be Baker et al's ODE models of a dairy slurry tank [3, 4]. An initial model is presented of the slurry tank modelling the spread of AMR in bacteria within the slurry flow [3] and highlights the importance of the rate of gene transfer to the prevalence of resistant bacteria. However, this model did not consider natural bacterial death or the effects of metal co-selection. This model was extended in later work to consider a wider number of antimicrobials including metals (and their potentially co-selective effects) [4]. This model formed part of a large interdisciplinary study which I had the opportunity to assist on by providing estimations of the antibiotic and metal concentrations within the slurry (based upon calculations done in the parametrisation of my farm flow model), and these were used to inform mini-tank experiments to provide microbiological data used in the MCMC parameter estimation for the Baker et al model. The model presented in Baker et al [4] helped form the basis for the bacterial growth and horizontal gene transfer dynamics in the farm flow model we have developed here.

1.4 Summary

In our search of the existing literature surrounding mathematical modelling of AMR in the environment we have been unable to find any examples of multiscale mathematical models that model the spread of resistance across bacterial populations flowing between different compartments in space where certain characteristics of each compartment are allowed to be variable: for example modelling bacterial populations in the flow of dairy slurry across different areas of a farm. Furthermore we have been unable to find any research in the existing literature into developing mathematical models of the co-selection of heavy metal and antimicrobial resistance. We propose to develop a multiscale mathematical model for the spread of AMR among bacterial populations within the flow of dairy slurry across different spatially segregated areas of a UK dairy farm which includes co-selection of antibiotic and heavy metal resistances and using this model we shall evaluate whether any factors on the farm could drive or reduce the spread of AMR.

Bibliography

[1] S. Arya, H. Todman, M. Baker, S. Hooton, A. Millard, J. Kreft, J.L. Hobman, and D.J. Stekel. A generalised model for generalised transduction: the importance of co-evolution and stochasticity in phage mediated antimicrobial resistance transfer. *FEMS Microbiology Ecology*, 96(7), 2020.

[2] P Aul, D F Ey, Homas J S Afranek, Ark E R Upp, Ileen F D Unne, Eter C I Wen, Atricia A B Radford, F Rederick, and J A Ngulo. Ceftriaxone-resistant salmonella infection acquired by a child from cattle. *New England Journal of Medicine*, 342(17):1242–1249, 2000.

[3] Michelle Baker, Jon L. Hobman, Christine E. R. Dodd, Stephen J. Ramsden, and Dov J. Stekel. Mathematical modelling of antimicrobial resistance in agricultural waste highlights importance of gene transfer rate. *FEMS Microbiology Ecology*, 92(4), 2016.

[4] Michelle Baker, Alexander D. Williams, Steven P.T. Hooton, Richard Helliwell, Elizabeth King, Thomas Dodsworth, Rosa María Baena-Nogueras, Andrew Warry, Catherine A. Ortori, Henry Todman, Charlotte J. Gray-Hammerton, Alexander C.W. Pritchard, Ethan Iles, Ryan Cook, Richard D. Emes, Michael A. Jones, Theodore Kypraios, Helen West, David A. Barrett, Stephen J. Ramsden, Rachel L. Gomes, Chris Hudson, Andrew D. Millard, Sujatha Raman, Carol Morris, Christine E.R. Dodd, Jan-Ulrich Kreft, Jon L. Hobman, and Dov J. Stekel. Antimicrobial resistance in dairy slurry tanks: A critical point for measurement and control. *Environment International*, 169:107516, 2022.

[5] Craig Baker-Austin, Meredith S. Wright, Ramunas Stepanauskas, and J.V. McArthur. Co-selection of antibiotic and metal resistance. *Trends in Microbiology*, 14(4):176–182, 2006.

[6] Carmen Bednorz, Kathrin Oelgeschläger, Bianca Kinnemann, Susanne Hartmann, Konrad Neumann, Robert Pieper, Astrid Bethe, Torsten Semmler, Karsten Tedin, Peter Schierack, Lothar H. Wieler, and Sebastian Guenther. The broader context of antibiotic resistance: Zinc feed supplementation of piglets increases the proportion of multi-resistant Escherichia coli in vivo. *International Journal of Medical Microbiology*, 303(6-7):396–403, 2013.

[7] Peter Borriello, Fraser Broadfoot, Kitty Healey, Stacey Brown, and Ana Vidal. UK veterinary antibiotic resistance & sales surveillance report. Technical report, Veterinary Medicines Directorate, Department for Environment, Farming and Rural Affairs, 2017.

[8] CL. Cazer, L. Ducrot, VV. Volkova, and YT Gröhn. Monte Carlo simulations suggest current chlorotetracycline drug-residue based withdrawal periods would not control antimicrobial resistance dissemination from feedlot to slaughterhouse. *Frontiers in Microbiology*, 8(1753), 2017.

[9] J.M. Conly and B.L. Johnston. Where are all the new antibiotics? The new antibiotic paradox. *Canadian Journal of Infectious Diseases and Medical Microbiology*, 16(3):159–160, 2005.

[10] Julian Davies and Dorothy Davies. Origins and evolution of antibiotic resistance. *Microbiology and Molecular Biology Reviews*, 74(3):417–33, 2010.

[11] Food, U.S. Department of Health Drug Administration, and Human Services. Guidance for industry veterinary feed directive regulation questions and answers. Technical report, Center for Veterinary Medicine, 2015.

[12] P. Greulich, B. Waclaw, and Allen RJ. Mutational pathway determines whether drug gradients accelerate evolution of drug-resistant cells. *Physics Review Letters*, 109(8), 2012.

[13] Boucher H., Talbot G., Benjamin D., Bradley J., and Guidos R. et. al. 10 x '20 Progress–development of new drugs active against gram-negative bacilli: an update from the Infectious Diseases Society of America. *Clinical Infectious Diseases*, 56(12):1685–1694, 2013.

[14] R. Hermsen, JB. Deris, and Hwa T. On the rapidity of antibiotic resistance evolution facilitated by a concentration gradient. *Proceedings of the National Academy of Sciences*, 109(27), 2012.

[15] Holger Heuer, Heike Schmitt, and Kornelia Smalla. Antibiotic resistance gene spread due to manure application on agricultural fields. *Current Opinion In Microbiology*, 14:236–243, 2011.

[16] Jon L. Hobman and Lisa C. Crossman. Bacterial antimicrobial metal ion resistance. *Journal of Medical Microbiology*, 64(5):471–497, 2015.

[17] R. Hummel, H. Tschape, and M. Witte. Spread of plasmid-mediated nourseothricin resistance due to antibiotic use in animal husbandry. *Journal of Basic Microbiology*, 26(8):461–466, 1986.

[18] Daniela Jabes. The antibiotic R&D pipeline: an update. *Current Opinions in Microbiology*, 14(5):564–569, 2011.

[19] G.G. Khachatourians1998. Agricultural use of antibiotics and the evolution and transfer of antibiotic-resistant bacteria. *Canadian Medical Association Journal*, 159(3):1129–1136, 1998.

[20] Q. Leclerc, J. Lindsay, and G. Knight. Mathematical modelling to study the horizontal transfer of antimicrobial resistance genes in bacteria: current state of the field and recommendations. *J. R. Soc. Interface*, 16, 2019.

[21] Bonnie M Marshall and Stuart B Levy. Food animals and antimicrobials: impacts on human health. *Clinical Microbiology Reviews*, 24(4):718–733, 2011.

[22] J. Medardus, B. Molla, M. Nicol, W. Morrow, P. Rajala-Schultz, R. Kazwala, and W. Gebreyes. In-feed use of heavy metal micronutrients in U.S. swine production systems and its role in persistence of multidrug-resistant salmonellae. *Appl Environ Microbiol.*, 80(7), 2014.

[23] Center For Veterinary Medicine. Summary Report On Antimicrobials Sold or Distributed for Use in Food-Producing Animals. Technical report, U.S. Food And Drug Administration, 2016.

[24] Jim O'Neill. Tackling drug resistant infections globally: final report and recommendations. Technical report, The Review on Antimicrobial Resistance, 2016.

[25] Chandan Pal, Karishma Asiani, Sankalp Arya, Christopher Rensing, Dov J. Stekel, D.G. Joakim Larsson, and Jon L. Hobman. Metal resistance and Its association with antibiotic resistance. *Advances in microbial physiology*, 70:261–313, 2017.

[26] Keith Poole. At the Nexus of Antibiotics and Metals: The Impact of Cu and Zn on Antibiotic Activity and Resistance. *Trends in Microbiology*, 25(10):820–832, 2017.

[27] M.H. Richmond, M.T. Parker, M. Patricia Jevons, and Madeleine John. High Penicillinase Production Correlated With Multiple Antibiotic Resistance in Staphylococcus Aureus. *The Lancet*, 283(7328):293 – 296, 1964.

[28] Tomoo Saga and Keizo Yamaguchi. History of Antimicrobial Agents and Resistant Bacteria. *Japan Medical Association Journal*, 52(2):103–108, 2009.

[29] Simon Silver and Le T Phung. Bacterial Heavy Metal Resistance: New Surprises. *Annu. Rev. Microbiol*, 50:753–789, 1996.

[30] Richard Smith and Joanna Coast. The true cost of antimicrobial resistance. *British Medical Journal*, 346, 2013.

[31] M Swann. Report of the Joint Committee on the Use of Antibiotics in Animal Husbandry and Veterinary Medicine. Technical report, The Joint Committee on the use of Antibiotics in Animal Husbandry and Veterinary Medicine, 1969.

[32] Sophie Thanner, David Drissner, and Fiona Walsh. Antimicrobial resistance in agriculture. *mBio*, 7(4), 2016.

[33] H. Tschape. The spread of plasmids as a function of bacterial adaptability. *FEMS Microbiology Ecology*, 15:23–31, 1994.

[34] B. A. D. van Bunnik and M. E. J. Woolhouse. Modelling the impact of curtailing antibiotic usage in food animals on antibiotic resistance in humans. *Royal Society Open Science*, 4(4):161067, 2017.

[35] V. V. Volkova, C. L. Cazer, and Y. T. Gröhn. Models of antimicrobial pressure on intestinal bacteria of the treated host populations. *Epidemiology and Infection*, 145(10):2081–2094, 2017.

[36] VV. Volkova, C. Lanzas, Z. Lu, and Gröhn YT. Mathematical model of plasmid-mediated resistance to ceftiofur in commensal enteric escherichia coli of cattle. *PLoS ONE*, 7(5), 2012.

[37] VV. Volkova, Z. Lu, T. Besser, and Gröhn YT. Modeling the infection dynamics of bacteriophages in enteric escherichia coli: estimating the contribution of transduction to antimicrobial gene spread. *Applied and Environmental Microbiology*, 80(14), 2014.

[38] R Wang, L van Dorp, LP Shaw, et al. The global distribution and spread of the mobilized colistin resistance gene mcr-1. *Nature Communications*, 9(1179), 2018.

[39] World Health Organisation. Antimicrobial resistance: global report on surveillance. Technical report, World Health Organisation, 2014.

[40] Zhongyi Yu, Lynda Gunn, Patrick Wall, and Fanning Séamus. Antimicrobial resistance and its association with tolerance to heavy metals in agriculture production. *Food Microbiology*, 370, 2017.

[41] Q. Zhang, G. Lambert, D. Liao, H. Kim, K. Robin, C-K. Tung, N. Pourmand, and Austin RH. Acceleration of emergence of bacterial antibiotic resistance in connected microenvironments. *Science*, 333(6050), 2011.

Chapter 2

The development and calibration of a multiscale hybrid discrete-continuous model for the flow of waste and antimicrobial resistance on a dairy farm

Abstract

Antimicrobial resistance (AMR) presents a significant global health threat and requires a One Health approach to remediate the risk of this threat. The UK dairy farm industry produces approximately 28 million tonnes of manure each year, a significant proportion of which is liquid slurry. This represents a potential locus for the emergence of antimicrobially resistant bacterial populations, as slurry is mixed with other waste products (e.g. waste milk, formalin and heavy metal footbaths, and antimicrobials) providing an ideal co-selective environment for antibiotic resistance genes (ARGs). This presents a significant risk as a transmission path to humans when slurry is spread onto fields as fertiliser and so we should consider potential mitigating action. Previous studies have shown that reducing antibiotic usage in livestock does not significantly affect the spread of AMR from livestock to humans, and it would be difficult to further reduce antimicrobial usage without affecting the health and welfare of the animals, so it may be more productive to consider the effects of changes to farming infrastructure and management practices. We have developed a multiscale hybrid discrete-continuous ODE mathematical model of a typical high-performance dairy farm in the UK to model the flow of slurry, bacteria, metals and antibiotics across the different areas of the farm, incorporating discrete events to model different farming practices. This model is calibrated using metal concentration data collected from the slurry tank at 27 time points over a six month period. In the next chapter, we shall use this model to evaluate the impact of different farm layout scenarios on the dynamics and prevalence of antimicrobially resistant bacteria across the farm.

2.1 Introduction

The use of antibiotics (Ab) in agriculture can result in drug-resistant strains of pathogens infecting human populations through the food chain [1, 2], or may lead to the transfer of novel antibiotic resistance genes (ARGs) from livestock-associated bacteria to human-acquired infections [3, 4, 5]. The importance of mitigating the risks of AMR in the agricultural sector has been recognised by many countries, including the UK and European Union[6, 7], with reductions and restrictions being imposed on Ab usage in agriculture (particularly on "critically important" Ab). However, despite a 50% reduction in Ab usage in the UK agriculture sector since 2014 [8], usage still remains high representing 36% of the total UK Ab use [9] and represents a risk of spread of ARGs and AMR. Further reduction in usage of Ab will be extremely challenging for countries that have already made major reductions due to the need for antibiotics in the care and welfare of diseased animals. Therefore it may be appropriate to consider whether changes in farm management and infrastructure can reduce selection for resistance.

In addition to antibiotics, other antimicrobials such as metals (e.g. copper and zinc) and other chemicals (e.g. formalin) are widely used across farms globally, particularly in footbaths to prevent lameness in livestock - a prevalent concern in dairy and sheep farming [10]. Metals and other antimicrobial agents (such as formalin and glutaraldehyde) are known to have a co-selective effect on antibiotic resistance, allowing for the persistence of ARBs in the absence of antibiotic selective pressures [11, 12, 13, 14, 15, 16].

Farm waste management is of particular interest as large volumes of manure and slurry present a system in which faecal bacteria and antibiotics mix, alongside other co-selective antimicrobial agents such as metals and formalin and presenting a possible locus for the selection and co-selection of resistance [17]. The UK dairy farm industry produces on average 2.8 $\times 10^{10}$ kg of manure each year (approximately 1.8 $\times 10^{10}$ kg of which is undiluted dairy slurry) [18]. Dairy slurry is often stored in slurry tanks or lagoons for long periods of time, and such accumulated storage of agricultural waste may act as a hotspot for the spread of ARGs and AMR, potentially giving rise to multi-drug resistance (MDR) - microbiological studies on a dairy farm at the University of Nottingham found resistances to multiple antibiotics in over two thirds of *Escherichia coli* strains that were cultured [19, 17].

The spreading of slurry/manure onto field soil as fertiliser may then release ARGs and ARBs into the surrounding environment. Studies of fields that have been spread with dairy slurry have observed a higher proportion of ARGs [20, 21, 22], while studies of crops fertilised with dairy slurry have been shown to accumulate ARGs associated with the slurry [20, 23, 24, 25]. This is of particular concern as this opens potential transmission pathways for these ARGs to transfer to human pathogens [26] and as well as the risk for the more widespread dissemination of such ARGs in the environment through waterways and the food chain.

Hence there is a clear and potentially significant risk of AMR spread from agricultural waste, and efforts should be made to reduce this contamination risk. However, many developed countries have already made major reductions in the usage of antibiotics in livestock and further reduction will be extremely difficult without potentially compromising the care and welfare of diseased animals. Indeed modelling studies have shown that further reduction in antibiotic usage in livestock has little impact in reducing the levels of AMR in human populations [27].

Therefore it is important to consider other ways that we can effectively mediate the risks of AMR spread from manure, such as through changes in infrastructure or farm management practices [17]. However, it is often impractical to effectively study such structural changes since they would require potentially expensive changes to infrastructure or management practice, with numerous unknown welfare and business risks. In this regard mathematical modelling is a powerful tool as it allows us to model alternative scenarios through changes in simulations' parameters or processes to which adverse outcomes (i.e. proliferation of ARBs) are especially sensitive can be identified, which serve as potential points of control [17].

Most mathematical models studying the impact of AMR in dairy farms (or other livestock farm environments) consider a single area of a farm [28, 29, 30, 31, 17], treat the entire farm as a single compartment [27], or are interested in within-host dynamics of the livestock [32]. While such approaches are undoubtedly useful, to our knowledge, there are no modelling studies that investigate the effects of farm layout, the farm practices associated across different areas of the farm, and the impact these may have upon the emergence and/or spread of AMR across the farm.

We have developed and evaluated a mathematical model of a typical UK dairy farm that considers the entire flow of dairy waste from its source in the cattle sheds to the slurry tank where waste is stored until it is needed for spreading on fields. Informed by ethnographic observations of the dairy farm (performed by Richard Helliwell, University of Nottingham), this model considers many sources of waste input across the farm, as well as contaminants such as antibiotics and metals. This model is then calibrated against data of observed metal concentrations in the slurry tank [17] using a Bayesian estimation approach. This flow model is then coupled with a traditional horizontal gene transfer model to provide a multiscale hybrid discrete-continuous ODE model that models the dynamics of antimicrobially-resistant bacteria across the different areas of the farm.

2.2 Materials & Methods

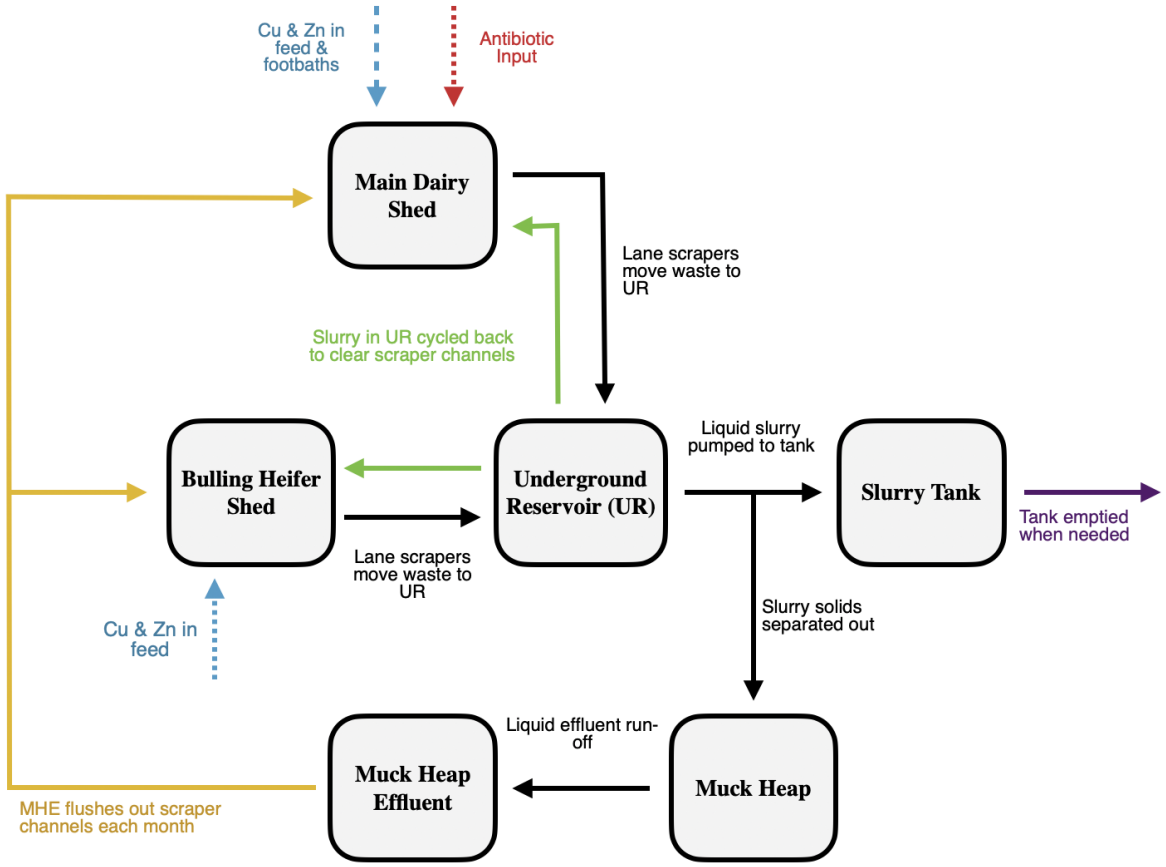

Figure 2.1: A flow diagram showing the different compartments of the dairy farm, and how waste flows between the compartments. Waste from the main dairy and bulling heifer sheds flows into an underground reservoir (UR) via scraper channels. Slurry is then passed through a separator where slurry solids are put on the muck heap, and liquid slurry is pumped into the slurry tank, which is then emptied when the tank is full or slurry is needed for spreading on fields (purple arrow). The only metal (blue arrows) and antibiotic (red arrows) inputs into the waste water flow system are through metal in the daily cow feed in both sheds and heavy metal footbaths used in the main dairy shed. There are two main feedback loops where waste water is recycled through the system to clear the scraper channels of any waste build up: slurry is pumped back from the UR into the scraper channels for 4 hours each day (green arrows), and effluent run-off from the muck heap is collected and used to flush out the scraper channels once every 3-4 weeks (yellow arrows).

Dairy Farm Background

This study considers a mid-sized, high performance commercial dairy farm in the East Midlands, UK, housing 200 milking Holstein Friesian cattle at the time of study. Milking cattle are housed indoors on concrete, and all excreta are regularly removed from cattle yards by automatic scrapers into a drainage system terminating at the 3 M litre slurry tank. The drainage system also receives used cleaning materials and wash water, used footbath, waste milk, and rainwater runoff. An automated screw press (Bauer S655 slurry separator with sieve size 0.75 mm; Bauer GmbH, Voitsberg, Austria) performs liquid-solid separation of the slurry before it is passed to the slurry tank. Liquids enter the slurry tank semi-continuously, while solids are removed to a muck heap. Calves, dry cows, and heifers are housed separately from the milking cows. Faeces and urine from calves drain into the common drainage system, whilst dirty straw from calf housing is taken directly to the muck heap. Excess slurry can be pumped to an 8 M litre lagoon for long term storage. Slurry is used to fertilize grassland and arable fields. Practice at this farm is typical of management methods at high-performance dairy farms, although all farms vary.

Mathematical Model

We have developed a mathematical model (2.1)-(2.24) to evaluate the risk of the spread of AMR across bacterial populations within dirty water as it flows around different areas of a typical UK dairy farm described in figure 2.1, using a multiscale, hybrid discrete-continuous, compartmental system of ordinary differential equations (ODEs). The six different farm compartments are described by a volumetric flow ODE model, to describe the flow of dirty water (V_i) between the compartments, in which the rates of flow between the different compartments follow first order mass action kinetics, and materials within the waste flow between compartments have the non-variable fractional flow rates. The flow model is then extended to include the concentrations of copper and zinc ($M_i^{[Cu]}$ and $M_i^{[Zn]}$), and antibiotics ($A_i^{[Oxy]}$ and $A_i^{[Cex]}$). The flow model was coupled with a bacterial resistance transfer ODE model [17], that describes populations of antimicrobial sensitive (S_i) and resistant ($R_i^{[x_1,x_2,x_3,x_4]}$ bacteria in each of the six compartments, where $[x_1, x_2, x_3, x_4] \in \{0, 1\}^4$, such that $x_1 = 1$ if the population is resistant to copper, while $x_1 = 0$ if it is sensitive to copper, and similarly x_2, x_3 and x_4 reflect zinc, oxytetracycline and cefalexin resistant bacteria. All the parameters of the model are described in table 2.B1-2.B6 with realistic value ranges for each parameter based on ethnographic observations of the Sutton Bonington dairy farm and available information in the existing literature. This hybrid discrete-continuous farm flow model was built on a continuous version of the farm flow model which we initially developed. The equations defining the continuous farm flow model are given in Appendix in Appendix 2.A.

$$\frac{dV_{\text{dairy}}}{dt} = a - \rho V_{\text{dairy}} + \frac{\sigma V_{\text{UR}}}{2} + \Theta\left(T_{\text{footbath}}\right) V_{\text{footbath}} + \Theta\left(T_{\text{extra foot.}}\right) V_{\text{extra foot.}} + \Theta\left(T_{\text{Eff. flush}}\right) \frac{\left(1-\epsilon_{\text{eff}}\right) V_{\text{eff}}}{2} \ , \tag{2.1}$$

$$\frac{dV_{\text{heifer}}}{dt} = b - \rho V_{\text{heifer}} + \frac{\sigma V_{\text{UR}}}{2} + \Theta\left(T_{\text{Eff. flush}}\right) \frac{\left(1-\epsilon_{\text{eff}}\right) V_{\text{eff}}}{2} \ , \tag{2.2}$$

$$\frac{dV_{\text{UR}}}{dt} = \rho\left(V_{\text{dairy}} + V_{\text{heifer}}\right) - \sigma V_{\text{UR}} - \gamma V_{\text{UR}} \ , \tag{2.3}$$

$$\frac{dV_{\text{muck}}}{dt} = \left(1-\varepsilon\right)\gamma V_{\text{UR}} - \eta V_{\text{muck}} - \kappa_{\text{muck}} V_{\text{muck}} \ , \tag{2.4}$$

$$\frac{dV_{\text{eff}}}{dt} = \eta V_{\text{muck}} + \iota_{\text{silage}} - \Theta\left(T_{\text{Eff. flush}}\right)\left(1-\epsilon_{\text{eff}}\right) V_{\text{eff}} \ , \tag{2.5}$$

$$\frac{dV_{\text{tank}}}{dt} = \varepsilon\gamma V_{\text{UR}} - \Theta\left(T_{\text{Tank empty}}\right)\left(1-\epsilon_{\text{Tank}}\right) V_{\text{tank}} \ , \tag{2.6}$$

where $\Theta(T) = \begin{cases} 1 & t \in T \\ 0 & \text{otherwise} \end{cases}$.

We assume that the amount of volume of daily waste inputs in the main dairy shed (a) and bulling heifer shed (b) (i.e. from faecal matter, trough water, footbaths, bedding etc.) are constant. Copper and zinc are used in the cattle feed for growth promotion purposes and a significant percentage of these metals are not absorbed by the cow ($\approx$ 99% and 85% for Cu and Zn respectively [33]) and enter the slurry flow system in the cow faeces. We also assume that the solid slurry matter separated onto the muck heap has no residual liquid and effluent run off is determined only by rainfall (η).

On top of the continuous flow model, three farm processes are represented by discrete processes within the model: the emptying of metal footbaths into the main dairy shed scraper channel; the flushing of the scraper channels with muck heap effluent; and the emptying of the slurry tank. To model these processes, we assert that at time T_{footbath} that the volume of the footbath (V_{footbath} and mass of copper and zinc ($a^{[Cu]}_{\text{footbath}}$ & $a^{[Zn]}_{\text{footbath}}$) is instantly added to the slurry volume and metal mass in the main dairy shed respectively. The emptying of the slurry tank is modelled similarly where at time T_{Tank}, the slurry tank compartments are emptied. We model the tank as not being completely emptied and that a small proportion ($0 < \epsilon_{\text{Tank}} \ll 1$) of the volume, mass of metals and antibiotics and population

of bacteria in the slurry tank contents remains. Similarly, at time $T_{\text{Eff. Flush}}$ we assume that a small fraction ($0 < \epsilon_{\text{eff}} \ll 1$) of the contents in the effluent tank contents remains and ${}^{(1-\epsilon_{\text{eff}})V_{\text{eff}}}/_{2}$ is added to the main dairy and bulling heifer sheds each. We also include the term ι_{silage} for the runoff from the farm silage clamp that is added to the effluent tank also. However, in the interest of model complexity we assume that this run-off is just water containing no additional metals, bacteria or antibiotics (although we appreciate that this is not a realistic assumption of silage clamp run-off and an interesting extension of the farm flow model could be to consider the silage clamp and the sheds which feed into it).

$$\begin{aligned}\frac{dM^{[j]}_{\text{dairy}}}{dt} = a^{[j]}_{\text{feed}} - \rho M^{[j]}_{\text{dairy}} + \frac{\sigma M^{[j]}_{\text{UR}}}{2} + \Theta\left(T_{\text{footbath}}\right) a^{[j]}_{\text{footbath}} \\ + \Theta\left(T_{\text{extra foot.}}\right) a^{[j]}_{\text{extra foot.}} + \Theta\left(T_{\text{Eff. flush}}\right) \frac{\left(1-\epsilon_{\text{eff}}\right) M^{[j]}_{\text{eff}}}{2} \ ,\end{aligned} \tag{2.7}$$

$$\frac{dM^{[j]}_{\text{heifer}}}{dt} = b^{[j]}_{\text{feed}} - \rho M^{[j]}_{\text{heifer}} + \frac{\sigma M^{[j]}_{\text{UR}}}{2} + \Theta\left(T_{\text{Eff. flush}}\right) \frac{\left(1-\epsilon_{\text{eff}}\right) M^{[j]}_{\text{eff}}}{2} \ , \tag{2.8}$$

$$\frac{dM^{[j]}_{\text{UR}}}{dt} = \rho\left(M^{[j]}_{\text{dairy}} + M^{[j]}_{\text{heifer}}\right) - \sigma M^{[j]}_{\text{UR}} - \gamma M^{[j]}_{\text{UR}}, \tag{2.9}$$

$$\frac{dM^{[j]}_{\text{muck}}}{dt} = \left(1-\varepsilon\right)\gamma M^{[j]}_{\text{UR}} - \eta M^{[j]}_{\text{muck}} - \kappa_{\text{muck}} M^{[j]}_{\text{muck}}, \tag{2.10}$$

$$\frac{dM^{[j]}_{\text{eff}}}{dt} = \eta M^{[j]}_{\text{muck}} - \Theta\left(T_{\text{Effluent}}\right)\left(1-\epsilon_{\text{eff}}\right) M^{[j]}_{\text{eff}} \ , , \tag{2.11}$$

$$\frac{dM^{[j]}_{\text{tank}}}{dt} = \varepsilon\gamma M^{[j]}_{\text{UR}} - \Theta\left(T_{\text{Tank empty}}\right)\left(1-\epsilon_{\text{Tank}}\right) M^{[j]}_{\text{tank}} \ , \tag{2.12}$$

where $j \in \{\text{Cu}, \text{Zn}\}$.

Antibiotics enter the slurry flow system in the main dairy shed sick pens as we assume the antibiotics pass into the scrapers channels in the sick pen cow's faeces and we model the antibiotic input ($a^{[j]}(t)$ for $j \in \{\text{Oxy, Cex}\}$ as a time-dependent discrete parameter based on the farm antibiotic usage records. We model the degradation of the antibiotics using previously identified first-order degradation kinetics[17]. The microbiological model is a subset of the model previously described[17], but with four rather than six antimicrobials (copper, zinc, oxytetracyline and cephalexin).

$$\frac{dA^{[j]}_{\text{dairy}}}{dt} = a^{[j]}(t) - \rho A^{[j]}_{\text{dairy}} + \frac{\sigma A^{[j]}_{\text{UR}}}{2} - \delta_{[j]} A^{[j]}_{\text{dairy}} + \Theta\left(T_{\text{Eff. flush}}\right) \frac{(1-\epsilon_{\text{eff}})\, A^{[j]}_{\text{eff}}}{2}\ , \tag{2.13}$$

$$\frac{dA^{[j]}_{\text{heifer}}}{dt} = -\rho A^{[j]}_{\text{heifer}} + \frac{\sigma A^{[j]}_{\text{UR}}}{2} - \delta_{[j]} A^{[j]}_{\text{heifer}} + \Theta\left(T_{\text{Eff. flush}}\right) \frac{(1-\epsilon_{\text{eff}})\, A^{[j]}_{\text{eff}}}{2}\ , \tag{2.14}$$

$$\frac{dA^{[j]}_{\text{UR}}}{dt} = \rho\left(A^{[j]}_{\text{dairy}} + A^{[j]}_{\text{heifer}}\right) - \sigma A^{[j]}_{\text{UR}} - \gamma A^{[j]}_{\text{UR}} - \delta_{[j]} A^{[j]}_{\text{UR}}, \tag{2.15}$$

$$\frac{dA^{[j]}_{\text{muck}}}{dt} = (1-\varepsilon)\,\gamma A^{[j]}_{\text{UR}} - \eta A^{[j]}_{\text{muck}} - \kappa_{\text{muck}} A^{[j]}_{\text{muck}} - \delta_{[j]} A^{[j]}_{\text{muck}}, \tag{2.16}$$

$$\frac{dA^{[j]}_{\text{eff}}}{dt} = \eta A^{[j]}_{\text{muck}} - \delta_{[j]} A^{[j]}_{\text{eff}} - \Theta\left(T_{\text{Effluent}}\right)(1-\epsilon_{\text{eff}})\, A^{[j]}_{\text{eff}}\ ,\ , \tag{2.17}$$

$$\frac{dA^{[j]}_{\text{tank}}}{dt} = \varepsilon\gamma A^{[j]}_{\text{UR}} - \delta_{[j]} A^{[j]}_{\text{tank}} - \Theta\left(T_{\text{Tank empty}}\right)(1-\epsilon_{\text{Tank}})\, A^{[j]}_{\text{tank}}\ , \tag{2.18}$$

where $j \in \{\text{Oxy}, \text{Cex}\}$.

We define Ω_i as the set of all bacterial populations within the compartment i:

$$\Omega_i = \left\{S_i, R_i^{[1,0,0,0]}, R_i^{[0,1,0,0]}, \ldots, R_i^{[1,1,1,1]}\right\},$$

and define Ω_i^* as the set of all bacterial populations carrying at least one resistance within the compartment i, i.e. $\Omega_i^* = \Omega_i \ / \{S_i\}$.

The flow of each bacterial population, $R_i^{[x_1,x_2,x_3,x_4]}$, between the different farm areas is described by the function $\mathscr{F} : \Omega_i \to \mathbb{R}$ such that:

$$\mathscr{F}(R_i^{[x_1,x_2,x_3,x_4]}) = \begin{cases} a\nu_{[x_1,x_2,x_3,x_4]}\psi_{\text{E.coli}} - \rho R^{[x_1,x_2,x_3,x_4]}_{\text{dairy}} + \frac{\sigma R^{[x_1,x_2,x_3,x_4]}_{\text{UR}}}{2}, & \text{for } i = \text{dairy} \\ b\nu_{[x_1,x_2,x_3,x_4]}\psi_{\text{E.coli}} - \rho R^{[x_1,x_2,x_3,x_4]}_{\text{heifer}} + \frac{\sigma R^{[x_1,x_2,x_3,x_4]}_{\text{UR}}}{2}, & \text{for } i = \text{heifer} \\ \rho\left(R^{[x_1,x_2,x_3,x_4]}_{\text{dairy}} + R^{[x_1,x_2,x_3,x_4]}_{\text{heifer}}\right) - \sigma R^{[x_1,x_2,x_3,x_4]}_{\text{UR}} - \gamma R^{[x_1,x_2,x_3,x_4]}_{\text{UR}}, & \text{for } i = \text{UR} \\ (1-\varepsilon)\,\gamma R^{[x_1,x_2,x_3,x_4]}_{\text{UR}} - \eta R^{[x_1,x_2,x_3,x_4]}_{\text{muck}} - \kappa_{\text{muck}} R^{[x_1,x_2,x_3,x_4]}_{\text{muck}}, & \text{for } i = \text{muck} \\ \eta R^{[x_1,x_2,x_3,x_4]}_{\text{muck}}, & \text{for } i = \text{eff} \\ \varepsilon\gamma R^{[x_1,x_2,x_3,x_4]}_{\text{UR}}, & \text{for } i = \text{tank} \end{cases} \tag{2.19}$$

We define the effect of the discrete farm processes on each bacterial population, $R_i^{[x_1,x_2,x_3,x_4]}$, by the function $\mathscr{D} : \Omega_i \to \mathbb{R}$ such that:

$$\mathscr{D}(R_i^{[x_1,x_2,x_3,x_4]}) = \begin{cases} \Theta\left(T_{\text{Eff. flush}}\right) \frac{(1-\epsilon_{\text{eff}}) R_{\text{eff}}^{[x_1,x_2,x_3,x_4]}}{2}, & \text{for } i = \text{dairy, heifer} \\ 0, & \text{for } i = \text{UR, muck} \\ -\Theta\left(T_{\text{Eff. flush}}\right)(1-\epsilon_{\text{eff}}) R_{\text{eff}}^{[x_1,x_2,x_3,x_4]}, & \text{for } i = \text{eff} \\ -\Theta\left(T_{\text{Tank empty}}\right)(1-\epsilon_{\text{tank}}) R_{\text{tank}}^{[x_1,x_2,x_3,x_4]}, & \text{for } i = \text{tank} \end{cases} \tag{2.20}$$

Similarly, we describe the growth and death of each bacterial population, $R_i^{[x_1,x_2,x_3,x_4]}$, by the function $\mathscr{G} : \Omega_i \to \mathbb{R}$ such that:

$$\begin{aligned} \mathscr{G}(R_i^{[x_1,x_2,x_3,x_4]}) =& r R_i^{[x_1,x_2,x_3,x_4]}) \left(1 - x_1\alpha_{[\text{Cu}]} - x_2\alpha_{[\text{Zn}]} - x_3\alpha_{[\text{Oxy}]} - x_4\alpha_{[\text{Cex}]}\right) \left(1 - \frac{N_{\text{i}}}{N_{\max}}\right) \\ & \left(1 - (1-x_3)ES_{[\text{Oxy}]}\right) - \left((1-x_1)ES_{[\text{Cu}]} - (1-x_2)ES_{[\text{Zn}]} - (1-x_4)ES_{[\text{Cex}]}\right. \\ & \left. - \delta\right) R_i^{[x_1,x_2,x_3,x_4]} \end{aligned} \tag{2.21}$$

Where N_{i} denotes the total bacterial population in the compartment $i \in \{\text{dairy, heifer, UR, muck, eff, tank}\}$, such that:

$$N_{\text{i}} = \sum_{\mathscr{R}_i \in \Omega_i} \left(\mathscr{R}_i\right), \tag{2.22}$$

and $E_{\text{i}}^{[j]}$ (for $i \in \{\text{dairy, heifer, UR, muck, eff, tank}\}$ and $j \in \{\text{Cu, Zn, Oxy, Cex}\}$) denotes the antimicrobial effect on the bacterial growth rate in the case of bacteriostatic antibiotics (e.g. oxytetracycline), or the antimicrobial effect on the bacterial death rate in the case of bacteriocidal antimicrobials (e.g. copper, zinc or cefalexin). Since $x_i \in \{0, 1\}$, the general equation for the bacterial growth dynamics, (2.21), includes the fitness cost, $\alpha_{[j]}$, incurred by the presence of resistance (i.e. when $x_i = 1$), as well as the negated bacteriocidal/bacteriostatic effects if the bacteria is resistant to that antibiotic.

$$E_{\text{i}}^{[j]} = \frac{E_{\max}^{[j]} \left(A_i/V_i\right)^{H_{[j]}}}{MIC_{[j]}{}^{H_{[j]}} + \left(A_i/V_i\right)^{H_{[j]}}} \tag{2.23}$$

Finally, the horizontal transfer of resistance between bacterial populations is defined by the function $\mathscr{H} : \Omega_i \to \mathbb{R}$ (the full definition of this $\mathscr{H}$ is given by (2.C25)-(2.C40) in Appendix 2.C.

The dynamics of each bacterial population in the farm flow system can therefore be described by the system of equations defined by:

$$\frac{dR_i^{[x_1,x_2,x_3,x_4]}}{dt} = \mathscr{F}(R_i^{[x_1,x_2,x_3,x_4]}) + \mathscr{D}(R_i^{[x_1,x_2,x_3,x_4]}) + \mathscr{G}(R_i^{[x_1,x_2,x_3,x_4]}) + \mathscr{H}(R_i^{[x_1,x_2,x_3,x_4]}),$$
$$\text{where } i \in \{\text{dairy, heifer, UR, muck, eff., tank}\} \ \& \ [x_1, x_2, x_3, x_4] \in \{0,1\}^4. \tag{2.24}$$

Simulations

We simulated our farm flow model using MATLAB R2020 [34]. We produced time course simulations with the standard parameter values (Table 2.B1) using the ODE45 solver to show the concentration of the different bacterial populations over time. For all simulations of the model, we used the steady state values of the continuous farm flow model for the initial conditions of the slurry volume and metal equations, and assume that the initial volume of the slurry tank is 1 $\times 10^6$ L and the effluent tank has recently been used and in a near empty state ($V_{\text{eff}}(0) = \omega$) to avoid division by zero errors in the HGT terms of the effluent bacterial populations). We initialise the bacterial populations in our model using the average *E. coli* counts sampled from each area of the farm and assume the proportion of each distinct resistant bacterial population is the same.

Model Calibration

We have calibrated the model using data sets of the metal concentrations across different areas in the slurry flow chain of the Sutton Bonington dairy farm using two different methods. We used HACH UV-Vis Spectrophotometer kits to determine copper and zinc concentrations in the slurry tank at 27 time points between 7th June 2017 and 23rd November 2017, as well as concentrations at a single time point from 23rd November 2017 for other areas of the farm flow system (the dairy shed and heifer shed scraper channels, underground reservoir and muck heap effluent). We also used ICP-MS analysis to give heavy metal concentrations of 9 samples from slurry tank taken on 2nd July 2015. We used both the HACH and ICP-MS metal concentration data to estimate the concentration of copper and zinc in the cattle feed as this was initially understood to be a significant component of the metal inputs into the slurry system (this concentration determined the value of $a_{\text{feed}}^{[j]}$ and $b_{\text{feed}}^{[j]}$ for $j \in \{\text{Cu, Zn}\}$ along with mass of feed per cow and number of cows in each shed). We estimated heavy metal content of the cow's daily feed using a Metropolis-Hastings Markov Chain Monte Carlo (MCMC) method on the continuous farm flow model with an uninformed uniform prior between 0 and the maximum permitted levels of heavy metal in dairy feed according to the European Food Safety Authority (EFSA) [35, 36, 37]. We estimated the feed copper and zinc concentrations individually as well as used each set of concentration data individually in our parameter estimations. For each estimate we used an initial estimate for the

parameter based on values calculated from the farm daily feed menu and ran the MCMC algorithm for 1000 iterations.

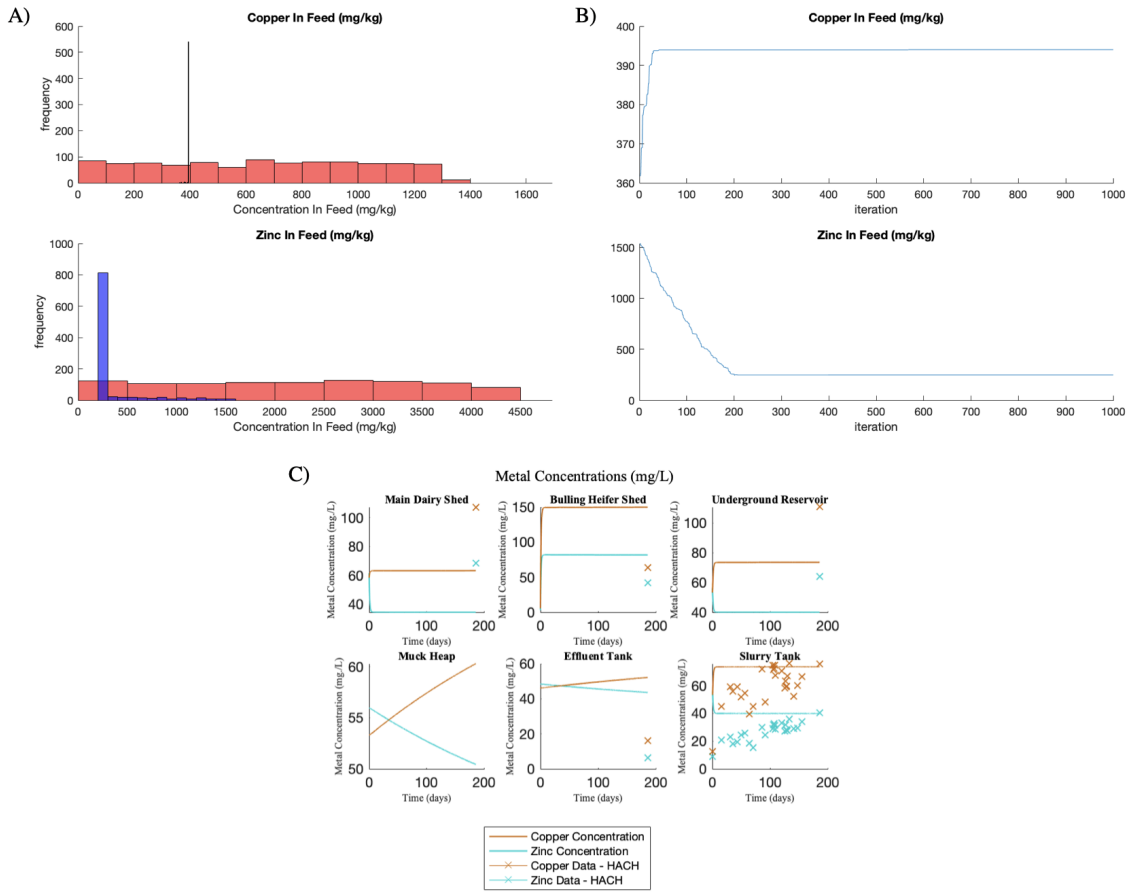

Figure 2.2: **Parameter estimation of cattle feed metal contents using MCMC approach against HACH UV-vis spectrophotometer data** (A) shows histograms of the uniform prior distributions (red) and the posterior distributions (blue) of the MCMC estimation against the HACH data. (B) shows the trace plots of the parameter estimation at each iteration of the Metropolis-Hasting algorithm. (C) is a time course of the continuous farm flow model for the metal mass across the different areas of the farm using the mean of the posterior distribution estimated in the MCMC (Cu: 393.997 and Zn: 247.926) against the metal concentrations observed in the slurry tank and across the farm measured using the HACH UV-vis spectrophotometer kits.

2.3 Results and Discussion

We initially developed the continuous volumetric model for the flow of dairy slurry around the Sutton Bonington dairy farm (2.A1)-(2.A6) and an analogous model for the mass of copper and zinc in the slurry flow (2.A7)-(2.A12).

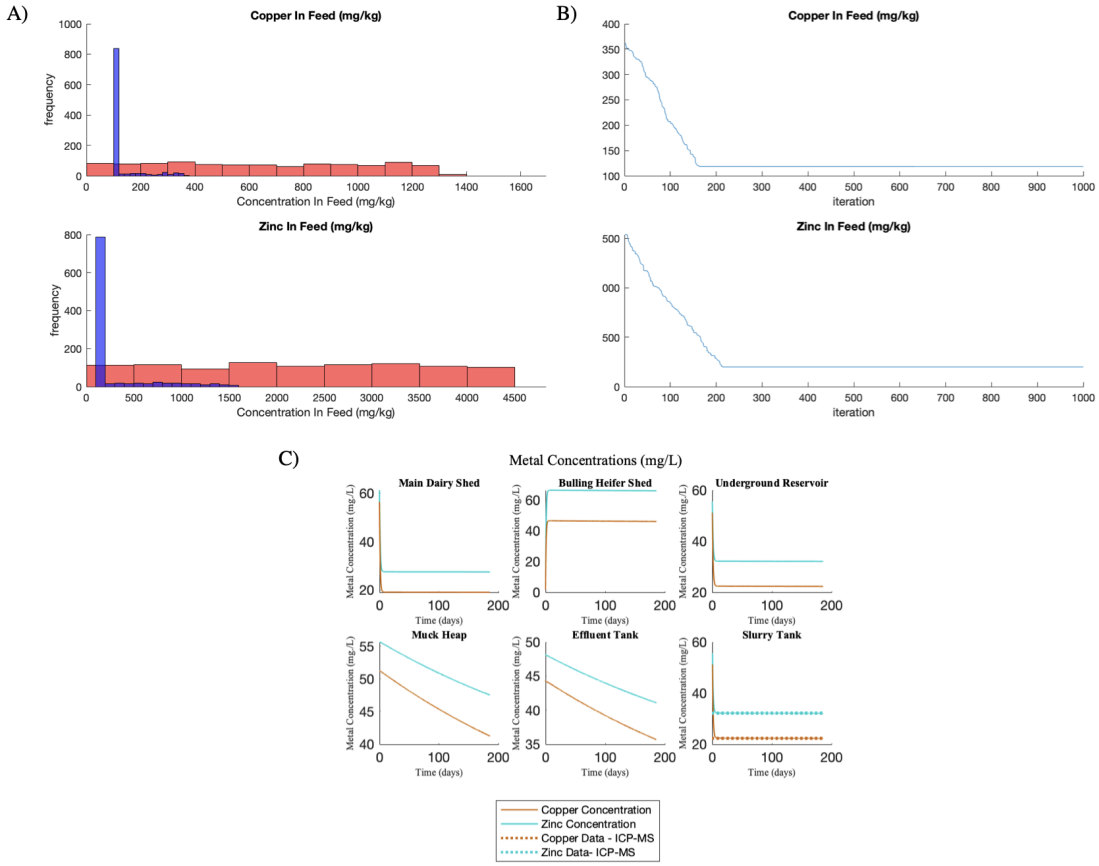

Figure 2.3: **Parameter estimation of cattle feed metal contents using MCMC approach against ICP-MS data**. (A) shows histograms of the uniform prior distributions (red) and the posterior distributions (blue) of the MCMC estimation against the HACH data. (B) shows the trace plots of the parameter estimation at each iteration of the Metropolis-Hasting algorithm. (C) is a time course of the continuous farm flow model for the metal mass across the different areas of the farm using the mean of the posterior distribution estimated in the MCMC (Cu: 118.233 and Zn: 198.877) against the metal concentrations observed in the slurry tank using ICP-MS (as this was only taken at a single time point before the period of interest we show this as a constant line).

We have attempted to calibrate the continuous model using metal concentrations observed on the

farm between 7th June 2017 and 23rd November 2017. In order to do this we have used this data to estimate the metal input from the milking herd feed (a value that we have also approximated using data from the farm's feeding menu and EFSA regulations [35, 36, 37]) using a Metropolis-Hastings algorithm and ran this method over 1000 iterations. For our estimation, we assumed a uniform prior distribution with an upper bound limit defined by the EFSA limits for Cu (30 mg/kg on 88% dry matter basis) and Zn (100 mg/kg on 88% dry matter basis) content in dairy cattle feed.

We evaluated the model in this way against two different data sets:

- Copper and zinc concentrations from the slurry tank gathered at 27 distinct time points between 7th June and 23rd November 2017 and analysed using HACH UV-Vis spectrophotometer kits. These also include a measurements across the other farm areas at a single time point (23rd November 2017) [17].

- Copper and zinc concentrations from the slurry tank from a single time point (2nd July 2015) measured using ICP-MS analysis.

The MCMC estimation using the HACH data as a sample set provides a reasonable estimate for the feed Cu content (figure 2.2) - we estimated the mean Cu fed per cow per day to be 393.997mg, where the value calculated from the farm feed menu was approximately 361.77mg per cow per day. However the MCMC estimate for the Zn content of the feed (247.926) is approximately five times lower than expected value based on the farm menu (1538.43mg).

When the MCMC estimation was run against the ICP-MS data (figure 2.3), both copper and zinc content in the feed - 118.233 mg and 198.877 mg respectively - were notably lower than the expected menu concentrations.

Figure 2.4 shows time course simulations of the hybrid discrete-continuous model using the mean MCMC estimates given for Cu and Zn inputs from the cattle feed. We can clearly observe that estimated feed metal concentration parameters do not provide a great fit when used in the discrete-continuous model.

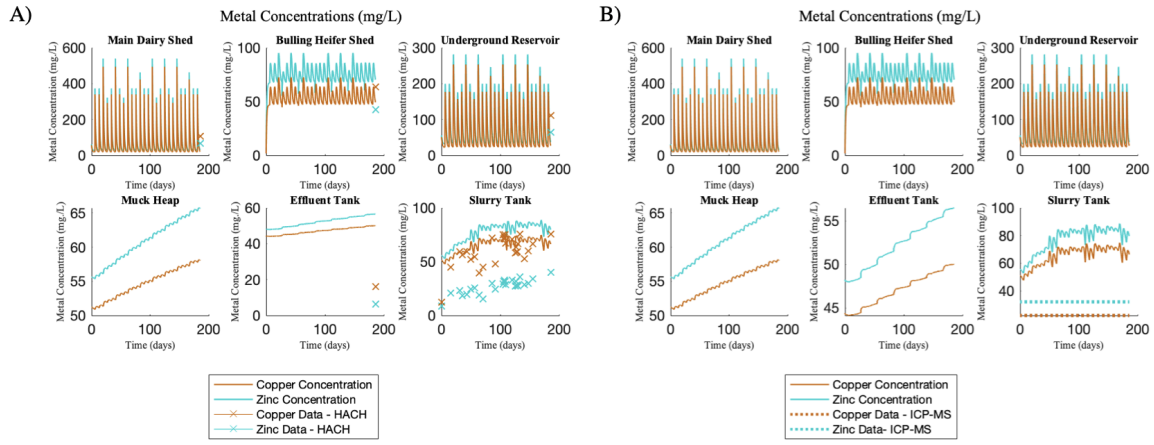

Figure 2.4: **Time course simulation of the hybrid discrete-continuous farm flow model using the parameters estimated using MCMC plotted against both the HACH and ICP-MS metal concentration data** These time course simulations of the discrete-continuous farm flow model use parameter values of metal footbath inputs based on the feed metal concentrations estimated using the continuous model (Figure 2.2-2.3).

It should be noted that the ICP-MS data is only taken from a single time point in 2015, while our model is based on knowledge of the farm practices carried out in 2017 and 2018, so our model may not accurately represent the practices on the farm at that time - e.g. the EFSA MPL for copper in dairy cattle feed was reduced in 2016 [36].

We also note that the concentration of copper in the slurry tank is measured to be nearly two-fold the zinc concentration using the HACH kits, while feed information from the farm and the EFSA MPLs for Cu and Zn, would suggest that there are significantly higher amounts of Zn entering the system than Cu. We suggest that this large discrepancy may be caused by a high-bias for copper due to interfering levels of iron in the dairy slurry - HACH have acknowledged interference in copper measurements for levels of iron above 15 mg/L [38, 39] and ICP-MS analysis shows average iron concentration of 25.27 mg/L in the slurry tank. Furthermore similar inaccuracies of the UV-Vis spectrophotometer method have been observed in method comparisons against ICP-MS and ICP-OES [40, 41].

Discrepancies between the estimation and the observed metal concentrations may also be partially explained by adsorption of the metals into slurry solids before and after the slurry passes through the screw press separator - an interesting extension to the model may be to include these adsorption dynamics.

2.4 Conclusion

In this chapter, we have presented a mathematical model for bacteria and antimicrobials within the flow of dairy slurry across the different areas of a typical UK dairy farm. We have attempted to calibrate the model against two different metal concentration data sets, and while the this calibration has not provided the best fit, there are numerous degrees of uncertainty that may have affected this outcome such as interference levels from iron in the HACH UV-vis spectrophotometer kits, an insufficient number of time points for the ICP-MS (as we only have a single time-point from outside the period of study). Another important consideration is that the mass of metal input due to the emptying of the footbaths is significantly higher than from the feed and this difference likely had a impact on the parameter estimation since the feed metal input accounts for such a small proportion of the total metal input. Therefore it would be more appropriate to have calibrated the model by estimating the metal footbath metal concentration instead.

2.5 Acknowledgements

Ethnographic observations of the University Of Nottingham Sutton Bonington Dairy Farm were performed by Richard Helliwell, and the metal concentration data from both the HACH UV-Vis spectrophotometer kits and the ICP-MS analysis was completed as a part of the EVAL-Farms research project [17] and was performed by Tom Dodsworth and Elizabeth King.

2.A Appendix: Continuous Farm Flow Model

We initially developed a continuous version of the farm flow model where all farm processes were considered to occur continuously at a constant rate. The continuous farm flow model is defined by the system of equations (2.A1) - (2.A24).

The volume of slurry equations in the continuous model are defined as:

$$\frac{dV_{\text{dairy}}}{dt} = a - \rho V_{\text{dairy}} + \frac{\sigma V_{\text{UR}}}{2} + a_{\text{footbath}} + \frac{\omega}{2} \ , \tag{2.A1}$$

$$\frac{dV_{\text{heifer}}}{dt} = b - \rho V_{\text{heifer}} + \frac{\sigma V_{\text{UR}}}{2} + \frac{\omega}{2} \ , \tag{2.A2}$$

$$\frac{dV_{\text{UR}}}{dt} = \rho \left(V_{\text{dairy}} + V_{\text{heifer}}\right) - \sigma V_{\text{UR}} - \gamma V_{\text{UR}} \ , \tag{2.A3}$$

$$\frac{dV_{\text{muck}}}{dt} = (1-\varepsilon)\,\gamma V_{\text{UR}} - \eta V_{\text{muck}} - \kappa_{\text{muck}} V_{\text{muck}} \ , \tag{2.A4}$$

$$\frac{dV_{\text{eff}}}{dt} = \eta V_{\text{muck}} + \iota_{\text{silage}} - \omega \ , \tag{2.A5}$$

$$\frac{dV_{\text{tank}}}{dt} = \varepsilon\gamma V_{\text{UR}} - \kappa_{\text{tank}} V_{\text{tank}} \ , \tag{2.A6}$$

where a_{footbath} represents the footbaths being emptied into the main dairy shed at a constant rate, ω is the constant rate of effluent being used to flush the scraper channels and $kappa_{\text{tank}}$ is the rate at which the slurry tank is emptied.

Similarly the equations for the metal mass, $M_i^{[j]}$, in the continuous farm flow model are given by:

$$\frac{dM^{[j]}_{\text{dairy}}}{dt} = a^{[j]}_{\text{feed}} - \rho M^{[j]}_{\text{dairy}} + \frac{\sigma M^{[j]}_{\text{UR}}}{2} + \bar{a}^{[j]}_{\text{footbath}} + \frac{\omega M^{[j]}_{\text{eff}}}{2V_{\text{eff}}} \ , \tag{2.A7}$$

$$\frac{dM^{[j]}_{\text{heifer}}}{dt} = b^{[j]}_{\text{feed}} - \rho M^{[j]}_{\text{heifer}} + \frac{\sigma M^{[j]}_{\text{UR}}}{2} + \frac{\omega M^{[j]}_{\text{eff}}}{2V_{\text{eff}}} \ , \tag{2.A8}$$

$$\frac{dM_{\text{UR}}^{[j]}}{dt} = \rho\left(M_{\text{dairy}}^{[j]} + M_{\text{heifer}}^{[j]}\right) - \sigma M_{\text{UR}}^{[j]} - \gamma M_{\text{UR}}^{[j]}, \tag{2.A9}$$

$$\frac{dM_{\text{muck}}^{[j]}}{dt} = (1-\varepsilon)\,\gamma M_{\text{UR}}^{[j]} - \eta M_{\text{muck}}^{[j]} - \kappa_{\text{muck}} M_{\text{muck}}^{[j]}, \tag{2.A10}$$

$$\frac{dM_{\text{eff}}^{[j]}}{dt} = \eta M_{\text{muck}}^{[j]} - \frac{\omega M_{\text{eff}}^{[j]}}{V_{\text{eff}}}\ ,, \tag{2.A11}$$

$$\frac{dM_{\text{tank}}^{[j]}}{dt} = \varepsilon\gamma M_{\text{UR}}^{[j]} - \kappa\text{tank} M_{\text{tank}}^{[j]}\ , \tag{2.A12}$$

where $j \in \{\text{Cu}, \text{Zn}\}$, and $\bar{a}_{\text{footbath}}^{[j]}$ is the constant rate of metals entering the main dairy shed scraper channel due to footbath emptying.

The antibiotic mass equations of the continuous case are similarly defined:

$$\frac{dA_{\text{dairy}}^{[j]}}{dt} = \ a^{[j]}(t) - \rho A_{\text{dairy}}^{[j]} + \frac{\sigma A_{\text{UR}}^{[j]}}{2} - \delta_{[j]} A_{\text{dairy}}^{[j]} + \frac{\omega A_{\text{eff}}^{[j]}}{2V_{\text{eff}}}\ , \tag{2.A13}$$

$$\frac{dA_{\text{heifer}}^{[j]}}{dt} = -\rho A_{\text{heifer}}^{[j]} + \frac{\sigma A_{\text{UR}}^{[j]}}{2} - \delta_{[j]} A_{\text{heifer}}^{[j]} + \frac{\omega A_{\text{eff}}^{[j]}}{2V_{\text{eff}}}\ , \tag{2.A14}$$

$$\frac{dA_{\text{UR}}^{[j]}}{dt} = \rho\left(A_{\text{dairy}}^{[j]} + A_{\text{heifer}}^{[j]}\right) - \sigma A_{\text{UR}}^{[j]} - \gamma A_{\text{UR}}^{[j]} - \delta_{[j]} A_{\text{UR}}^{[j]}, \tag{2.A15}$$

$$\frac{dA_{\text{muck}}^{[j]}}{dt} = (1-\varepsilon)\,\gamma A_{\text{UR}}^{[j]} - \eta A_{\text{muck}}^{[j]} - \kappa_{\text{muck}} A_{\text{muck}}^{[j]} - \delta_{[j]} A_{\text{muck}}^{[j]}, \tag{2.A16}$$

$$\frac{dA_{\text{eff}}^{[j]}}{dt} = \eta A_{\text{muck}}^{[j]} - \delta_{[j]} A_{\text{eff}}^{[j]} - \frac{\omega A_{\text{eff}}^{[j]}}{V_{\text{eff}}}\ ,, \tag{2.A17}$$

$$\frac{dA_{\text{tank}}^{[j]}}{dt} = \varepsilon\gamma A_{\text{UR}}^{[j]} - \delta_{[j]} A_{\text{tank}}^{[j]} - \kappa_{\text{tank}} A_{\text{tank}}^{[j]}\ , \tag{2.A18}$$

where $j \in \{\text{Oxy}, \text{Cex}\}$. Note that for both the continuous and the hybrid discrete-continuous farm flow models, we model the antibiotic input $(a^{[j]}(t)$ for $j \in \{\text{Oxy, Cex}\}$ as a time-dependent discrete parameter based on the farm antibiotic usage records.

The bacterial dynamics for the flow, $\mathscr{F} : \Omega_i \to \mathbb{R}$, growth $\mathscr{G} : \Omega_i \to \mathbb{R}$ and horizontal gene transfer $\mathscr{H} : \Omega_i \to \mathbb{R}$ of each bacterial population are the same as in the discrete farm flow model (2.19), (2.21) and (2.C25)-(2.C40).

The flow of each bacterial population, $R_i^{[x_1,x_2,x_3,x_4]}$, between the different farm areas is described by the function $\mathscr{F} : \Omega_i \to \mathbb{R}$ such that:

$$\mathscr{F}(R_i^{[x_1,x_2,x_3,x_4]}) = \begin{cases} a\nu_{[x_1,x_2,x_3,x_4]}\psi_{\text{E.coli}} - \rho R_{\text{dairy}}^{[x_1,x_2,x_3,x_4]} + \frac{\sigma R_{\text{UR}}^{[x_1,x_2,x_3,x_4]}}{2}, & \text{for } i = \text{dairy} \\ b\nu_{[x_1,x_2,x_3,x_4]}\psi_{\text{E.coli}} - \rho R_{\text{heifer}}^{[x_1,x_2,x_3,x_4]} + \frac{\sigma R_{\text{UR}}^{[x_1,x_2,x_3,x_4]}}{2}, & \text{for } i = \text{heifer} \\ \rho\left(R_{\text{dairy}}^{[x_1,x_2,x_3,x_4]} + R_{\text{heifer}}^{[x_1,x_2,x_3,x_4]}\right) - \sigma R_{\text{UR}}^{[x_1,x_2,x_3,x_4]} - \gamma R_{\text{UR}}^{[x_1,x_2,x_3,x_4]}, & \text{for } i = \text{UR} \\ (1-\varepsilon)\,\gamma R_{\text{UR}}^{[x_1,x_2,x_3,x_4]} - \eta R_{\text{muck}}^{[x_1,x_2,x_3,x_4]} - \kappa_{\text{muck}} R_{\text{muck}}^{[x_1,x_2,x_3,x_4]}, & \text{for } i = \text{muck} \\ \eta R_{\text{muck}}^{[x_1,x_2,x_3,x_4]}, & \text{for } i = \text{eff} \\ \varepsilon\gamma R_{\text{UR}}^{[x_1,x_2,x_3,x_4]}, & \text{for } i = \text{tank} \end{cases} \tag{2.A19}$$

$$\begin{aligned} \mathscr{G}(R_i^{[x_1,x_2,x_3,x_4]}) =& r R_i^{[x_1,x_2,x_3,x_4]} \left(1 - x_1\alpha_{[\text{Cu}]} - x_2\alpha_{[\text{Zn}]} - x_3\alpha_{[\text{Oxy}]} - x_4\alpha_{[\text{Cex}]}\right)\left(1 - \frac{N_{\text{i}}}{N_{\max}}\right) \\ & \left((1-x_3)E_{[\text{Oxy}]}\right) - \left((1-x_1)E_{[\text{Cu}]} - (1-x_2)E_{[\text{Zn}]} - (1-x_4)E_{[\text{Cex}]}\right. \\ & \left. - \delta\right) R_i^{[x_1,x_2,x_3,x_4]} \end{aligned} \tag{2.A20}$$

Where N_{i} denotes the total bacterial population in the compartment $i \in \{\text{dairy, heifer, UR, muck, eff, tank}\}$, such that:

$$N_{\text{i}} = \sum_{\mathscr{R}_i \in \Omega_i} (\mathscr{R}_i)\,, \tag{2.A21}$$

and $E_{\text{i}}^{[j]}$ (for $i \in \{\text{dairy, heifer, UR, muck, eff, tank}\}$ and $j \in \{\text{Cu, Zn, Oxy, Cex}\}$) denotes the antimicrobial effect on the bacterial growth rate in the case of bacteriostatic antibiotics (e.g. oxytetracycline), or the antimicrobial effect on the bacterial death rate in the case of bacteriocidal antimicrobials (e.g. copper, zinc or cefalexin).

$$E_{\text{i}}^{[j]} = \frac{E_{\max}^{[j]}\left(A_i/V_i\right)^{H_{[j]}}}{MIC_{[j]}{}^{H_{[j]}} + \left(A_i/V_i\right)^{H_{[j]}}} \tag{2.A22}$$

And the horizontal transfer of resistance between bacterial populations is defined by the function $\mathscr{H} : \Omega_i \to \mathbb{R}$ (the full definition of this $\mathscr{H}$ is given by (2.C25)-(2.C40) in Appendix 2.B.

However, the bacterial dynamics defined by the discrete farm practices differ from (2.20) since we assume that all farm processes occur at a continuous rate, e.g. effluent flushing occurs at rate ω and the emptying of the slurry tank at rate κ_{tank}. Note that we do not consider the impact of the footbath emptying here since since the emptying of the footbaths does not directly impact the inflow of bacteria,

but rather and the antimicrobial effect this change from discrete to continuous is encapsulated by the changes in $M_i^{[j]}$ given in the equations (2.A7) - (2.A12). In the continuous model, we define the effect of the farm processes on each bacterial population, $R_i^{[x_1,x_2,x_3,x_4]}$, by the function $\mathscr{D}_{\text{cts.}} : \Omega_i \to \mathbb{R}$ such that:

$$\mathscr{D}_{\text{cts.}}(R_i^{[x_1,x_2,x_3,x_4]}) = \begin{cases} \frac{\omega R_{\text{eff}}^{[x_1,x_2,x_3,x_4]}}{2V_{\text{dairy}}}, & \text{for } i = \text{dairy} \\ \frac{\omega R_{\text{eff}}^{[x_1,x_2,x_3,x_4]}}{2V_{\text{heifer}}}, & \text{for } i = \text{heifer} \\ 0, & \text{for } i = \text{UR, muck} \\ -\frac{\omega R_{\text{eff}}^{[x_1,x_2,x_3,x_4]}}{V_{\text{heifer}}}, & \text{for } i = \text{eff} \\ -\kappa_{\text{tank}} R_{\text{tank}}^{[x_1,x_2,x_3,x_4]}, & \text{for } i = \text{tank} \end{cases} \tag{2.A23}$$

The dynamics of each bacterial population in the continuous farm flow system are therefore described by the system of equations defined by:

$$\frac{dR_i^{[x_1,x_2,x_3,x_4]}}{dt} = \mathscr{F}(R_i^{[x_1,x_2,x_3,x_4]}) + \mathscr{D}_{\text{Cts}}(R_i^{[x_1,x_2,x_3,x_4]}) + \mathscr{G}(R_i^{[x_1,x_2,x_3,x_4]}) + \mathscr{H}(R_i^{[x_1,x_2,x_3,x_4]}),$$
$$\text{where } i \in \{\text{dairy, heifer, UR, muck, eff., tank}\} \ \& \ [x_1,x_2,x_3,x_4] \in \{0,1\}^4. \tag{2.A24}$$

2.B Appendix: Model Parameters

The tables 2.B1-2.B6 give the typical parameter values used in simulations of the farm flow model.

Parameter	Parameter Name	Parameter Values	Units	Source
	Volume Flow Parameters			
a	Main dairy shed waste volume input	1.238×10^{3}	L h^{-1}	farm observations, [42]
b	Bulling heifer shed waste volume input	1.358×10^{2}	L h^{-1}	farm observations, [42]
ρ	Scraper channel natural outflow rate	4.167×10^{-2}	h^{-1}	Assumed
γ	Pump rate from UR to slurry tank	9.625×10^{-2}	h^{-1}	farm observations, [43]
σ	Pump rate from UR to scraper channels	4.010×10^{-3}	h^{-1}	farm observations, [43]
ε	Fraction of slurry separated as liquid	0.950	-	farm observations
κ_{muck}	Muck heap emptying rate	7.500×10^{-5}	h^{-1}	farm observations
η	Muck heap effluent run off rate	2.083×10^{-5}	h^{-1}	farm observations
ι_{silage}	Volume of effluent run off from the silage clamp	2.382	L h^{-1}	farm observations

Table 2.B1:

Parameter	Parameter Name	Parameter Values	Units	Source
	Metal Parameters			
$a_{\text{feed}}^{[Cu]}$	Copper input from daily cow feed in main dairy shed	2.985×10^{3}	mg h^{-1}	farm observations, [35, 44]
$a_{\text{feed}}^{[Zn]}$	Zinc input from daily cow feed in main dairy shed	1.090×10^{4}	mg h^{-1}	farm observations, [37, 44]
$b_{\text{feed}}^{[Cu]}$	Copper input from daily cow feed in bulling heifer shed	8.954×10^{2}	mg h^{-1}	farm observations, [35, 44]
$b_{\text{feed}}^{[Zn]}$	Zinc input from daily cow feed in bulling heifer shed	3.269×10^{3}	mg h^{-1}	farm observations, [37, 44]

Table 2.B2:

Parameter	Parameter Name	Parameter Values	Units	Source
Antibiotic Parameters				
$\delta^{[Oxy]}$	Oxytetracycline degradation rate	3.269×10^{3}	h^{-1}	[17]
$\delta^{[Cex]}$	Cefalexin degradation rate	3.269×10^{3}	h^{-1}	[17]

Table 2.B3:

Parameter	Parameter Name	Parameter Values	Units	Source
Bacterial Parameters				
r	Specific growth rate	8.000×10^{-2}	h^{-1}	[17]
β	Horizontal gene transfer rate	1.000×10^{-6}	h^{-1}	[17]
N_{Max}	Carrying capacity	1.000×10^{10}	CFU L^{-1}	[17]
δ	Natural death rate of bacteria	4.684×10^{-2}	h^{-1}	Estimated, [17]
$\psi_{E.coli}$	Concentration of bacteria in slurry inflow	4.479×10^{7}	CFU L^{-1} h^{-1}	[17]
ν	Proportion of resistant bacteria in slurry inflow	3.178×10^{-4}	-	Estimated, [17]
$\alpha^{[Cu]}$	Fitness cost of copper resistance carried on plasmid	2.921×10^{-1}	-	Estimated, [17]
$\alpha^{[Zn]}$	Fitness cost of zinc resistance carried on plasmid	2.921×10^{-1}	-	Estimated, [17]
$\alpha^{[Oxy]}$	Fitness cost of Oxytetracycline resistance carried on plasmid	3.000×10^{-3}	-	[17]
$\alpha^{[Cex]}$	Fitness cost of Cefalexin resistance carried on plasmid	1.561×10^{-1}	-	Estimated, [17]

Table 2.B4:

Parameter	Parameter Name	Parameter Values	Units	Source
Pharmacodynamic Parameters				
$MIC^{[Cu]}$	Minimum inhibitory concentration of copper	212.79	mg L^{-1}	[45, 30, 17]
$MIC^{[Zn]}$	Minimum inhibitory concentration of zinc	2760.31	mg L^{-1}	[45, 30, 17]
$MIC^{[Oxy]}$	Minimum inhibitory concentration of Oxytetracycline	1	mg L^{-1}	[17]
$MIC^{[Cex]}$	Minimum inhibitory concentration of Cefalexin	8	mg L^{-1}	[17]
$E_{\text{Max}}^{[Cu]}$	Maximum death rate due to copper	1.74	h^{-1}	[45, 30, 17]
$E_{\text{Max}}^{[Zn]}$	Maximum death rate due to zinc	1.37	h^{-1}	[45, 30, 17]
$E_{\text{Max}}^{[Oxy]}$	Maximum death rate due to Oxytetracycline	1	h^{-1}	[17]
$E_{\text{Max}}^{[Cex]}$	Maximum death rate due to Cefalexin	1	h^{-1}	[17]
$H^{[Cu]}$	Hill coefficient for copper	1.54	-	[45, 30, 17]
$H^{[Zn]}$	Hill coefficient for zinc	0.72	-	[45, 30, 17]
$H^{[Oxy]}$	Hill coefficient for Oxytetracycline	2	-	[17]
$H^{[Cex]}$	Hill coefficient for Cefalexin	2	-	[17]

Table 2.B5:

Parameter	Parameter Name	Parameter Values	Units	Source
Discrete Farm Parameters				
T_{footbath}	Days on which metal footbaths are emptied into the main dairy shed scraper channels	$\{7, 14, 21, \ldots, 364\}$	days	Assumed
$T_{\text{extra foot.}}$	Days on which additional metal footbaths are emptied into the main dairy shed scraper channels	$\{21, 42, 63, \ldots, 357\}$	days	Assumed
$T_{\text{eff. flushing}}$	Days on which MHE is used to flush out the main dairy shed and bulling heifer shed scraper channels	$\{28, 56, 74, \ldots, 364\}$	days	Assumed
$T_{\text{Empty Tank}}$	Days on which the slurry tank is emptied	$\{50, 110, 170, \ldots, 350\}$	days	Assumed, [17]

Table 2.B6:

2.C Appendix: Horizontal Gene Transfer Equations

We define the horizontal transfer of resistance between bacterial populations by the function $\mathscr{H} : \Omega_i \to \mathbb{R}$ such that:

$$\begin{aligned}\mathscr{H}(S_i) = -\beta S_i \Bigg(& \frac{R_i^{[1,0,0,0]}}{S_i + R_i^{[1,0,0,0]}} + \frac{R_i^{[0,1,0,0]}}{S_i + R_i^{[0,1,0,0]}} + \frac{R_i^{[0,0,1,0]}}{S_i + R_i^{[0,0,1,0]}} + \frac{R_i^{[0,0,0,1]}}{S_i + R_i^{[0,0,0,1]}} + \\ & \frac{R_i^{[1,1,0,0]}}{S_i + R_i^{[1,1,0,0]}} + \frac{R_i^{[1,0,1,0]}}{S_i + R_i^{[1,0,1,0]}} + \frac{R_i^{[1,0,0,1]}}{S_i + R_i^{[1,0,0,1]}} + \frac{R_i^{[0,1,1,0]}}{S_i + R_i^{[0,1,1,0]}} + \\ & \frac{R_i^{[0,1,0,1]}}{S_i + R_i^{[0,1,0,1]}} + \frac{R_i^{[0,0,1,1]}}{S_i + R_i^{[0,0,1,1]}} + \frac{R_i^{[1,1,1,0]}}{S_i + R_i^{[1,1,1,0]}} + \frac{R_i^{[1,1,0,1]}}{S_i + R_i^{[1,1,0,1]}} + \\ & \frac{R_i^{[1,0,1,1]}}{S_i + R_i^{[1,0,1,1]}} + \frac{R_i^{[0,1,1,1]}}{S_i + R_i^{[0,1,1,1]}} + \frac{R_i^{[1,1,1,1]}}{S_i + R_i^{[1,1,1,1]}} \Bigg),\end{aligned} \tag{2.C25}$$

$$\begin{aligned}\mathscr{H}\left(R_i^{[1,0,0,0]}\right) = & \frac{\beta S_i R_i^{[1,0,0,0]}}{S_i + R_i^{[1,0,0,0]}} - \beta R_i^{[1,0,0,0]} \Bigg(\frac{R_i^{[0,1,0,0]}}{R_i^{[1,0,0,0]} + R_i^{[0,1,0,0]}} + \frac{R_i^{[0,0,1,0]}}{R_i^{[1,0,0,0]} + R_i^{[0,0,1,0]}} + \\ & \frac{R_i^{[0,0,0,1]}}{R_i^{[1,0,0,0]} + R_i^{[0,0,0,1]}} + \frac{R_i^{[1,1,0,0]}}{R_i^{[1,0,0,0]} + R_i^{[1,1,0,0]}} + \frac{R_i^{[1,0,1,0]}}{R_i^{[1,0,0,0]} + R_i^{[1,0,1,0]}} + \\ & \frac{R_i^{[1,0,0,1]}}{R_i^{[1,0,0,0]} + R_i^{[1,0,0,1]}} + \frac{R_i^{[0,1,1,0]}}{R_i^{[1,0,0,0]} + R_i^{[0,1,1,0]}} + \frac{R_i^{[0,1,0,1]}}{R_i^{[1,0,0,0]} + R_i^{[0,1,0,1]}} + \\ & \frac{R_i^{[0,0,1,1]}}{R_i^{[1,0,0,0]} + R_i^{[0,0,1,1]}} + \frac{R_i^{[1,1,1,0]}}{R_i^{[1,0,0,0]} + R_i^{[1,1,1,0]}} + \frac{R_i^{[1,1,0,1]}}{R_i^{[1,0,0,0]} + R_i^{[1,1,0,1]}} + \\ & \frac{R_i^{[1,0,1,1]}}{R_i^{[1,0,0,0]} + R_i^{[1,0,1,1]}} + \frac{R_i^{[0,1,1,1]}}{R_i^{[1,0,0,0]} + R_i^{[0,1,1,1]}} + \frac{R_i^{[1,1,1,1]}}{R_i^{[1,0,0,0]} + R_i^{[1,1,1,1]}} \Bigg),\end{aligned} \tag{2.C26}$$

$$\begin{aligned}\mathscr{H}\left(R_i^{[0,1,0,0]}\right) = & \frac{\beta S_i R_i^{[0,1,0,0]}}{S_i + R_i^{[0,1,0,0]}} - \beta R_i^{[0,1,0,0]} \Bigg(\frac{R_i^{[1,0,0,0]}}{R_i^{[0,1,0,0]} + R_i^{[1,0,0,0]}} + \frac{R_i^{[0,0,1,0]}}{R_i^{[0,1,0,0]} + R_i^{[0,0,1,0]}} + \\ & \frac{R_i^{[0,0,0,1]}}{R_i^{[0,1,0,0]} + R_i^{[0,0,0,1]}} + \frac{R_i^{[1,1,0,0]}}{R_i^{[0,1,0,0]} + R_i^{[1,1,0,0]}} + \frac{R_i^{[1,0,1,0]}}{R_i^{[0,1,0,0]} + R_i^{[1,0,1,0]}} + \\ & \frac{R_i^{[1,0,0,1]}}{R_i^{[0,1,0,0]} + R_i^{[1,0,0,1]}} + \frac{R_i^{[0,1,1,0]}}{R_i^{[0,1,0,0]} + R_i^{[0,1,1,0]}} + \frac{R_i^{[0,1,0,1]}}{R_i^{[0,1,0,0]} + R_i^{[0,1,0,1]}} + \\ & \frac{R_i^{[0,0,1,1]}}{R_i^{[0,1,0,0]} + R_i^{[0,0,1,1]}} + \frac{R_i^{[1,1,1,0]}}{R_i^{[0,1,0,0]} + R_i^{[1,1,1,0]}} + \frac{R_i^{[1,1,0,1]}}{R_i^{[0,1,0,0]} + R_i^{[1,1,0,1]}} + \\ & \frac{R_i^{[1,0,1,1]}}{R_i^{[0,1,0,0]} + R_i^{[1,0,1,1]}} + \frac{R_i^{[0,1,1,1]}}{R_i^{[0,1,0,0]} + R_i^{[0,1,1,1]}} + \frac{R_i^{[1,1,1,1]}}{R_i^{[0,1,0,0]} + R_i^{[1,1,1,1]}} \Bigg),\end{aligned} \tag{2.C27}$$

$$\mathscr{H}\left(R_i^{[0,0,1,0]}\right) = \frac{\beta S_i R_i^{[0,0,1,0]}}{S_i + R_i^{[0,0,1,0]}} - \beta R_i^{[0,0,1,0]} \left(\frac{R_i^{[1,0,0,0]}}{R_i^{[0,0,1,0]} + R_i^{[1,0,0,0]}} + \frac{R_i^{[0,1,0,0]}}{R_i^{[0,0,1,0]} + R_i^{[0,1,0,0]}} + \right.$$
$$\frac{R_i^{[0,0,0,1]}}{R_i^{[0,0,1,0]} + R_i^{[0,0,0,1]}} + \frac{R_i^{[1,1,0,0]}}{R_i^{[0,0,1,0]} + R_i^{[1,1,0,0]}} + \frac{R_i^{[1,0,1,0]}}{R_i^{[0,0,1,0]} + R_i^{[1,0,1,0]}} +$$
$$\frac{R_i^{[1,0,0,1]}}{R_i^{[0,0,1,0]} + R_i^{[1,0,0,1]}} + \frac{R_i^{[0,1,1,0]}}{R_i^{[0,0,1,0]} + R_i^{[0,1,1,0]}} + \frac{R_i^{[0,1,0,1]}}{R_i^{[0,0,1,0]} + R_i^{[0,1,0,1]}} +$$
$$\frac{R_i^{[0,0,1,1]}}{R_i^{[0,0,1,0]} + R_i^{[0,0,1,1]}} + \frac{R_i^{[1,1,1,0]}}{R_i^{[0,0,1,0]} + R_i^{[1,1,1,0]}} + \frac{R_i^{[1,1,0,1]}}{R_i^{[0,0,1,0]} + R_i^{[1,1,0,1]}} +$$
$$\left. \frac{R_i^{[1,0,1,1]}}{R_i^{[0,0,1,0]} + R_i^{[1,0,1,1]}} + \frac{R_i^{[0,1,1,1]}}{R_i^{[0,0,1,0]} + R_i^{[0,1,1,1]}} + \frac{R_i^{[1,1,1,1]}}{R_i^{[0,0,1,0]} + R_i^{[1,1,1,1]}} \right), \tag{2.C28}$$

$$\mathscr{H}\left(R_i^{[0,0,0,1]}\right) = \frac{\beta S_i R_i^{[0,0,0,1]}}{S_i + R_i^{[0,0,0,1]}} - \beta R_i^{[0,0,0,1]} \left(\frac{R_i^{[1,0,0,0]}}{R_i^{[0,0,0,1]} + R_i^{[1,0,0,0]}} + \frac{R_i^{[0,1,0,0]}}{R_i^{[0,0,0,1]} + R_i^{[0,1,0,0]}} + \right.$$
$$\frac{R_i^{[0,0,1,0]}}{R_i^{[0,0,0,1]} + R_i^{[0,0,1,0]}} + \frac{R_i^{[1,1,0,0]}}{R_i^{[0,0,0,1]} + R_i^{[1,1,0,0]}} + \frac{R_i^{[1,0,1,0]}}{R_i^{[0,0,0,1]} + R_i^{[1,0,1,0]}} +$$
$$\frac{R_i^{[1,0,0,1]}}{R_i^{[0,0,0,1]} + R_i^{[1,0,0,1]}} + \frac{R_i^{[0,1,1,0]}}{R_i^{[0,0,0,1]} + R_i^{[0,1,1,0]}} + \frac{R_i^{[0,1,0,1]}}{R_i^{[0,0,0,1]} + R_i^{[0,1,0,1]}} +$$
$$\frac{R_i^{[0,0,1,1]}}{R_i^{[0,0,0,1]} + R_i^{[0,0,1,1]}} + \frac{R_i^{[1,1,1,0]}}{R_i^{[0,0,0,1]} + R_i^{[1,1,1,0]}} + \frac{R_i^{[1,1,0,1]}}{R_i^{[0,0,0,1]} + R_i^{[1,1,0,1]}} +$$
$$\left. \frac{R_i^{[1,0,1,1]}}{R_i^{[0,0,0,1]} + R_i^{[1,0,1,1]}} + \frac{R_i^{[0,1,1,1]}}{R_i^{[0,0,0,1]} + R_i^{[0,1,1,1]}} + \frac{R_i^{[1,1,1,1]}}{R_i^{[0,0,0,1]} + R_i^{[1,1,1,1]}} \right), \tag{2.C29}$$

$$\mathscr{H}\left(R_i^{[1,1,0,0]}\right) = \beta R_i^{[1,1,0,0]} \left(\frac{S_i}{S_i + R_i^{[1,1,0,0]}} + \frac{R_i^{[1,0,0,0]}}{R_i^{[1,0,0,0]} + R_i^{[1,1,0,0]}} + \frac{R_i^{[0,1,0,0]}}{R_i^{[0,1,0,0]} + R_i^{[1,1,0,0]}} \right) +$$
$$2\frac{\beta R_i^{[1,0,0,0]} R_i^{[0,1,0,0]}}{R_i^{[1,0,0,0]} + R_i^{[0,1,0,0]}} - \beta R_i^{[1,1,0,0]} \left(\frac{R_i^{[0,0,1,0]}}{R_i^{[1,1,0,0]} + R_i^{[0,0,1,0]}} + \right.$$
$$\frac{R_i^{[0,0,0,1]}}{R_i^{[1,1,0,0]} + R_i^{[0,0,0,1]}} + \frac{R_i^{[1,0,1,0]}}{R_i^{[1,1,0,0]} + R_i^{[1,0,1,0]}} + \frac{R_i^{[1,0,0,1]}}{R_i^{[1,1,0,0]} + R_i^{[1,0,0,1]}} +$$
$$\frac{R_i^{[0,1,1,0]}}{R_i^{[1,1,0,0]} + R_i^{[0,1,1,0]}} + \frac{R_i^{[0,1,0,1]}}{R_i^{[1,1,0,0]} + R_i^{[0,1,0,1]}} + \frac{R_i^{[0,0,1,1]}}{R_i^{[1,1,0,0]} + R_i^{[0,0,1,1]}} +$$
$$\frac{R_i^{[1,1,1,0]}}{R_i^{[1,1,0,0]} + R_i^{[1,1,1,0]}} + \frac{R_i^{[1,1,0,1]}}{R_i^{[1,1,0,0]} + R_i^{[1,1,0,1]}} + \frac{R_i^{[1,0,1,1]}}{R_i^{[1,1,0,0]} + R_i^{[1,0,1,1]}} +$$
$$\left. \frac{R_i^{[0,1,1,1]}}{R_i^{[1,1,0,0]} + R_i^{[0,1,1,1]}} + \frac{R_i^{[1,1,1,1]}}{R_i^{[1,1,0,0]} + R_i^{[1,1,1,1]}} \right), \tag{2.C30}$$

$$\mathscr{H}\left(R_i^{[1,0,1,0]}\right) = \beta R_i^{[1,0,1,0]}\left(\frac{S_i}{S_i + R_i^{[1,0,1,0]}} + \frac{R_i^{[1,0,0,0]}}{R_i^{[1,0,0,0]} + R_i^{[1,0,1,0]}} + \frac{R_i^{[0,0,1,0]}}{R_i^{[0,0,1,0]} + R_i^{[1,0,1,0]}}\right) + 2\frac{\beta R_i^{[1,0,0,0]} R_i^{[0,0,1,0]}}{R_i^{[1,0,0,0]} + R_i^{[0,0,1,0]}} - \beta R_i^{[1,0,1,0]}\left(\frac{R_i^{[0,1,0,0]}}{R_i^{[1,0,1,0]} + R_i^{[0,1,0,0]}} + \frac{R_i^{[0,0,0,1]}}{R_i^{[1,0,1,0]} + R_i^{[0,0,0,1]}} + \frac{R_i^{[1,1,0,0]}}{R_i^{[1,0,1,0]} + R_i^{[1,1,0,0]}} + \frac{R_i^{[1,0,0,1]}}{R_i^{[1,0,1,0]} + R_i^{[1,0,0,1]}} + \frac{R_i^{[0,1,1,0]}}{R_i^{[1,0,1,0]} + R_i^{[0,1,1,0]}} + \frac{R_i^{[0,1,0,1]}}{R_i^{[1,0,1,0]} + R_i^{[0,1,0,1]}} + \frac{R_i^{[0,0,1,1]}}{R_i^{[1,0,1,0]} + R_i^{[0,0,1,1]}} + \frac{R_i^{[1,1,1,0]}}{R_i^{[1,0,1,0]} + R_i^{[1,1,1,0]}} + \frac{R_i^{[1,1,0,1]}}{R_i^{[1,0,1,0]} + R_i^{[1,1,0,1]}} + \frac{R_i^{[1,0,1,1]}}{R_i^{[1,0,1,0]} + R_i^{[1,0,1,1]}} + \frac{R_i^{[0,1,1,1]}}{R_i^{[1,0,1,0]} + R_i^{[0,1,1,1]}} + \frac{R_i^{[1,1,1,1]}}{R_i^{[1,0,1,0]} + R_i^{[1,1,1,1]}}\right), \tag{2.C31}$$

$$\mathscr{H}\left(R_i^{[1,0,0,1]}\right) = \beta R_i^{[1,0,0,1]}\left(\frac{S_i}{S_i + R_i^{[1,0,0,1]}} + \frac{R_i^{[1,0,0,0]}}{R_i^{[1,0,0,0]} + R_i^{[1,0,0,1]}} + \frac{R_i^{[0,0,0,1]}}{R_i^{[0,0,1,0]} + R_i^{[1,0,0,1]}}\right) + 2\frac{\beta R_i^{[1,0,0,0]} R_i^{[0,0,0,1]}}{R_i^{[1,0,0,0]} + R_i^{[0,0,0,1]}} - \beta R_i^{[1,0,0,1]}\left(\frac{R_i^{[0,1,0,0]}}{R_i^{[1,0,0,1]} + R_i^{[0,1,0,0]}} + \frac{R_i^{[0,0,1,0]}}{R_i^{[1,0,0,1]} + R_i^{[0,0,1,0]}} + \frac{R_i^{[1,1,0,0]}}{R_i^{[1,0,0,1]} + R_i^{[1,1,0,0]}} + \frac{R_i^{[1,0,1,0]}}{R_i^{[1,0,0,1]} + R_i^{[1,0,1,0]}} + \frac{R_i^{[0,1,1,0]}}{R_i^{[1,0,0,1]} + R_i^{[0,1,1,0]}} + \frac{R_i^{[0,1,0,1]}}{R_i^{[1,0,0,1]} + R_i^{[0,1,0,1]}} + \frac{R_i^{[0,0,1,1]}}{R_i^{[1,0,0,1]} + R_i^{[0,0,1,1]}} + \frac{R_i^{[1,1,1,0]}}{R_i^{[1,0,0,1]} + R_i^{[1,1,1,0]}} + \frac{R_i^{[1,1,0,1]}}{R_i^{[1,0,0,1]} + R_i^{[1,1,0,1]}} + \frac{R_i^{[1,0,1,1]}}{R_i^{[1,0,0,1]} + R_i^{[1,0,1,1]}} + \frac{R_i^{[0,1,1,1]}}{R_i^{[1,0,0,1]} + R_i^{[0,1,1,1]}} + \frac{R_i^{[1,1,1,1]}}{R_i^{[1,0,0,1]} + R_i^{[1,1,1,1]}}\right), \tag{2.C32}$$

$$\mathscr{H}\left(R_i^{[0,1,1,0]}\right) = \beta R_i^{[0,1,1,0]}\left(\frac{S_i}{S_i+R_i^{[0,1,1,0]}}+\frac{R_i^{[0,1,0,0]}}{R_i^{[0,1,0,0]}+R_i^{[0,1,1,0]}}+\frac{R_i^{[0,0,1,0]}}{R_i^{[0,0,1,0]}+R_i^{[0,1,1,0]}}\right)+$$
$$2\frac{\beta R_i^{[0,1,0,0]}R_i^{[0,0,1,0]}}{R_i^{[0,1,0,0]}+R_i^{[0,0,1,0]}}-\beta R_i^{[0,1,1,0]}\left(\frac{R_i^{[1,0,0,0]}}{R_i^{[0,1,1,0]}+R_i^{[1,0,0,0]}}+\right.$$
$$\frac{R_i^{[0,0,0,1]}}{R_i^{[0,1,1,0]}+R_i^{[0,0,0,1]}}+\frac{R_i^{[1,1,0,0]}}{R_i^{[0,1,1,0]}+R_i^{[1,1,0,0]}}+\frac{R_i^{[1,0,1,0]}}{R_i^{[0,1,1,0]}+R_i^{[1,0,1,0]}}+$$
$$\frac{R_i^{[1,0,0,1]}}{R_i^{[0,1,1,0]}+R_i^{[1,0,0,1]}}+\frac{R_i^{[0,1,0,1]}}{R_i^{[0,1,1,0]}+R_i^{[0,1,0,1]}}+\frac{R_i^{[0,0,1,1]}}{R_i^{[0,1,1,0]}+R_i^{[0,0,1,1]}}+$$
$$\frac{R_i^{[1,1,1,0]}}{R_i^{[0,1,1,0]}+R_i^{[1,1,1,0]}}+\frac{R_i^{[1,1,0,1]}}{R_i^{[0,1,1,0]}+R_i^{[1,1,0,1]}}+\frac{R_i^{[1,0,1,1]}}{R_i^{[0,1,1,0]}+R_i^{[1,0,1,1]}}+$$
$$\left.\frac{R_i^{[0,1,1,1]}}{R_i^{[0,1,1,0]}+R_i^{[0,1,1,1]}}+\frac{R_i^{[1,1,1,1]}}{R_i^{[0,1,1,0]}+R_i^{[1,1,1,1]}}\right), \tag{2.C33}$$

$$\mathscr{H}\left(R_i^{[0,1,0,1]}\right) = \beta R_i^{[0,1,0,1]}\left(\frac{S_i}{S_i+R_i^{[0,1,0,1]}}+\frac{R_i^{[0,1,0,0]}}{R_i^{[0,1,0,0]}+R_i^{[0,1,0,1]}}+\frac{R_i^{[0,0,0,1]}}{R_i^{[0,0,1,0]}+R_i^{[0,1,0,1]}}\right)+$$
$$2\frac{\beta R_i^{[0,1,0,0]}R_i^{[0,0,0,1]}}{R_i^{[0,1,0,0]}+R_i^{[0,0,0,1]}}-\beta R_i^{[0,1,0,1]}\left(\frac{R_i^{[1,0,0,0]}}{R_i^{[0,1,0,1]}+R_i^{[1,0,0,0]}}+\right.$$
$$\frac{R_i^{[0,0,1,0]}}{R_i^{[0,1,0,1]}+R_i^{[0,0,1,0]}}+\frac{R_i^{[1,1,0,0]}}{R_i^{[0,1,0,1]}+R_i^{[1,1,0,0]}}+\frac{R_i^{[1,0,1,0]}}{R_i^{[0,1,0,1]}+R_i^{[1,0,1,0]}}+$$
$$\frac{R_i^{[1,0,0,1]}}{R_i^{[0,1,0,1]}+R_i^{[1,0,0,1]}}+\frac{R_i^{[0,1,1,0]}}{R_i^{[0,1,0,1]}+R_i^{[0,1,1,0]}}+\frac{R_i^{[0,0,1,1]}}{R_i^{[0,1,0,1]}+R_i^{[0,0,1,1]}}+$$
$$\frac{R_i^{[1,1,1,0]}}{R_i^{[0,1,0,1]}+R_i^{[1,1,1,0]}}+\frac{R_i^{[1,1,0,1]}}{R_i^{[0,1,0,1]}+R_i^{[1,1,0,1]}}+\frac{R_i^{[1,0,1,1]}}{R_i^{[0,1,0,1]}+R_i^{[1,0,1,1]}}+$$
$$\left.\frac{R_i^{[0,1,1,1]}}{R_i^{[0,1,0,1]}+R_i^{[0,1,1,1]}}+\frac{R_i^{[1,1,1,1]}}{R_i^{[0,1,0,1]}+R_i^{[1,1,1,1]}}\right), \tag{2.C34}$$

$$
\begin{aligned}
\mathscr{H}\left(R_i^{[0,0,1,1]}\right) = \beta R_i^{[0,0,1,1]} \Bigg(& \frac{S_i}{S_i + R_i^{[0,0,1,1]}} + \frac{R_i^{[0,0,1,0]}}{R_i^{[0,0,1,0]} + R_i^{[0,0,1,1]}} + \frac{R_i^{[0,0,0,1]}}{R_i^{[0,0,1,0]} + R_i^{[0,0,1,1]}} \Bigg) + \\
& 2\frac{\beta R_i^{[0,0,1,0]} R_i^{[0,0,0,1]}}{R_i^{[0,0,1,0]} + R_i^{[0,0,0,1]}} - \beta R_i^{[0,0,1,1]} \Bigg(\frac{R_i^{[1,0,0,0]}}{R_i^{[0,0,1,1]} + R_i^{[1,0,0,0]}} + \\
& \frac{R_i^{[0,1,0,0]}}{R_i^{[0,0,1,1]} + R_i^{[0,1,0,0]}} + \frac{R_i^{[1,1,0,0]}}{R_i^{[0,0,1,1]} + R_i^{[1,1,0,0]}} + \frac{R_i^{[1,0,1,0]}}{R_i^{[0,0,1,1]} + R_i^{[1,0,1,0]}} + \\
& \frac{R_i^{[1,0,0,1]}}{R_i^{[0,0,1,1]} + R_i^{[1,0,0,1]}} + \frac{R_i^{[0,1,1,0]}}{R_i^{[0,0,1,1]} + R_i^{[0,1,1,0]}} + \frac{R_i^{[0,1,0,1]}}{R_i^{[0,0,1,1]} + R_i^{[0,1,0,1]}} + \\
& \frac{R_i^{[1,1,1,0]}}{R_i^{[0,0,1,1]} + R_i^{[1,1,1,0]}} + \frac{R_i^{[1,1,0,1]}}{R_i^{[0,0,1,1]} + R_i^{[1,1,0,1]}} + \frac{R_i^{[1,0,1,1]}}{R_i^{[0,0,1,1]} + R_i^{[1,0,1,1]}} + \\
& \frac{R_i^{[0,1,1,1]}}{R_i^{[0,0,1,1]} + R_i^{[0,1,1,1]}} + \frac{R_i^{[1,1,1,1]}}{R_i^{[0,0,1,1]} + R_i^{[1,1,1,1]}} \Bigg),
\end{aligned}
\tag{2.C35}
$$

$$
\begin{aligned}
\mathscr{H}\left(R_i^{[1,1,1,0]}\right) = \beta R_i^{[1,1,1,0]} \Bigg(& \frac{S_i}{S_i + R_i^{[1,1,1,0]}} + \frac{R_i^{[1,0,0,0]}}{R_i^{[1,0,0,0]} + R_i^{[1,1,1,0]}} + \frac{R_i^{[0,1,0,0]}}{R_i^{[0,1,0,0]} + R_i^{[1,1,1,0]}} + \\
& \frac{R_i^{[0,0,1,0]}}{R_i^{[0,0,1,0]} + R_i^{[1,1,1,0]}} + \frac{R_i^{[1,1,0,0]}}{R_i^{[1,1,0,0]} + R_i^{[1,1,1,0]}} + \frac{R_i^{[1,0,1,0]}}{R_i^{[1,0,1,0]} + R_i^{[1,1,1,0]}} + \\
& \frac{R_i^{[0,1,1,0]}}{R_i^{[0,1,1,0]} + R_i^{[1,1,1,0]}} \Bigg) + \\
& \beta R_i^{[1,1,0,0]} \Bigg(\frac{R_i^{[0,0,1,0]}}{R_i^{[0,0,1,0]} + R_i^{[1,1,0,0]}} + \frac{R_i^{[1,0,1,0]}}{R_i^{[1,0,1,0]} + R_i^{[1,1,0,0]}} + \frac{R_i^{[0,1,1,0]}}{R_i^{[1,0,1,0]} + R_i^{[1,1,0,0]}} \Bigg) + \\
& \beta R_i^{[1,0,1,0]} \Bigg(\frac{R_i^{[0,1,0,0]}}{R_i^{[0,1,0,0]} + R_i^{[1,0,1,0]}} + \frac{R_i^{[1,1,0,0]}}{R_i^{[1,1,0,0]} + R_i^{[1,0,1,0]}} + \frac{R_i^{[0,1,1,0]}}{R_i^{[0,1,1,0]} + R_i^{[1,0,1,0]}} \Bigg) + \\
& \beta R_i^{[0,1,1,0]} \Bigg(\frac{R_i^{[1,0,0,0]}}{R_i^{[1,0,0,0]} + R_i^{[0,1,1,0]}} + \frac{R_i^{[1,1,0,0]}}{R_i^{[1,1,0,0]} + R_i^{[0,1,1,0]}} + \frac{R_i^{[1,0,1,0]}}{R_i^{[1,0,1,0]} + R_i^{[0,1,1,0]}} \Bigg) + \\
& \frac{\beta R_i^{[1,0,0,0]} R_i^{[0,1,1,0]}}{R_i^{[1,0,0,0]} + R_i^{[0,1,1,0]}} + \frac{\beta R_i^{[0,1,0,0]} R_i^{[1,0,1,0]}}{R_i^{[0,1,0,0]} + R_i^{[1,0,1,0]}} + \frac{\beta R_i^{[0,0,1,0]} R_i^{[1,1,0,0]}}{R_i^{[0,0,1,0]} + R_i^{[1,1,0,0]}} - \\
& \beta R_i^{[1,1,1,0]} \Bigg(\frac{R_i^{[0,0,0,1]}}{R_i^{[0,0,0,1]} + R_i^{[1,1,1,0]}} + \frac{R_i^{[1,0,0,1]}}{R_i^{[1,0,0,1]} + R_i^{[1,1,1,0]}} + \frac{R_i^{[0,1,0,1]}}{R_i^{[0,1,0,1]} + R_i^{[1,1,1,0]}} + \\
& \frac{R_i^{[0,0,1,1]}}{R_i^{[0,0,1,1]} + R_i^{[1,1,1,0]}} + \frac{R_i^{[1,1,0,1]}}{R_i^{[1,1,0,1]} + R_i^{[1,1,1,0]}} + \frac{R_i^{[1,0,1,1]}}{R_i^{[1,0,1,1]} + R_i^{[1,1,1,0]}} + \\
& \frac{R_i^{[0,1,1,1]}}{R_i^{[0,1,1,1]} + R_i^{[1,1,1,0]}} + \frac{R_i^{[1,1,1,1]}}{R_i^{[1,1,1,1]} + R_i^{[1,1,1,0]}} \Bigg),
\end{aligned}
\tag{2.C36}
$$

$$\mathscr{H}\left(R_i^{[1,1,0,1]}\right) = \beta R_i^{[1,1,0,1]}\left(\frac{S_i}{S_i+R_i^{[1,1,0,1]}}+\frac{R_i^{[1,0,0,0]}}{R_i^{[1,0,0,0]}+R_i^{[1,1,0,1]}}+\frac{R_i^{[0,1,0,0]}}{R_i^{[0,1,0,0]}+R_i^{[1,1,0,1]}}+\right.$$
$$\frac{R_i^{[0,0,0,1]}}{R_i^{[0,0,0,1]}+R_i^{[1,1,0,1]}}+\frac{R_i^{[1,1,0,0]}}{R_i^{[1,1,0,0]}+R_i^{[1,1,0,1]}}+\frac{R_i^{[1,0,0,1]}}{R_i^{[1,0,0,1]}+R_i^{[1,1,0,1]}}+$$
$$\left.\frac{R_i^{[0,1,0,1]}}{R_i^{[0,1,0,1]}+R_i^{[1,1,0,1]}}\right)+$$
$$\beta R_i^{[1,1,0,0]}\left(\frac{R_i^{[0,0,0,1]}}{R_i^{[0,0,0,1]}+R_i^{[1,1,0,0]}}+\frac{R_i^{[1,0,0,1]}}{R_i^{[1,0,0,1]}+R_i^{[1,1,0,0]}}+\frac{R_i^{[0,1,0,1]}}{R_i^{[0,1,0,1]}+R_i^{[1,1,0,0]}}\right)+$$
$$\beta R_i^{[1,0,0,1]}\left(\frac{R_i^{[0,1,0,0]}}{R_i^{[0,1,0,0]}+R_i^{[1,0,0,1]}}+\frac{R_i^{[1,1,0,0]}}{R_i^{[1,1,0,0]}+R_i^{[1,0,0,1]}}+\frac{R_i^{[0,1,0,1]}}{R_i^{[0,1,0,1]}+R_i^{[1,0,0,1]}}\right)+$$
$$\beta R_i^{[0,1,0,1]}\left(\frac{R_i^{[1,0,0,0]}}{R_i^{[1,0,0,0]}+R_i^{[0,1,0,1]}}+\frac{R_i^{[1,1,0,0]}}{R_i^{[1,1,0,0]}+R_i^{[0,1,0,1]}}+\frac{R_i^{[1,0,0,1]}}{R_i^{[1,0,0,1]}+R_i^{[0,1,0,1]}}\right)+$$
$$\frac{\beta R_i^{[1,0,0,0]}R_i^{[0,1,0,1]}}{R_i^{[1,0,0,0]}+R_i^{[0,1,0,1]}}+\frac{\beta R_i^{[0,1,0,0]}R_i^{[1,0,0,1]}}{R_i^{[0,1,0,0]}+R_i^{[1,0,0,1]}}+\frac{\beta R_i^{[0,0,0,1]}R_i^{[1,1,0,0]}}{R_i^{[0,0,0,1]}+R_i^{[1,1,0,0]}}-$$
$$\beta R_i^{[1,1,0,1]}\left(\frac{R_i^{[0,0,1,0]}}{R_i^{[0,0,1,0]}+R_i^{[1,1,0,1]}}+\frac{R_i^{[1,0,1,0]}}{R_i^{[1,0,1,0]}+R_i^{[1,1,0,1]}}+\frac{R_i^{[0,1,1,0]}}{R_i^{[0,1,1,0]}+R_i^{[1,1,0,1]}}+\right.$$
$$\frac{R_i^{[0,0,1,1]}}{R_i^{[0,0,1,1]}+R_i^{[1,1,0,1]}}+\frac{R_i^{[1,1,1,0]}}{R_i^{[1,1,1,0]}+R_i^{[1,1,0,1]}}+\frac{R_i^{[1,0,1,1]}}{R_i^{[1,0,1,1]}+R_i^{[1,1,0,1]}}+$$
$$\left.\frac{R_i^{[0,1,1,1]}}{R_i^{[0,1,1,1]}+R_i^{[1,1,0,1]}}+\frac{R_i^{[1,1,1,1]}}{R_i^{[1,1,1,1]}+R_i^{[1,1,0,1]}}\right), \tag{2.C37}$$

$$\mathscr{H}\left(R_i^{[1,0,1,1]}\right) = \beta R_i^{[1,0,1,1]}\left(\frac{S_i}{S_i+R_i^{[1,0,1,1]}}+\frac{R_i^{[1,0,0,0]}}{R_i^{[1,0,0,0]}+R_i^{[1,0,1,1]}}+\frac{R_i^{[0,0,1,0]}}{R_i^{[0,0,1,0]}+R_i^{[1,0,1,1]}}+\right.$$
$$\frac{R_i^{[0,0,0,1]}}{R_i^{[0,0,0,1]}+R_i^{[1,0,1,1]}}+\frac{R_i^{[1,0,1,0]}}{R_i^{[1,0,1,0]}+R_i^{[1,0,1,1]}}+\frac{R_i^{[1,0,0,1]}}{R_i^{[1,0,0,1]}+R_i^{[1,0,1,1]}}+$$
$$\left.\frac{R_i^{[0,0,1,1]}}{R_i^{[0,0,1,1]}+R_i^{[1,0,1,1]}}\right)+$$
$$\beta R_i^{[1,0,1,0]}\left(\frac{R_i^{[0,0,0,1]}}{R_i^{[0,0,0,1]}+R_i^{[1,0,1,0]}}+\frac{R_i^{[1,0,0,1]}}{R_i^{[1,0,0,1]}+R_i^{[1,0,1,0]}}+\frac{R_i^{[0,0,1,1]}}{R_i^{[0,0,1,1]}+R_i^{[1,0,1,0]}}\right)+$$
$$\beta R_i^{[1,0,0,1]}\left(\frac{R_i^{[0,0,1,0]}}{R_i^{[0,0,1,0]}+R_i^{[1,0,0,1]}}+\frac{R_i^{[1,0,1,0]}}{R_i^{[1,0,1,0]}+R_i^{[1,0,0,1]}}+\frac{R_i^{[0,0,1,1]}}{R_i^{[0,0,1,1]}+R_i^{[1,0,0,1]}}\right)+$$
$$\beta R_i^{[0,0,1,1]}\left(\frac{R_i^{[1,0,0,0]}}{R_i^{[1,0,0,0]}+R_i^{[0,0,1,1]}}+\frac{R_i^{[1,0,1,0]}}{R_i^{[1,0,1,0]}+R_i^{[0,0,1,1]}}+\frac{R_i^{[1,0,0,1]}}{R_i^{[1,0,0,1]}+R_i^{[0,0,1,1]}}\right)+$$
$$\frac{\beta R_i^{[1,0,0,0]}R_i^{[0,0,1,1]}}{R_i^{[1,0,0,0]}+R_i^{[0,0,1,1]}}+\frac{\beta R_i^{[0,0,1,0]}R_i^{[1,0,0,1]}}{R_i^{[0,0,1,0]}+R_i^{[1,0,0,1]}}+\frac{\beta R_i^{[0,0,0,1]}R_i^{[1,0,1,0]}}{R_i^{[0,0,0,1]}+R_i^{[1,0,1,0]}}-$$
$$\beta R_i^{[1,0,1,1]}\left(\frac{R_i^{[0,1,0,0]}}{R_i^{[0,1,0,0]}+R_i^{[1,0,1,1]}}+\frac{R_i^{[1,1,0,0]}}{R_i^{[1,1,0,0]}+R_i^{[1,0,1,1]}}+\frac{R_i^{[0,1,1,0]}}{R_i^{[0,1,1,0]}+R_i^{[1,0,1,1]}}+\right.$$
$$\frac{R_i^{[0,1,0,1]}}{R_i^{[0,1,0,1]}+R_i^{[1,0,1,1]}}+\frac{R_i^{[1,1,1,0]}}{R_i^{[1,1,1,0]}+R_i^{[1,0,1,1]}}+\frac{R_i^{[1,1,0,1]}}{R_i^{[1,1,0,1]}+R_i^{[1,0,1,1]}}+$$
$$\left.\frac{R_i^{[0,1,1,1]}}{R_i^{[0,1,1,1]}+R_i^{[1,0,1,1]}}+\frac{R_i^{[1,1,1,1]}}{R_i^{[1,1,1,1]}+R_i^{[1,0,1,1]}}\right), \tag{2.C38}$$

$$\mathscr{H}\left(R_i^{[0,1,1,1]}\right) = \beta R_i^{[0,1,1,1]}\left(\frac{S_i}{S_i+R_i^{[0,1,1,1]}}+\frac{R_i^{[0,1,0,0]}}{R_i^{[0,1,0,0]}+R_i^{[0,1,1,1]}}+\frac{R_i^{[0,0,1,0]}}{R_i^{[0,0,1,0]}+R_i^{[0,1,1,1]}}+\right.$$
$$\frac{R_i^{[0,0,0,1]}}{R_i^{[0,0,0,1]}+R_i^{[0,1,1,1]}}+\frac{R_i^{[0,1,1,0]}}{R_i^{[0,1,1,0]}+R_i^{[0,1,1,1]}}+\frac{R_i^{[0,1,0,1]}}{R_i^{[0,1,0,1]}+R_i^{[0,1,1,1]}}+$$
$$\left.\frac{R_i^{[0,0,1,1]}}{R_i^{[0,0,1,1]}+R_i^{[0,1,1,1]}}\right)+$$
$$\beta R_i^{[0,1,1,0]}\left(\frac{R_i^{[0,0,0,1]}}{R_i^{[0,0,0,1]}+R_i^{[0,1,1,0]}}+\frac{R_i^{[0,1,0,1]}}{R_i^{[0,1,0,1]}+R_i^{[0,1,1,0]}}+\frac{R_i^{[0,0,1,1]}}{R_i^{[0,0,1,1]}+R_i^{[0,1,1,0]}}\right)+$$
$$\beta R_i^{[0,1,0,1]}\left(\frac{R_i^{[0,0,1,0]}}{R_i^{[0,0,1,0]}+R_i^{[0,1,0,1]}}+\frac{R_i^{[0,1,1,0]}}{R_i^{[0,1,1,0]}+R_i^{[0,1,0,1]}}+\frac{R_i^{[0,0,1,1]}}{R_i^{[0,0,1,1]}+R_i^{[0,1,0,1]}}\right)+$$
$$\beta R_i^{[0,0,1,1]}\left(\frac{R_i^{[0,1,0,0]}}{R_i^{[0,1,0,0]}+R_i^{[0,0,1,1]}}+\frac{R_i^{[0,1,1,0]}}{R_i^{[0,1,1,0]}+R_i^{[0,0,1,1]}}+\frac{R_i^{[0,1,0,1]}}{R_i^{[0,1,0,1]}+R_i^{[0,0,1,1]}}\right)+$$
$$\frac{\beta R_i^{[0,1,0,0]}R_i^{[0,0,1,1]}}{R_i^{[0,1,0,0]}+R_i^{[0,0,1,1]}}+\frac{\beta R_i^{[0,0,1,0]}R_i^{[0,1,0,1]}}{R_i^{[0,0,1,0]}+R_i^{[0,1,0,1]}}+\frac{\beta R_i^{[0,0,0,1]}R_i^{[0,1,1,0]}}{R_i^{[0,0,0,1]}+R_i^{[0,1,1,0]}}-$$
$$\beta R_i^{[0,1,1,1]}\left(\frac{R_i^{[1,0,0,0]}}{R_i^{[1,0,0,0]}+R_i^{[0,1,1,1]}}+\frac{R_i^{[1,1,0,0]}}{R_i^{[1,1,0,0]}+R_i^{[0,1,1,1]}}+\frac{R_i^{[1,0,1,0]}}{R_i^{[1,0,1,0]}+R_i^{[0,1,1,1]}}+\right.$$
$$\frac{R_i^{[1,0,0,1]}}{R_i^{[1,0,0,1]}+R_i^{[0,1,1,1]}}+\frac{R_i^{[1,1,1,0]}}{R_i^{[1,1,1,0]}+R_i^{[0,1,1,1]}}+\frac{R_i^{[1,1,0,1]}}{R_i^{[1,1,0,1]}+R_i^{[0,1,1,1]}}+$$
$$\left.\frac{R_i^{[1,0,1,1]}}{R_i^{[1,0,1,1]}+R_i^{[0,1,1,1]}}+\frac{R_i^{[1,1,1,1]}}{R_i^{[1,1,1,1]}+R_i^{[0,1,1,1]}}\right), \tag{2.C39}$$

$$
\begin{aligned}
&\mathscr{H}\left(R_i^{[1,1,1,1]}\right) = \\
&\frac{\beta S_i R_i^{[1,1,1,1]}}{S_i + R_i^{[1,1,1,1]}} + \beta R_i^{[1,0,0,0]}\left(\frac{R_i^{[1,1,1,1]}}{R_i^{[1,0,0,0]} + R_i^{[1,1,1,1]}} + \frac{R_i^{[0,1,1,1]}}{R_i^{[1,0,0,0]} + R_i^{[0,1,1,1]}}\right) + \\
&\beta R_i^{[0,1,0,0]}\left(\frac{R_i^{[1,1,1,1]}}{R_i^{[0,1,0,0]} + R_i^{[1,1,1,1]}} + \frac{R_i^{[1,0,1,1]}}{R_i^{[0,1,0,0]} + R_i^{[1,0,1,1]}}\right) + \\
&\beta R_i^{[0,0,1,0]}\left(\frac{R_i^{[1,1,1,1]}}{R_i^{[0,0,1,0]} + R_i^{[1,1,1,1]}} + \frac{R_i^{[1,1,0,1]}}{R_i^{[0,0,1,0]} + R_i^{[1,1,0,1]}}\right) + \\
&\beta R_i^{[0,0,0,1]}\left(\frac{R_i^{[1,1,1,1]}}{R_i^{[0,0,0,1]} + R_i^{[1,1,1,1]}} + \frac{R_i^{[1,1,1,0]}}{R_i^{[0,0,0,1]} + R_i^{[1,1,1,0]}}\right) + \beta R_i^{[1,1,0,0]}\left(\frac{R_i^{[1,1,1,1]}}{R_i^{[1,1,0,0]} + R_i^{[1,1,1,1]}} + \right. \\
&\left.\frac{R_i^{[1,0,1,1]}}{R_i^{[1,1,0,0]} + R_i^{[1,0,1,1]}} + \frac{R_i^{[0,1,1,1]}}{R_i^{[1,1,0,0]} + R_i^{[0,1,1,1]}} + \frac{R_i^{[0,0,1,1]}}{R_i^{[1,1,0,0]} + R_i^{[0,0,1,1]}}\right) + \beta R_i^{[1,0,1,0]}\left(\frac{R_i^{[1,1,1,1]}}{R_i^{[1,0,1,0]} + R_i^{[1,1,1,1]}} + \right. \\
&\left.\frac{R_i^{[1,1,0,1]}}{R_i^{[1,0,1,0]} + R_i^{[1,1,0,1]}} + \frac{R_i^{[0,1,1,1]}}{R_i^{[1,0,1,0]} + R_i^{[0,1,1,1]}} + \frac{R_i^{[0,1,0,1]}}{R_i^{[1,0,1,0]} + R_i^{[0,1,0,1]}}\right) + \beta R_i^{[1,0,0,1]}\left(\frac{R_i^{[1,1,1,1]}}{R_i^{[1,0,0,1]} + R_i^{[1,1,1,1]}} + \right. \\
&\left.\frac{R_i^{[1,1,1,0]}}{R_i^{[1,0,0,1]} + R_i^{[1,1,1,0]}} + \frac{R_i^{[0,1,1,1]}}{R_i^{[1,0,0,1]} + R_i^{[0,1,1,1]}} + \frac{R_i^{[0,1,1,0]}}{R_i^{[1,0,0,1]} + R_i^{[0,1,1,0]}}\right) + \beta R_i^{[0,1,1,0]}\left(\frac{R_i^{[1,1,1,1]}}{R_i^{[0,1,1,0]} + R_i^{[1,1,1,1]}} + \right. \\
&\left.\frac{R_i^{[1,1,0,1]}}{R_i^{[0,1,1,0]} + R_i^{[1,1,0,1]}} + \frac{R_i^{[1,0,1,1]}}{R_i^{[0,1,1,0]} + R_i^{[1,0,1,1]}} + \frac{R_i^{[1,00,1]}}{R_i^{[0,1,1,0]} + R_i^{[1,0,0,1]}}\right) + \beta R_i^{[0,1,0,1]}\left(\frac{R_i^{[1,1,1,1]}}{R_i^{[0,1,0,1]} + R_i^{[1,1,1,1]}} + \right. \\
&\left.\frac{R_i^{[1,1,1,0]}}{R_i^{[0,1,0,1]} + R_i^{[1,1,1,0]}} + \frac{R_i^{[1,0,1,1]}}{R_i^{[0,1,0,1]} + R_i^{[1,0,1,1]}} + \frac{R_i^{[1,0,1,0]}}{R_i^{[0,1,0,1]} + R_i^{[1,0,1,0]}}\right) + \beta R_i^{[0,0,1,1]}\left(\frac{R_i^{[1,1,1,1]}}{R_i^{[0,0,1,1]} + R_i^{[1,1,1,1]}} + \right. \\
&\left.\frac{R_i^{[1,1,1,0]}}{R_i^{[0,0,1,1]} + R_i^{[1,1,1,0]}} + \frac{R_i^{[1,1,0,1]}}{R_i^{[0,0,1,1]} + R_i^{[1,1,0,1]}} + \frac{R_i^{[1,1,0,0]}}{R_i^{[0,0,1,1]} + R_i^{[1,1,0,0]}}\right) + \beta R_i^{[1,1,1,0]}\left(\frac{R_i^{[1,1,1,1]}}{R_i^{[1,1,1,0]} + R_i^{[1,1,1,1]}} + \right. \\
&\left.\frac{R_i^{[1,1,0,1]}}{R_i^{[1,1,1,0]} + R_i^{[1,1,0,1]}} + \frac{R_i^{[1,0,1,1]}}{R_i^{[1,1,1,0]} + R_i^{[1,0,1,1]}} + \frac{R_i^{[0,1,1,1]}}{R_i^{[1,1,1,0]} + R_i^{[0,1,1,1]}} + \frac{R_i^{[1,0,0,1]}}{R_i^{[1,1,1,0]} + R_i^{[1,0,0,1]}} + \right. \\
&\left.\frac{R_i^{[0,1,0,1]}}{R_i^{[1,1,1,0]} + R_i^{[0,1,0,1]}} + \frac{R_i^{[0,0,1,1]}}{R_i^{[1,1,1,0]} + R_i^{[0,0,1,1]}} + \frac{R_i^{[0,0,0,1]}}{R_i^{[1,1,1,0]} + R_i^{[0,0,0,1]}}\right) + \beta R_i^{[1,1,0,1]}\left(\frac{R_i^{[1,1,1,1]}}{R_i^{[1,1,0,1]} + R_i^{[1,1,1,1]}} + \right. \\
&\left.\frac{R_i^{[1,1,1,0]}}{R_i^{[1,1,0,1]} + R_i^{[1,1,1,0]}} + \frac{R_i^{[1,0,1,1]}}{R_i^{[1,1,0,1]} + R_i^{[1,0,1,1]}} + \frac{R_i^{[0,1,1,1]}}{R_i^{[1,1,0,1]} + R_i^{[0,1,1,1]}} + \frac{R_i^{[1,0,1,0]}}{R_i^{[1,1,0,1]} + R_i^{[1,0,1,0]}} + \right. \\
&\left.\frac{R_i^{[0,1,1,0]}}{R_i^{[1,1,0,1]} + R_i^{[0,1,1,0]}} + \frac{R_i^{[0,0,1,1]}}{R_i^{[1,1,0,1]} + R_i^{[0,0,1,1]}} + \frac{R_i^{[0,0,1,0]}}{R_i^{[1,1,0,1]} + R_i^{[0,0,1,0]}}\right) + \beta R_i^{[1,0,1,1]}\left(\frac{R_i^{[1,1,1,1]}}{R_i^{[1,0,1,1]} + R_i^{[1,1,1,1]}} + \right. \\
&\left.\frac{R_i^{[1,1,1,0]}}{R_i^{[1,0,1,1]} + R_i^{[1,1,1,0]}} + \frac{R_i^{[1,1,0,1]}}{R_i^{[1,0,1,1]} + R_i^{[1,1,0,1]}} + \frac{R_i^{[0,1,1,1]}}{R_i^{[1,0,1,1]} + R_i^{[0,1,1,1]}} + \frac{R_i^{[1,1,0,0]}}{R_i^{[1,0,1,1]} + R_i^{[1,1,0,0]}} + \right. \\
&\left.\frac{R_i^{[0,1,1,0]}}{R_i^{[1,0,1,1]} + R_i^{[0,1,1,0]}} + \frac{R_i^{[0,1,0,1]}}{R_i^{[1,0,1,1]} + R_i^{[0,1,0,1]}} + \frac{R_i^{[0,1,0,0]}}{R_i^{[1,0,1,1]} + R_i^{[0,1,0,0]}}\right) + \beta R_i^{[0,1,1,1]}\left(\frac{R_i^{[1,1,1,1]}}{R_i^{[0,1,1,1]} + R_i^{[1,1,1,1]}} + \right. \\
&\left.\frac{R_i^{[1,1,1,0]}}{R_i^{[0,1,1,1]} + R_i^{[1,1,1,0]}} + \frac{R_i^{[1,1,0,1]}}{R_i^{[0,1,1,1]} + R_i^{[1,1,0,1]}} + \frac{R_i^{[1,0,1,1]}}{R_i^{[0,1,1,1]} + R_i^{[1,0,1,1]}} + \frac{R_i^{[1,1,0,0]}}{R_i^{[0,1,1,1]} + R_i^{[1,1,0,0]}} + \right. \\
&\left.\frac{R_i^{[1,0,1,0]}}{R_i^{[0,1,1,1]} + R_i^{[1,0,1,0]}} + \frac{R_i^{[1,0,0,1]}}{R_i^{[0,1,1,1]} + R_i^{[1,0,0,1]}} + \frac{R_i^{[1,0,0,0]}}{R_i^{[0,1,1,1]} + R_i^{[1,0,0,0]}}\right).
\end{aligned}
\tag{2.C40}
$$

References

[1] Raymond Ruimy, Anne Brisabois, Claire Bernede, David Skurnik, Saïda Barnat, Guillaume Arlet, Sonia Momcilovic, Sandrine Elbaz, Frédérique Moury, Marie-Anne Vibet, Patrice Courvalin, Didier Guillemot, and Antoine Andremont. Organic and conventional fruits and vegetables contain equivalent counts of gram-negative bacteria expressing resistance to antibacterial agents. *Environmental Microbiology*, 12(3):608–615, 2010.

[2] Samantha L. Lammie and James M. Hughes. Antimicrobial resistance, food safety, and one health: The need for convergence. *Annual Review of Food Science and Technology*, 7(1):287–312, 2016. PMID: 26772408.

[3] R. Hummel, H. Tschape, and M. Witte. Spread of plasmid-mediated nourseothricin resistance due to antibiotic use in animal husbandry. *Journal of Basic Microbiology*, 26(8):461–466, 1986.

[4] Yi-Yun Liu, Yang Wang, Timothy R Walsh, Ling-Xian Yi, Rong Zhang, James Spencer, Yohei Doi, Guobao Tian, Baolei Dong, Xianhui Huang, Lin-Feng Yu, Danxia Gu, Hongwei Ren, Xiaojie Chen, Luchao Lv, Dandan He, Hongwei Zhou, Zisen Liang, Jian-Hua Liu, and Jianzhong Shen. Emergence of plasmid-mediated colistin resistance mechanism mcr-1 in animals and human beings in china: a microbiological and molecular biological study. *The Lancet Infectious Diseases*, 16(2):161 – 168, 2016.

[5] Rongsui Gao, Yongfei Hu, Zhencui Li, Jian Sun, Qingjing Wang, Jingxia Lin, Huiyan Ye, Fei Liu, Swaminath Srinivas, Defeng Li, Baoli Zhu, Ya-Hong Liu, Guo-Bao Tian, and Youjun Feng. Dissemination and mechanism for the mcr-1 colistin resistance. *PLOS Pathogens*, 12(11):1–19, 11 2016.

[6] Jim O'Neill. Tackling drug resistant infections globally: final report and recommendations. Technical report, The Review on Antimicrobial Resistance, 2016.

[7] World Health Organisation. Antimicrobial resistance: global report on surveillance. Technical report, World Health Organisation, 2014.

[8] UK-VARSS. Veterinary Antibiotic Resistance and Sales Surveillance Report (UK-VARSS 2019). Technical report, Veterinary Medicines Directorate, New Haw, Addlestone, 2020.

[9] Veterinary Medicines Directorate. UK One Health Report - Joint report on antibiotic use and antibiotic resistance, 2013–2017. Technical report, Veterinary Medicines Directorate, New Haw, Addlestone, 2019.

[10] Bethany Griffiths, Dai White, and Georgios Oikonomou. A cross-sectional study into the prevalence of dairy cattle lameness and associated herd-level risk factors in england and wales. *Frontiers in Veterinary Science*, 5:65, 04 2018.

[11] Craig Baker-Austin, Meredith S. Wright, Ramunas Stepanauskas, and J.V. McArthur. Co-selection of antibiotic and metal resistance. *Trends in Microbiology*, 14(4):176–182, 2006.

[12] Julius J Medardus, Bayleyegn Z Molla, Matthew Nicol, W Morgan Morrow, Paivi J Rajala-Schultz, Rudovick Kazwala, and Wondwossen A Gebreyes. In-feed use of heavy metal micronutrients in U.S. swine production systems and its role in persistence of multidrug-resistant salmonellae. *Applied and environmental microbiology*, 80(7):2317–2325, 2014.

[13] Jon L. Hobman and Lisa C. Crossman. Bacterial antimicrobial metal ion resistance. *Journal of Medical Microbiology*, 64(5):471–497, 2015.

[14] Chandan Pal, Karishma Asiani, Sankalp Arya, Christopher Rensing, Dov J. Stekel, D.G. Joakim Larsson, and Jon L. Hobman. Metal resistance and Its association with antibiotic resistance. *Advances in microbial physiology*, 70:261–313, 2017.

[15] Keith Poole. At the Nexus of Antibiotics and Metals: The Impact of Cu and Zn on Antibiotic Activity and Resistance. *Trends in Microbiology*, 25(10):820–832, 2017.

[16] Robert Davies and Andrew Wales. Antimicrobial resistance on farms: A review including biosecurity and the potential role of disinfectants in resistance selection. *Comprehensive Reviews in Food Science and Food Safety*, 18(3):753–774, 2019.

[17] Michelle Baker, Alexander D. Williams, Steven P.T. Hooton, Richard Helliwell, Elizabeth King, Thomas Dodsworth, Rosa María Baena-Nogueras, Andrew Warry, Catherine A. Ortori, Henry Todman, Charlotte J. Gray-Hammerton, Alexander C.W. Pritchard, Ethan Iles, Ryan Cook, Richard D. Emes, Michael A. Jones, Theodore Kypraios, Helen West, David A. Barrett, Stephen J. Ramsden, Rachel L. Gomes, Chris Hudson, Andrew D. Millard, Sujatha Raman, Carol Morris, Christine E.R. Dodd, Jan-Ulrich Kreft, Jon L. Hobman, and Dov J. Stekel. Antimicrobial resistance in dairy slurry tanks: A critical point for measurement and control. *Environment International*, 169:107516, 2022.

[18] K. A. Smith and A. G. Williams. Production and management of cattle manure in the uk and implications for land application practice. *Soil Use and Management*, 32(S1):73–82, 2016.

[19] Delveen R. Ibrahim, Christine E. R. Dodd, Dov J. Stekel, Stephen J. Ramsden, and Jon L. Hobman. Multidrug resistant, extended spectrum beta-lactamase (ESBL)-producing Escherichia coli isolated from a dairy farm. *FEMS Microbiology Ecology*, 92(4), 02 2016.

[20] Holger Heuer, Heike Schmitt, and Kornelia Smalla. Antibiotic resistance gene spread due to manure application on agricultural fields. *Current Opinion In Microbiology*, 14:236–243, 2011.

[21] Sven Jechalke, Holger Heuer, Jan Siemens, Wulf Amelung, and Kornelia Smalla. Fate and effects of veterinary antibiotics in soil. *Trends in Microbiology*, 22(9):536 – 545, 2014.

[22] Hiie Nõlvak, Marika Truu, Kärt Kanger, Mailiis Tampere, Mikk Espenberg, Evelin Loit, Henn Raave, and Jaak Truu. Inorganic and organic fertilizers impact the abundance and proportion of antibiotic resistance and integron-integrase genes in agricultural grassland soil. *Science of The Total Environment*, 562:678 – 689, 2016.

[23] Yuan-Ching Tien, Bing Li, Tong Zhang, Andrew Scott, Roger Murray, Lyne Sabourin, Romain Marti, and Edward Topp. Impact of dairy manure pre-application treatment on manure composition, soil dynamics of antibiotic resistance genes, and abundance of antibiotic-resistance genes on vegetables at harvest. *Science of The Total Environment*, 581-582:32 – 39, 2017.

[24] Yu-Jing Zhang, Hang-Wei Hu, Qing-Lin Chen, Brajesh K. Singh, Hui Yan, Deli Chen, and Ji-Zheng He. Transfer of antibiotic resistance from manure-amended soils to vegetable microbiomes. *Environment International*, 130:104912, 2019.

[25] Xiang Zhao, Jinhua Wang, Lusheng Zhu, and Jun Wang. Field-based evidence for enrichment of antibiotic resistance genes and mobile genetic elements in manure-amended vegetable soils. *Science of The Total Environment*, 654:906 – 913, 2019.

[26] W.-Y. Xie, Q. Shen, and F. J. Zhao. Antibiotics and antibiotic resistance from animal manures to soil: a review. *European Journal of Soil Science*, 69(1):181–195, 2018.

[27] B. A. D. van Bunnik and M. E. J. Woolhouse. Modelling the impact of curtailing antibiotic usage in food animals on antibiotic resistance in humans. *Royal Society Open Science*, 4(4):161067, 2017.

[28] Michelle Baker, Jon L. Hobman, Christine E. R. Dodd, Stephen J. Ramsden, and Dov J. Stekel. Mathematical modelling of antimicrobial resistance in agricultural waste highlights importance of gene transfer rate. *FEMS Microbiology Ecology*, 92(4), 2016.

[29] Sankalp Arya, Henry Todman, Michelle Baker, Steven Hooton, Andrew Millard, Jan-Ulrich Kreft, Jon L Hobman, and Dov J Stekel. A generalised model for generalised transduction: the importance of co-evolution and stochasticity in phage mediated antimicrobial resistance transfer. *FEMS Microbiology Ecology*, 96(7), 06 2020.

[30] Sankalp Arya, Alexander Williams, Saul Vazquez Reina, Charles W. Knapp, Jan-Ulrich Kreft, Jon L. Hobman, and Dov J. Stekel. Towards a general model for predicting minimal metal concentrations co-selecting for antibiotic resistance plasmids. *Environmental Pollution*, 275, 2021.

[31] C.W. Lanyon, J.R King, D.J. Stekel, and R.L. Gomes. A Model to Investigate the Impact of Farm Practice on Antimicrobial Resistance in UK Dairy Farms. *Bulletin Of Mathematical Biology*, 83(36), 2021.

[32] Victoriya V. Volkova, Cristina Lanzas, Zhao Lu, and Yrjö Tapio Gröhn. Mathematical Model of Plasmid-Mediated Resistance to Ceftiofur in Commensal Enteric Escherichia coli of Cattle. *PLoS ONE*, 7(5), 2012.

[33] National Research Council. *Nutrient Requirements of Dairy Cattle: Seventh Revised Edition, 2001.* The National Academies Press, Washington, DC, 2001.

[34] MATLAB. *version 9.9.0 (R2020b).* The MathWorks Inc., Natick, Massachusetts, 2020.

[35] EFSA Panel on Additives and Products or Substances used in Animal Feed (FEEDAP) . Scientific opinion on the safety and efficacy of copper compounds (e4) as feed additives for all animal species (cupric acetate, monohydrate; basic cupric carbonate, monohydrate; cupric chloride, dihydrate; cupric oxide; cupric sulphate, pentahydrate; cupric chelate of amino acids, hydrate; cupric chelate of glycine, hydrate), based on a dossier submitted by fefana asbl. *EFSA Journal*, 13(4), 2015.

[36] EFSA Panel on Additives and Products or Substances used in Animal Feed (FEEDAP) . Revision of the currently authorised maximum copper content in complete feed. *EFSA Journal*, 14(8), 2016.

[37] EFSA Panel on Additives and Products or Substances used in Animal Feed (FEEDAP) . Scientific opinion on the safety and efficacy of zinc compounds (e6) as feed additives for all animal species (zinc acetate, dihydrate; zinc chloride, anhydrous; zinc oxide; zinc sulphate, heptahydrate; zinc sulphate, monohydrate; zinc chelate of amino acids, hydrate; zinc chelate of glycine, hydrate), based on a dossier submitted by fefana asbl. *EFSA Journal*, 13(4), 2015.

[38] HACH Lange Ltd. *Working procedure LCK329 Copper*, 2014.

[39] HACH Lange Ltd. *Working procedure LCK360 Zinc*, 2014.

[40] M.F. Ali and S.A. Shakrani. A Comparison of ICP-OES and UV-Vis Spectrophotometer for Heavy Metals Determination in Soil Irrigated with Secondary Treated Wastewater. *International Journal of Civil and Environmental Engineering*, 14:8–15, 2014.

[41] Christine F. Wellborn. Naturally Occurring Arsenic Levels: A Method Comparison. *Geological Society of America Abstracts with Programs*, 44(4):3, 2012.

[42] American Society of Agricultural Engineers. Manure Production and Characteristics. Technical report, American Society of Agricultural Engineers, 2005.

[43] Landia. *Submersible Slurry Pump DG*, n.d.

[44] INRA-CIRAD-AFZ. Feedtables: Tables of composition and nutritional values of feed materials. https://feedtables.com/, 2018. [Online; accessed 31-May-2019].

[45] A Ivask, T Rolova, and Kahru A. A suite of recombinant luminescent bacterial strains for the quantification of bioavailable heavy metals and toxicity testing. *BMC Biotechnology*, 9(1), 2009.

Chapter 3

Modelling the impact of farm waste water management on antimicrobial resistance in dairy farms

Acknowledgements

Please note that this chapter comprises of a draft paper which includes research work not completed by myself. Ethanographic study of the farm was completed by Richard Helliwell, Sujatha Raman & Carol Morris, while microbiological sampling work was done by Elizabeth King, Jon Hobman and Christine Dodd. Charlotte Gray-Hammerton completed genome sequencing work on the chromosomally encoded ISEcp1 element. The mathematical model, sensitivity analysis and other model analysis presented here is my own work.

Abstract

Dairy slurry is one of the world's largest sources of environmental contamination with antimicrobial resistant genes and bacteria. However, it is not known to what extent waste water management practises on farms can contribute to or control antimicrobial resistance (AMR) in slurry. We use mathematical modelling, informed by detailed anthropological research, to investigate how AMR depends on farm infrastructure and practises around waste water use. We find that experimentally observed temporal fluctuations in cephalosporin-resistant Escherichia coli can be explained by periodic farm activities, notably the emptying of spent copper and zinc footwash into the slurry system, leading to co-selection of metal and antibiotic resistance. The model shows that resistance to cephalosporins is also more observable when relevant genes are encoded chromosomally rather than on plasmids, a finding backed up with genome sequence analysis. Resistance is also predicted to be reduced in conditions with lower growth rate and higher environmental death rate. In contrast, temporal fluctuations in cephalosporin resistance were not explained by the re-use of muck heap effluent, despite survival of cephalosporin resistant *Escherichia coli* in the muck heap even in cold weather. We conclude that farm practises can have a material impact on AMR in slurry spread on land, and so provide farm-specific opportunities to reduce AMR pollution beyond reduction of overall antibiotic use.

3.1 Introduction

Antimicrobial resistance (AMR) is one of the most important global public health problems. It is estimated that there are over 700,000 deaths a year attributable to AMR across the globe, and, unless suitable countermeasures are taken, that number is predicted to rise to 10 million by 2050 [1]. AMR is driven by antibiotic use; the majority (73%) of antibiotic (Ab) sales are for use for food-producing livestock [2]. The use of Abs in agriculture can result in drug-resistant strains infecting human populations through the food chain [3, 4], or may lead to the transfer of antibiotic resistance genes (ARGs) from livestock-associated bacteria to human-acquired infections [5, 6, 7]. The importance of mitigating the risks of AMR in the agricultural sector has been recognised by many countries, including the UK and European Union [1, 8], with reductions and restrictions being imposed on Ab use in agriculture, particularly on critically important Ab. However, despite a 50% reduction in Ab use in the UK agriculture sector since 2014 [9], use still remains high, representing 36% of the total UK Ab use [10], with consequent risk of spread of ARGs and AMR.

In addition to antibiotics, other antimicrobials such as metals (copper and zinc) and other chemicals (e.g. formalin) are widely used across farms globally, particularly in footbaths to prevent lameness in livestock - a prevalent concern in dairy and sheep farming [11]. Metals and other antimicrobial agents (such as formalin and glutaraldehyde) are known to have a coselective effect on antibiotic resistance [12], allowing for the persistence of ARBs in the absence of antibiotic selective pressures [13, 14, 15, 16, 17, 18].

Cattle account for approximately 50% of global livestock (by Livestock Standard Units) including approximately 265 million dairy cows (www.faostat.org). These are estimated to produce 3 billion tonnes of manure per year. This study is based in the UK, whose agriculture sector produces approximately 83 million tonnes of livestock manure each year, with a significant amount of this due to dairy cattle farming (28 million tonnes) where 63% of the dairy waste produced is undiluted liquid slurry [19]. Liquid slurry is often stored in slurry tanks or lagoons for several months, principally to avoid spreading on land due to Nitrogen Vulnerable Zone restrictions. Dairy slurry is known to contain bacteria resistant to many antibiotics, including ESBL-producing *E. coli*[20, 21]. The spreading of slurry/manure onto field soil as fertiliser may then release ARGs and ARBs into the surrounding environment, which may then allow for potential transmission to human pathogens [22]. Studies of fields that have been spread with dairy slurry have demonstrated increased levels of resistance present [23, 24, 25]. Similar studies have shown that crops fertilized with manure can accumulate ARGs associated with the slurry [23, 26, 27, 28].

Thus there is a clear need to reduce AMR contamination from agricultural waste. However, further reduction in usage of Ab will be extremely challenging for countries that have already made major reductions, due to the need for antibiotics in the care and welfare of diseased animals. Therefore it

is appropriate to consider whether changes in farm management, infrastructure or practice can reduce selection for resistance[21]. Such changes are often difficult to evaluate empirically, because they would need expensive changes to infrastructure, or changes in management practise, with consequent welfare or business risks. Mathematical modelling is a powerful tool in such studies, because alternative strategies can be readily evaluated through simulations, and parameters or processes to which adverse outcomes (i.e. proliferation of ARBs) are especially sensitive can be identified, which serve as potential points of control[21].

Most mathematical models studying the impact of AMR in dairy farms (or other livestock farm environments) consider a single area of a farm [29, 30, 12, 31, 21], treat the entire farm as a single compartment [32], or are interested in within-host dynamics of the livestock [33]. While such approaches are undoubtedly useful, to our knowledge, there are no modelling studies that investigate the effects of farm layout, the farm practices associated across different areas of the farm, and the impact these may have upon the emergence and/or spread of AMR across the farm.

In this study, we specifically aim to understand how fluctuations in important ARBs could arise as a result of farm infrastructure and practise. This is motivated by previous empirical work, in which we observed the sporadic appearance of ESBL-producing *E. coli* in the slurry tank [21]. At the core of this paper is the development and analysis of a multi-scale whole-farm mathematical model for AMR, that describes the flow of waste water around a dairy farm, and the spread of resistance within and between farm compartments. In order to develop the model, we have carried out anthropological research on farm management practise on a typical high performance dairy farm, that has allowed us to identify deep understanding of farm operations, which are then incorporated into the model. Moreover, we have also taken additional microbiological measurements on *E. coli* counts and genome sequencing in different farm locations, in order to support the model process. We used the model to explain ARB outcomes and fluctuations, testing hypotheses derived from the ethnographic and microbiological data, by using sensitivity analyses and counterfactual simulations. We also test whether resistance levels will depend upon plasmid or chromosomal carriage of genes conferring cephalosporin resistance, backed up with genome sequence analysis. In this way, we show how an interdisciplinary approach, combining mathematical modelling, anthropology and microbiology, can show how large-scale farm activities can have a material impact on AMR at a molecular genetic level.

3.2 Materials & Methods

Dairy Farm Background

The study considers a mid-sized, high performance commercial dairy farm in the East Midlands, UK, housing 200 milking Holstein Friesian cattle at the time of study. Milking cattle are housed indoors on concrete, and all excreta are regularly removed from cattle yards by automatic scrapers into a drainage system terminating at the 3 M litre slurry tank. The drainage system also receives used cleaning materials and wash water, used footbath, waste milk, and rainwater runoff. An automated screw press (Bauer S655 slurry separator with sieve size 0.75 mm; Bauer GmbH, Voitsberg, Austria) performs liquid-solid separation of the slurry tank influent. Liquids enter the slurry tank semi-continuously, while solids are removed to a muck heap. Calves, dry cows, and heifers are housed separately from the milking cows. Faeces and urine from calves drain into the common drainage system, whilst dirty straw from calf housing is taken directly to the muck heap. Excess slurry can be pumped to an 8 M litre lagoon for long term storage. Slurry is used to fertilize grassland and arable fields. Practice at this farm is typical of management methods at high-performance dairy farms, although all farms vary.

Ethnographic Methods

The farm flow model was informed by ethnographic participant observations with farm staff on the dairy farm. Ethnography is a well-established qualitative method in rural research [34]. At its core it involves detailed and prolonged engagement with a specific actor or set of actors within their social context. This method is valuable in elucidating habitual or 'hidden' practices that would not be readily highlighted through seated interviewing or a survey as was the case in this study. The ethnographic research was conducted over a four-month period beginning September 2017. It involved two weeks of continuous on-farm participant-observations shadowing farm staff through their daily routines. Following this, the farm was visited regularly throughout the remaining period for short engagements (one to two days or half days) to observe specific re-occurring practices of interest and in response to events of interest arising on the farm. All members of staff were shadowed at different times over this period. Observations focused on the farm staff's everyday practices of animal management, animal disease diagnosis and treatment, and waste management. Further detail on the method and the broader ethnographic findings are reported in Helliwell, et al. (2019, 2020) [35, 36] These participant observations identified additional waste management infrastructure and practices that resulted in two feedback loops within the system that had not been previously identified through discussions with farm staff. These feedback loops are identified via the yellow and green arrows on the farm flow diagram Figure (3.1).

Mathematical Model

We have developed a mathematical model ((A1)-(A40) in Supplementary Material A) to evaluate the risk of the spread of AMR across bacterial populations within dirty water as it flows around different areas of a typical UK dairy farm described in figure 3.1, using a multiscale, hybrid discrete-continuous, compartmental system of ordinary differential equations (ODEs). The six different farm compartments are described by a volumetric flow ODE model, to describe the flow of dirty water (V_i) between the compartments, in which the rates of flow between the different compartments follow first order mass action kinetics, and materials within the waste flow between compartments have the non-variable fractional flow rates. The flow model is then extended to include the concentrations of copper and zinc ($M_i^{[Cu]}$ and $M_i^{[Zn]}$), and antibiotics ($A_i^{[Oxy]}$ and $A_i^{[Cex]}$). The flow model was coupled with a bacterial resistance transfer ODE model[21], that describes populations of antimicrobial sensitive (S_i) and resistant ($R_i^{[x_1,x_2,x_3,x_4]}$) bacteria in each of the six compartments, where $[x_1, x_2, x_3, x_4] \in \{0, 1\}^4$, such that $x_1 = 1$ if the population is resistant to copper, while $x_1 = 0$ if it is sensitive to copper, and similarly x_2, x_3 and x_4 reflect zinc, oxytetracycline and cefalexin resistant bacteria. All the parameters of the model are described in table A1 with realistic value ranges for each parameter based on ethnographic observations of the Sutton Bonington dairy farm and available information in the existing literature.

We assume that the amount of volume of daily waste inputs in the main dairy shed (a) and bulling heifer shed (b) (i.e. from faecal matter, trough water, footbaths, bedding etc.) are constant. Copper and zinc are used in the cattle feed for growth promotion purposes and a significant percentage of these metals are not absorbed by the cow ($\approx$ 99% and 85% for Cu and Zn respectively [37]) and enter the slurry flow system in the cow faeces. We also assume that the solid slurry matter separated onto the muck heap has no residual liquid and effluent run off is determined only by rainfall (η).

On top of the continuous flow model, three farm processes are represented by discrete processes within the model: the emptying of metal footbaths into the main dairy shed scraper channel; the flushing of the scraper channels with muck heap effluent; and the emptying of the slurry tank. To model these processes, we assert that at time T_{footbath} that the volume of the footbath (V_{footbath}) and mass of copper and zinc ($a_{\text{footbath}}^{[Cu]}$ & $a_{\text{footbath}}^{[Zn]}$) is instantly added to the slurry volume and metal mass in the main dairy shed respectively. The emptying of the slurry tank is modelled similarly where at time T_{Tank}, the slurry tank compartments are emptied. We model the tank as not being completely emptied and that a small proportion ($0 < \epsilon_{\text{Tank}} \ll 1$) of the volume, mass of metals and antibiotics and population of bacteria in the slurry tank contents remains. Similarly, at time $T_{\text{Eff. Flush}}$ we assume that a small fraction ($0 < \epsilon_{\text{Tank}} \ll 1$) of the contents in the slurry tank contents remains and $^{(1-\epsilon_{\text{eff}})V_{\text{eff}}}/_2$ is added to the main dairy and bulling heifer sheds each.

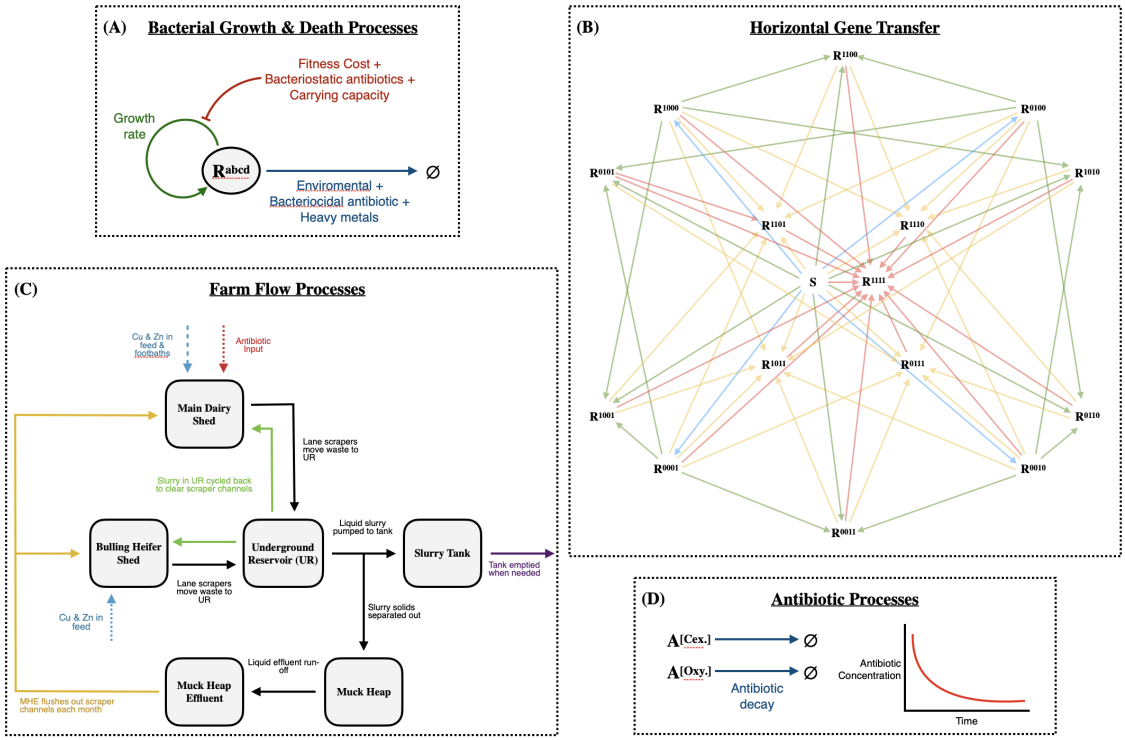

Figure 3.1: **Schematic diagrams explaining the processes included in the farm flow model.** ***(A)*** Bacterial growth and death processes: bacteria growth occurs according to a logistic-style growth determined by the carrying capacity of the slurry. The rate of growth may be reduced by the fitness cost associated with carriage of ARGs on plasmids, or by the effects of bacteriostatic antibiotics. The bacterial death rate is determined by environmental conditions (e.g. due to unsuitable temperature, pH, oxygen levels, or predation by phage, protozoa or bacteria), as well as due to the toxic effects of heavy metals and bactericidal antibiotics. ***(B)*** Horizontal gene transfer: this diagram shows the possible pathways for resistance to spread between different bacterial sub-populations. Blue arrows show sensitive bacteria acquiring a single resistance gene, green arrows and yellow arrows indicate the paths where bacteria become resistant to 2 or 3 antimicrobials respectively, and red arrows bacteria acquiring resistance to all 4 antimicrobials considered in this study. ***(C)*** A flow diagram showing the different compartments of the dairy farm, and how waste flows between the compartments. For a full description of this diagram, see Figure 2.1 in Chapter 2. ***(D)*** Antibiotic processes: antibiotics decay according to first-order mass action kinetics.

Antibiotics enter the slurry flow system in the main dairy shed sick pens as we assume the antibiotics pass into the scrapers channels in the sick pen cow's faeces and we model the antibiotic input ($a^{[j]}(t)$ for

$j \in \{\text{Oxy, Cex}\}$) as a time-dependent discrete parameter based on the farm antibiotic usage records. We model the degradation of the antibiotics using previously identified first-order degradation kinetics[21]. The microbiological model is a subset of the model previously described[21], but with four rather than six antimicrobials (copper, zinc, oxytetracyline and cephalexin).

We also consider a variation of the farm flow model where cefelexin-resistance is chromosomally-encoded. As cefelexin-resistance is now chromosomal, there is no fitness cost for cefelexin-resistance (i.e. $\alpha_{[Cex]} = 0$) and cefelexin-resistance genes can not be transferred via conjugation (although resistance to oxytetracycline, zinc and copper can still be spread via HGT). The system of equations (C17) describing the farm flow model with chromosomal cefelexin-resistance can be found in supplementary material C.

Simulations

We simulated our farm flow model using MATLAB R2020 [38]. We produced time course simulations with the standard parameter values (Table A1) using the ODE45 solver to show the concentration of the different bacterial populations over time. For all simulations of the model, we used the steady state values of the continuous farm flow model for the initial conditions of the slurry volume and metal equations, and assume that the initial volume of the slurry tank is 1×10^6 L and the effluent tank has recently been used and in a near empty state ($V_{\text{eff}}(0) = \omega$) to avoid division by zero errors in the HGT terms of the effluent bacterial populations). We initialise the bacterial populations in our model using the average *E. coli* counts sampled from each area of the farm and assume the proportion of each distinct resistant bacterial population is the same.

Sensitivity Analysis

We perform a global sensitivity analysis of bacterial parameters and discrete farm practice parameters to determine what factors have the most influence on the concentration of oxytetracyline- and cefelexin-resistance within the slurry tank. For each parameter, we take 1000 parameter values sampled from the feasible parameter space (Table B7 and B8) using the Latin hypercube sampling method. We then complete a local one-at-a-time sensitivity analysis for each parameter values and calculate the relative sensitivity of each parameter, as described in [29]. The relative sensitivity, S_p^X, of the output of interest X relative to a change in the model parameter p is given by:

$$S_p^X = \frac{\delta X/X}{\delta p/p}.$$

Due to the significant oscillatory nature of the model, we were unable to consider the sensitivity at the steady state, so instead we evaluated the sensitivity of the max and mean of the resistant bacteria

population over the time period. We use MATLAB R2020b [38] to carry out the sensitivity analysis and plot the outputs as box plots.

Microbiological Sampling

Liquid samples were collected from different areas on the farm on two different dates. On 21st November 2017, samples were taken from the dairy lane inside, dairy lane outside dairy shed scraper channel, bulling heifer shed scraper channel, underground reservoir, slurry tank, heifer shed (older cows), muck heap effluent and silage clamp effluent. On 12th December 2017, samples were taken from the heifer shed with older cows (as before), the heifer shed with younger cows, muck heap straw, muck heap effluent, slurry tank, feed from the floor, concentrated feed pellets and straw from the heifer shed. *Escherichia coli* strains were isolated using Tryptone Bile X-Glucuronide (TBX) or MacConkey agar or TBX/MacConkey supplemented with 16μg ml^{-1} ampicillin (AMP), or 2 μg ml^{-1} cefotaxime (CTX); or on CHROMagar ESBL ^{TM} agar. Putative *E. coli* isolates were subcultured onto TBX agar or TBX agar supplemented with 2 μg ml^{-1} CTX. *E. coli* strains were confirmed using oxidase and catalase tests as described[20].

3.3 Results

Farm practices leads to high variability in the bacterial load across the farm

Time course simulation of the farm flow model (figure 3.2) using the default parameter set (table A1-A6) shows high variability in the bacterial populations corresponding to different farm practices. First, we observe oscillations with a frequency of 7 days in all bacterial populations across the dairy shed, bulling heifer shed, underground reservoir and slurry tank, associated with the emptying of the metal footbaths into the scraper channels, as this causes significant increases in the metal concentration within the slurry (Cu and Zn increases by up to 115-fold and 38-fold respectively in the main dairy shed). This results in increased bacterial death due to the antimicrobial effects of copper and zinc, as we see the total bacterial concentration in the main dairy shed fall by approximately 98% each time the footbaths are emptied.

A second timescale is associated with the use of additional metal footbaths every 21 days (figure 3.2). This leads to increased reductions in the total bacterial population, and we see the Ab-sensitive bacteria sharply decline (from the order of 10^6 CFU/L to 10^4 CFU/L) while the resistant populations are significantly less affected by the increased metal concentration, leading to an significantly increased resistant proportion of the bacterial population, especially those resistant to copper and zinc (from 0.5% to 20%).

Finally, there is a third time scale of fluctuations within the slurry tank associated with emptying of

the tank. We observe increases in the concentration of all bacterial populations due to the tank being emptied before the concentrations return to the continuous steady state. However, the emptying of the slurry tank has a less pronounced effect on the bacterial populations than the effects of adding metal footbaths. No observed fluctuations in bacterial dynamics appear to be associated with the effluent flushing of the scraper channels every 28 days.

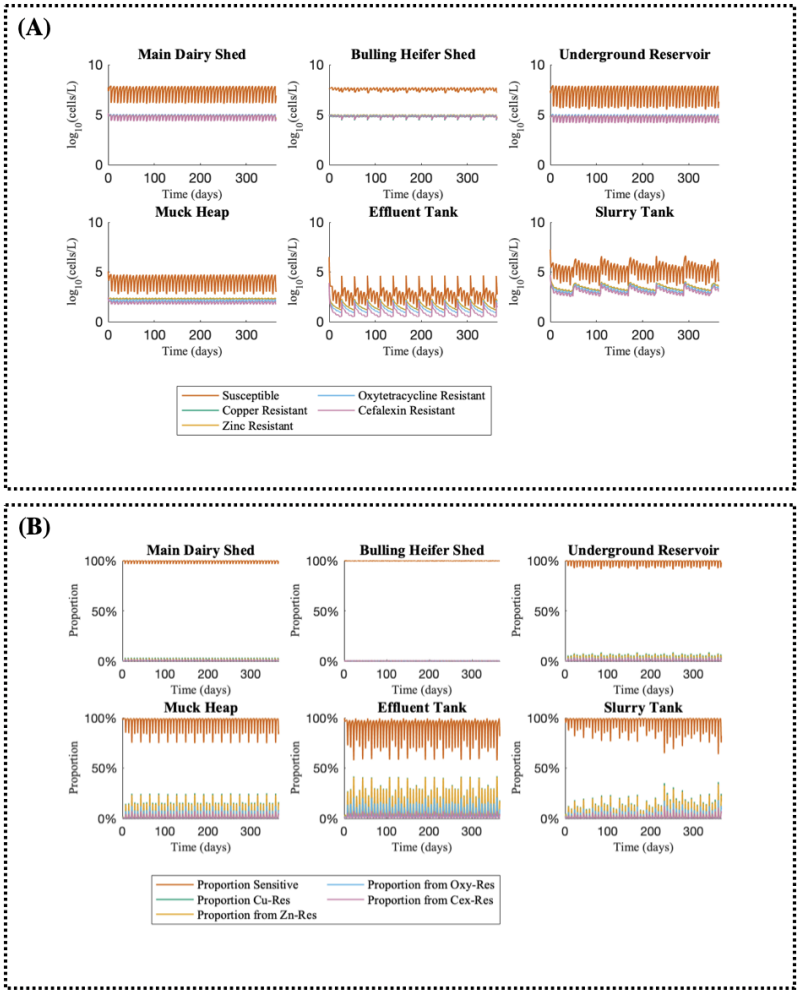

Figure 3.2: **Time course simulations of farm flow model where resistance is plasmid-encoded.** ***(A)*** Time course simulation showing the concentration of bacterial populations across different areas of the farm over a time period of 365 days. ***(B)*** Figure showing the relative proportion that each sub-population (sensitive, Cu-, Zn-, Oxy- and Cex-resistant bacteria) make up of the total bacterial load over the time course. We simulated this time course using parameter values gathered from farm data (given in supplementary material A). In this simulation, resistance genes to oxytetracycline, cefelexin, copper and zinc are assumed to be encoded on plasmids and may be transferred horizontally between populations.

However, the fluctuations of cephalexin resistant bacteria in these simulations are considerably smaller than those observed empirically[21]. Specifically, experimental sampling of the slurry tank found *E. coli* counts with spikes up to approximately $10^{5.6}$CFU L^{-1}, while simulation of our farm flow model only suggests increases in Cex-resistance up to approximately $10^{3.5}$CFU L^{-1}. In order to identify possible sources of this discrepancy, we carried out a global sensitivity analysis of the model to its continuous process parameters.

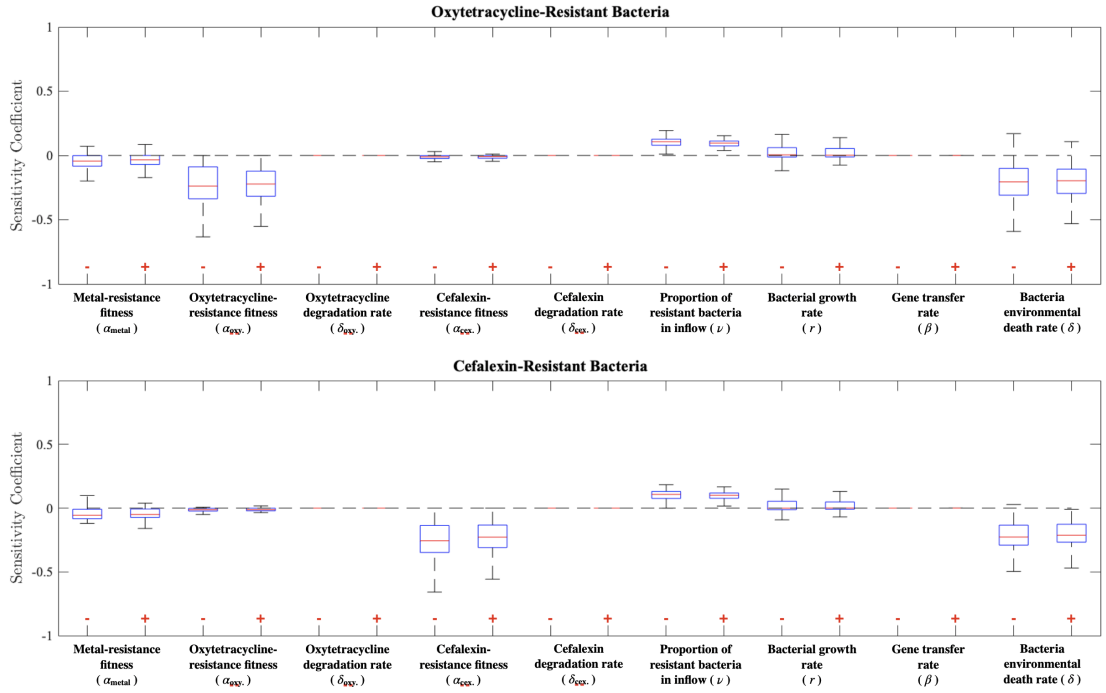

Figure 3.3: **Global sensitivity analysis of bacterial parameters.** Boxplots of the relative sensitivity of the average oxytetracycline- and cefelexin resistant bacteria populations in the slurry tank to ±1% change in each key bacterial parameter. This sensitivity analysis considers 1000 values of each individual parameter sampled from the realistic parameter ranges (given in supplementary material A) by the Latin hypercube sampling method. We observe that each resistant population is most sensitive to the fitness cost associated with plasmid-borne resistance ($\alpha_{[i]}$), and the bacterial death rate due to environmental factors such as temperature, pH, or predation (δ_S). Conversely, we note that the sensitivity coefficients of the degradation rate of both antibiotics (δ_{Oxy} and δ_{Cex}) and the rate of horizontal gene transfer (β) are negligible for both resistant bacterial populations.

Concentrations of antimicrobial-resistant bacteria are most sensitive to the fitness cost and the natural bacterial death rate

We conducted a global sensitivity analysis of the biologically-relevant parameter space to determine those parameters that most affect the concentration of resistant bacteria across the farm in our model (figure 3.3). We find that the antimicrobial-resistant bacterial population levels are most sensitive to the fitness cost of carrying resistance ($\alpha_{[j]}$) and the environmental bacterial death rate (δ).

The average concentration of resistant bacteria is also shown to be sensitive to the proportion of resistant bacteria (ν) entering the farm flow system in the heifer waste in the main dairy and bulling heifer sheds and also to the bacterial growth rate (r).

Interestingly, the sensitivity analysis showed that the average concentration of both oxytetracycline- and cefalexin-resistant bacteria are not sensitive to variation in the rate of horizontal gene transfer (β). This contrasts with the original slurry tank model [29], likely due to the fact that this model only considered the slurry tank in isolation and did not include factors like natural death rate (δ) or metal co-selection. We also observe that our sensitivity analysis results are consistent with observations of similar mathematical models considering metal co-selection [12].

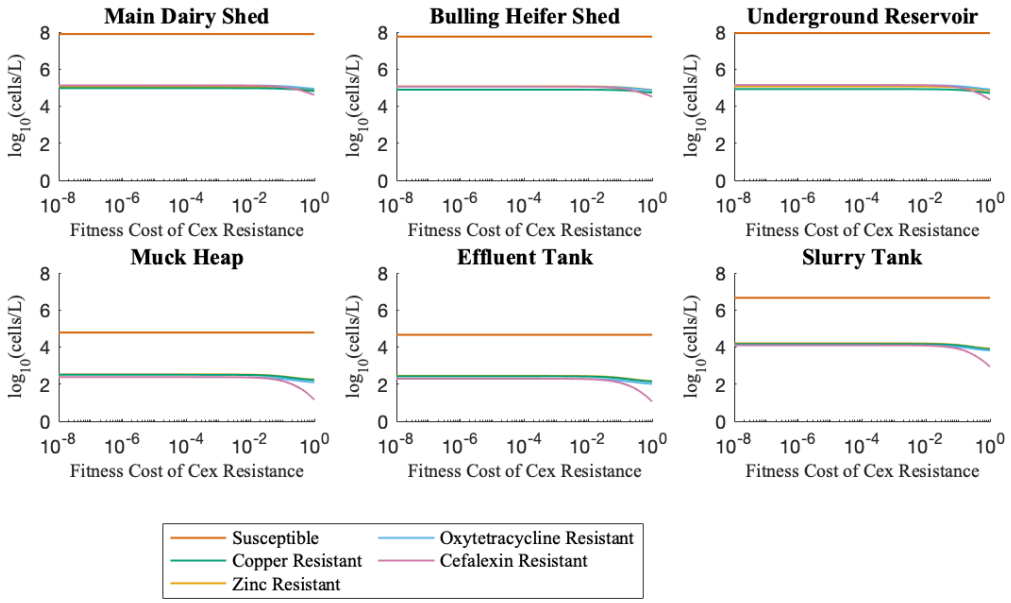

Figure 3.4: **Parameter analysis of the fitness cost of carrying cefelexin resistance against the maximum bacterial populations.** This figure shows how the maximum bacterial populations in the hybrid discrete-continuous farm flow model vary as the fitness cost of cefelexin resistance varies across the parameter space $\alpha_{[\mathrm{Cex}]} \in [0, 1]$.

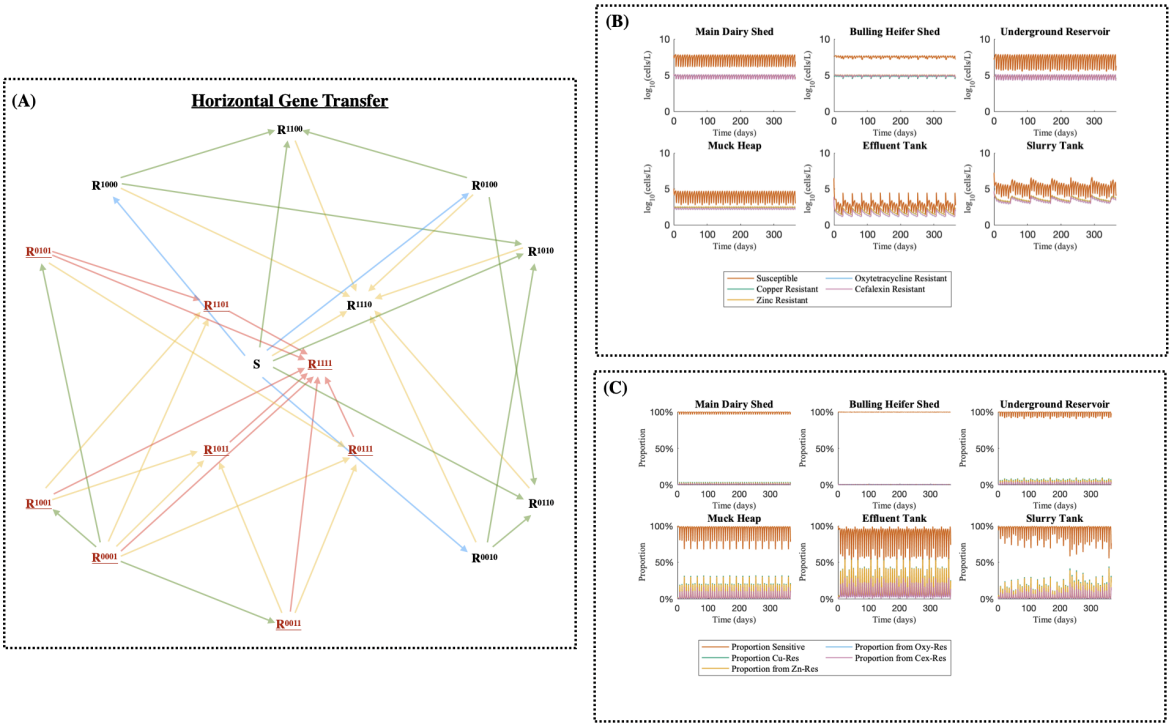

Figure 3.5: **Time course of farm flow model when cefelexin-resistance is chromosomal** ***(A)*** A schematic diagram describing the horizontal gene transfer dynamics in the case where cefelexin resistance is encoded chromosomally (rather than on a plasmid). As cex-resistance is located on the chromosome, bacteria carrying cex-resistance do not incur a fitness cost as in figure 3.2. Metal and oxytetracline resistances are still plasmid mediated in this case and transfer of these resistances can occur horizontally, however, cex-resistance cannot be transferred from one cell to another horizontally. Bacteria labelled in red denotes bacterial populations which have cefelexin-resistance, while bacteria labelled in black do not. ***(B)*** Time course simulation of farm flow model where Cex-resistance is chromosomally-encoded (described in supplementary material C). ***(C)*** Figure showing the relative proportion that each sub-population (sensitive, Cu-, Zn-, Oxy- and Cex-resistant bacteria) make up of the total bacterial load over the time course. This time course uses the same model parameters as in the simulation where cefelexin-resistance is plasmid-encoded (figure 3.2).

Spikes in ESBLs are consistent with chromosomal carriage of Cex-resistance genes

Following the global sensitivity analysis, single parameter variation analysis of the maximum bacterial populations as the fitness cost of carrying a plasmid with cefelexin-resistance genes is varied (figure

3.4) indicates that the spike concentration of cefelexin-resistant bacteria only reaches the experimentally observed maximum levels in the periodic spikes when the fitness cost is below 10^{-2}. We therefore simulated the scenario where cefelexin resistance is encoded on the chromosome instead of the plasmid. In this simulation, we assert that cefelexin-resistance confers no fitness cost, but also that the resistance genes for cefelexin can no longer be transferred horizontally.

In simulations of the chromosomal cefelexin-resistance case (figure 3.5), the temporal dynamics are similar to the case where cefelexin-resistance is plasmid-encoded (figure 3.2). However, the amplitudes of the spikes in cefelexin-resistant populations due to periodic footbath emptying are considerably greater when resistance is chromosomally encoded as compared with plasmid-enocded: in the plasmid case, the proportion of the bacterial load possessing cefelexin-resistance fluctuates between 0.1% and 11.9%, whilst with chromosomal encoding, the proportion of the bacterial load fluctuates between 0.2% and 21%. These concentrations are more consistent with the observed levels of spiked ESBL-producing *E.coli* from the slurry tank.

Resistant bacterial populations are insensitive to effluent flushing and highly sensitive to heavy metal footbath use

Two different farm activities could potentially explain the regular re-appearance of ESBL-producing *E. coli* in the slurry tank: periodic flushing the scraper channels with muck heap effluent, leading to possible re-seeding of the farm with ESBLs living in the muck heap; or periodic emptying of the metal footbaths into the slurry tank, leading to possible co-selection of ESBLs by copper and zinc. Support for the first hypothesis is given by microbial counts of *E. coli* cells grown on TBX/CTX media in different farm location. On 21st November, ESBL *E. coli*s were detected in 7 of the 9 locations tested, including the heifer shed, scraper channels, underground reservoir, slurry tank and muck heap effluent. On 12th December, ESBL *E. coli* cells were only detected in the muck heap effluent, and not in any other compartments. From 8th December that year, the temperature had been below 2°C, and the temperature was -0.5°C at the time of sampling. The muck heap is the one part of of the external farm environment with mesophyllic temperatures, and so it is reasonable that use of muck heap effluent could lead to spread of ESBL *E. coli* cells to other parts of the farm.

However, a global sensitivity analysis of the farm management parameters in this model (figure 3.6A) showed that the long-term average levels of antimicrobial resistance around the farm are extremely sensitive to the metal footbath emptying frequency, and not sensitive to the scraper channel effluent flushing frequency, nor to the volumes used for the metal footbath or effluent flushing. Negative sensitivity was seen to the frequency of slurry tank emptying, as would be expected, because of the physical removal

of bacteria. This is a clear indication that it is the metal footbath use that is responsible for spikes of ESBLs rather than the use of muck heap effluent.

To investigate the footbath use further, we show the impact of the different bactericidal antimicrobials (cefelexin, copper and zinc) to the death rate of sensitive bacteria (δ_S) 3.6B. Due to the limited use and relatively high degradation rate of cefelexin, it has an extremely limited impact on δ_S across the different areas, where we see the most impact in the main dairy shed reaching a brief maximum of 6.7% of δ_S, however, it largely has a near-zero impact on the death rate of sensitive bacteria in all areas. The bactericidal effects of copper and zinc have a much more pronounced effect on δ_S. There are substantial oscillations in the impact of both copper and zinc across the farm due to the metal footbath emptying in the main dairy shed once a week: we see the most considerable impact of this in the main dairy shed and UR where the effect of copper dramatically increases to 80% of δ_S when the footbaths are emptied from a minimum of 0.01%, though there is still considerable variation in the bactericidal effect of copper in the slurry tank oscillating between 25.7% and 63.0% of δ_S. We also see substantial oscillations in the bactericidal effect of zinc on the sensitive death rate due to the footbath emptying: both the main dairy shed and UR varying between 15% and 42% while the slurry tank fluctuates between 24.0% and 39.9%. Comparing the concentrations of copper and zinc in the different areas of the farm with the minimum inhibitory concentrations (MIC) of copper and zinc (103.7 mg/L and 1205.8 mg/L respectively [21]), we observe that the concentration of copper in the main dairy shed and underground reservoir is well in excess of the MIC (477.6 mg/L and 234.2 mg/L), while the concentration of zinc in these areas when the footbaths are emptied (521.8 mg/L and 260.1 mg/L) remains below the MIC of zinc when the metal footbath is emptied, hence why copper contributes up to 80% of δ_S in the areas of the farm.

In time course simulations of both plasmid-encoded (figure 3.2) and chromosomally-encoded (figure 3.5) resistance farm flow models we observe significant variation in the bacterial population due to the bactericidal effects of Cu and Zn when the metal footbaths are emptied into the slurry flow. A closer look at the resistant profiles of the different resistant bacterial populations shows that bacteria with resistance to both copper and zinc quickly become the dominant resistant populations, while bacterial populations which have resistances to oxytetracycline and/or cefelexin but are not resistant to both metals have trivial population size. For example, the average concentration of *E. coli* in the slurry tank with chromosomally encoded cex-resistance is approximately 5 CFU/L when there is no metal resistance, and approx. 20 CFU/L and 100 CFU/L when the bacteria has no Cu-resistance and Zn-resistance respectively. This suggests that the farm practice of emptying the heavy metal footwash into the slurry waste system inputs excessive metal into the systems creating a potentially co-selective environment.

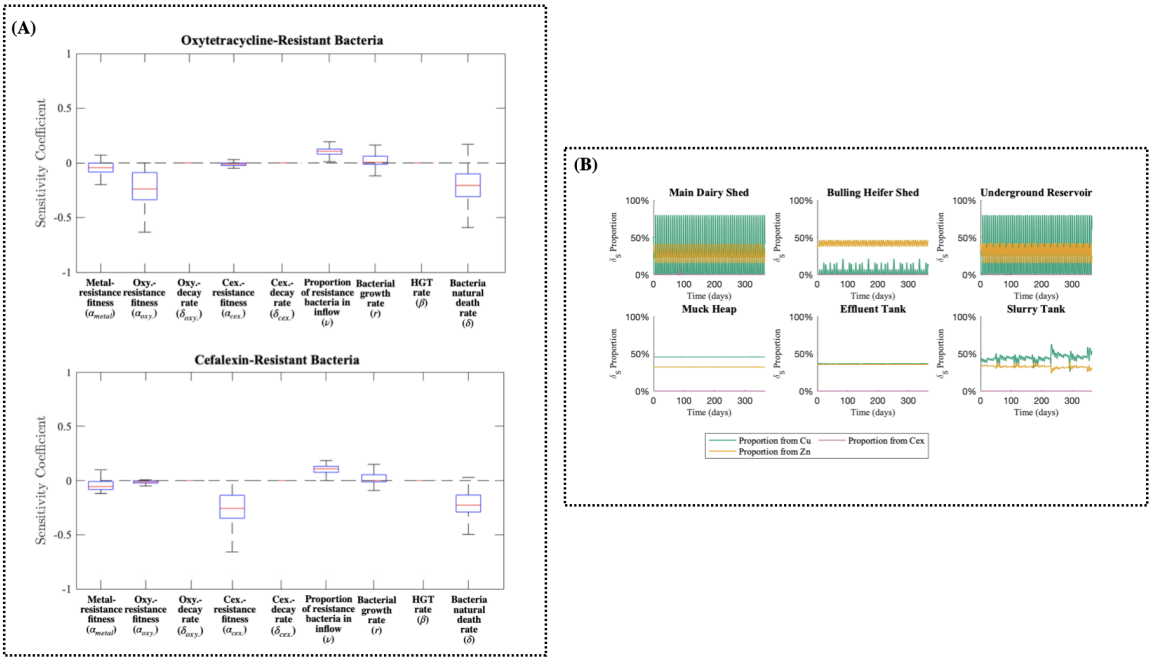

Figure 3.6: ***(A)*** Global sensitivity analysis of the discrete farm management parameters. Boxplots of the relative sensitivity of the average oxytetracycline- and cefelexin resistant bacteria populations in the slurry tank to +1% change in key parameters for the discrete farm processes. This sensitivity analysis consider 1000 values of each individual parameter sampled from the realistic parameter ranges (given in supplementary material A) by the Latin hypercube sampling method. We observe that the system is extremely sensitive to the frequency of the emptying of metal footbaths. ***(B)*** This figure shows the what proportion of the overall sensitive bacterial death rate (δ_S) over the time period by each bactericidal antimicrobial. At each time point, the total death rate for sensitive bacteria is the sum of the environmental death rate (δ) and the bactericidal effects of cefelexin ($E^{[}Cex]_i$), copper $E^{[}Cu]_i$) and zinc $E^{[}Zn]_i$).

Further confirmation of this finding can be given by running counterfactual simulations, in which either the footbaths are no longer emptied into the slurry system (Figure 3.7), or in which the muck heap effluent is no longer reused (Figure 3.8). In the first counter-factual scenario (Figure 3.7), the proportion of the total bacterial population carrying resistance is substantially lower than in the standard model simulations: in the case where cex-resistance is carried on the plasmid, oxytetracycline- and cefelexin-resistant sub-populations on average consist of 0.08% and 0.03% of of the total bacterial load (compared to 1.98% and 1.19% in the standard model), while in the case where cex-resistance is contained on the chromosome, these sub-populations both make up on average 0.14% of the total *E.coli* population

(compared to 2.65% and 2.67% in the chromosomal resistance case of the standard model). However, despite significantly lower proportions of resistance in this counter-factual scenario, we can see in the time course simulation (figure 3.7A) that the total bacterial load across the farm is significantly higher (10^9 CFU/L compared to 10^6 CFU/L). Without the system receiving the repetitive bactericidal injections of the metal footbaths, the selective pressures for copper and zinc resistance are removed, and we observe significant rises in oxytetracycline-resistance to 10^6 CFU/L in the slurry tank.

In the case where cex-resistance is chromosomally encoded (Figure 3.7B), we also observe a sustained increased concentration level of 10^6 CFU/L in the slurry tank (similar to oxy-resistance), however, in the case where cex-resistance is plasmid-mediated, the concentration of cex-resistant bacteria in the slurry tank varies between $10^3.7$ and $10^4.3$ CFU/L (slightly higher than the maximums reached in to the standard model, $10^3.8$ CFU/L). The significantly increased bacterial load appears to be a result of copper and zinc resistances no longer being necessary for Cex- and Oxy-resistant bacterial populations to survive as the bacterial cells are no longer exposed to high levels of antimicrobial metals from the footbaths ,and hence the fitness cost for carrying these genes is no longer outweighed by the excess presence of copper and zinc from the metal footbaths.

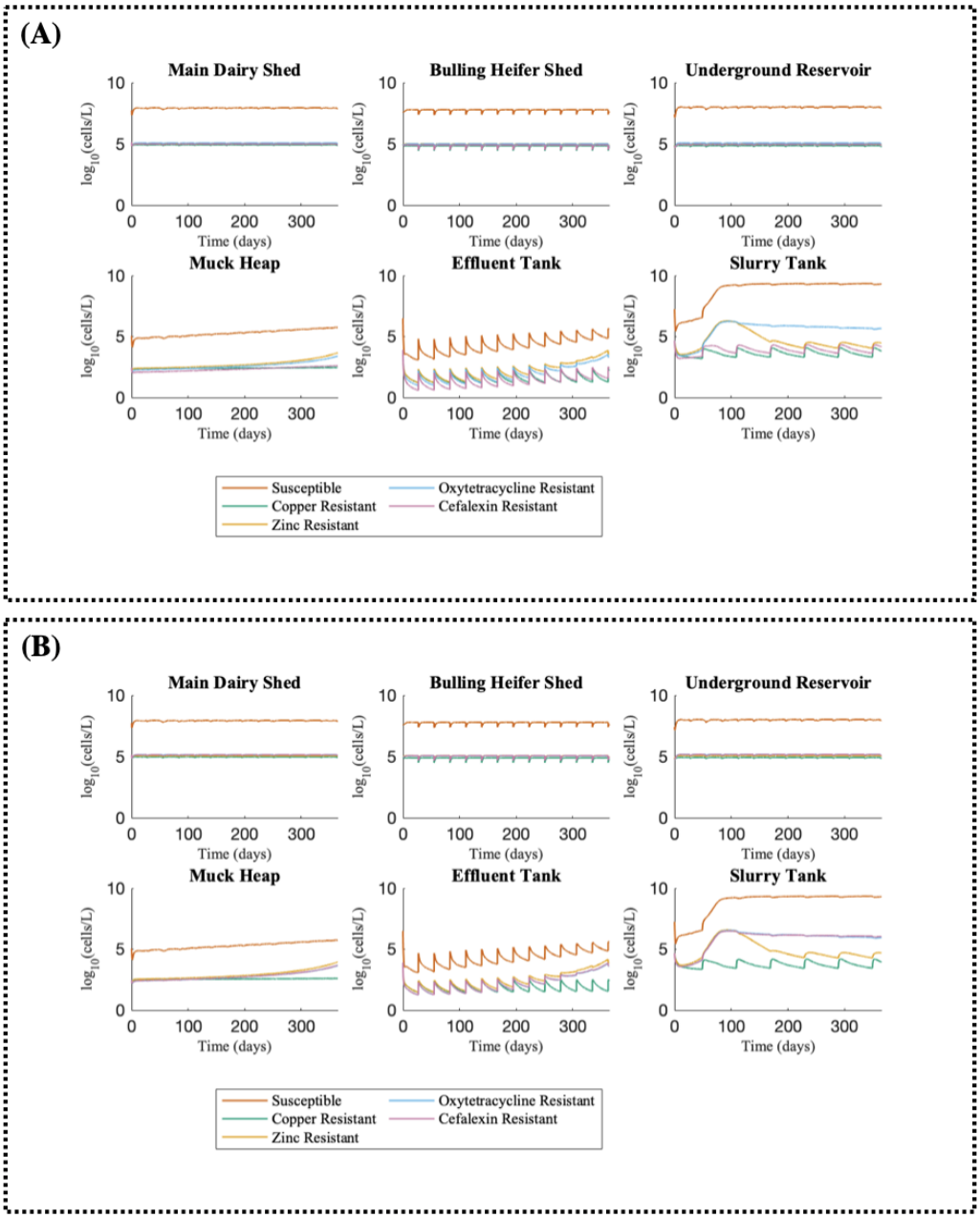

Figure 3.7: **Time course of counterfactual case of farm flow model (with no metal footbaths).** ***(A)*** Plasmid-encoded resistance ***(B)*** Cefelexin-resistance encoded on the chromosome. The counterfactual simulations of both plasmid and chromosomal resistance case use the same model equations and parameters as in previous simulations (given in supplementary material A-C), however, we no longer include the emptying of the metal footbaths: i.e $T_{\text{footbath}} = T_{\text{extra foot.}} = \emptyset$. We observe that in both ***(A)*** and ***(B)***, the removal of the metal footbaths from the system results in a reduction in the proportion of resistance, but also a significant increase in the total bacterial concentration to over 10^9 CFU/L.

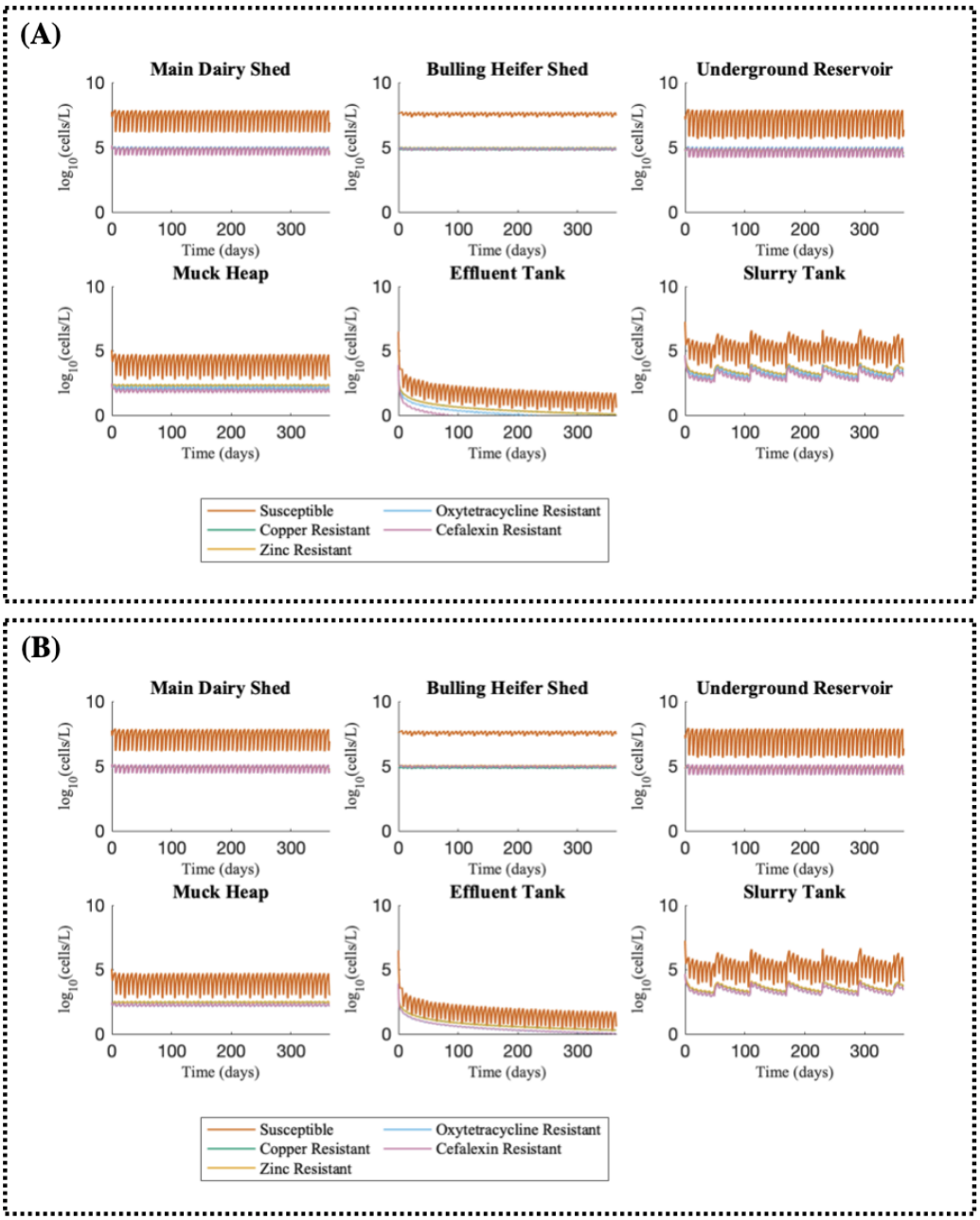

Figure 3.8: **Time course of counterfactual case of farm flow model with no effluent flushing feedback loop.** ***(A)*** Plasmid-encoded resistance ***(B)*** Cefelexin-resistance encoded on the chromosome. The counterfactual simulations of both plasmid and chromosomal resistance case use the same model equations and parameters as in previous simulations (given in supplementary material A-C), however, we no longer include the flushing of the main dairy and bulling heifer shed scraper lanes with muck heap effluent: i.e $T_{\text{Eff. Flushing}} = \emptyset$. We observe that in both ***(A)*** and ***(B)***, the removal of the effluent flushing feedback loop results in no significant difference in the bacterial populations across the farm compared to Figure 3.2A and 3.5B.

3.4 Discussion

Farm practices can have a material impact on AMR dynamics

The farm flow model we have developed uses a multiscale modelling approach that exhibits behaviour not captured by more homogeneous approaches. Many mathematical models considering AMR in agricultural settings have focussed on a within-host model [33, 39] or on a particular area of the farm, e.g. cattle shed [40], manure heaps or slurry tanks [29, 12, 31, 21]. While within-host models do provide scope to consider the effects of farm management on AMR, for example antimicrobial usage [32] or the effectiveness of sequestering of animals undergoing treatment [39], it is not practical for these models to assess the effects of structural farm management practices. Other models considering the spread of AMR in slurry tanks can provide useful analysis of farm management such as the role of water troughs in maintaining bacterial loads in cattle pens [40], how altering slurry storage time [29, 31] or the use of a two-tank slurry storage system [21] may control spread of resistance in dairy slurry. However, such models may not capture salient effects of practices in other areas of the farm as we have observed in the comparison of our farm flow model and a model focussing on the slurry tank only. This suggests that the multiscale modelling approach to consider the wider farm layout could be an important modelling tool in future work considering how farm practices may affect bacterial dynamics and the spread of resistance, given the wide view of the modelling approach and the versatility of a modelling approach to consider alternate scenarios for comparison through altering certain parameters - such as how we have considered counter-factual scenarios where the farm uses an alternative to metal footbaths in the dairy sheds.

While our farm flow model is uniquely designed to model the layout of the particular farm considered in this study, the use of sensitivity analyses provide generality by considering a wide range of realistic farm parameters. Moreover, the model could readily be adapted to the layout and waste management practices of other farms by the adjustment of the farm specific parameters and introducing (or removing) compartments dependent on the farm layout.

The inherent flexibility of this modelling approach to explore variations on the farm system that would be a serious challenge to test empirically can provide insight into the effect that making changes to farm management practices may have on the dynamics of AMR within bacterial communities on the farm. From seeing the significant impact of the emptying of the heavy metal footbaths on the system creating a potentially co-selective environment, one may consider the simplest solution may be to stop emptying heavy metal footbaths into the main dairy shed scraper lanes. However, counter-factual simulations of the farm flow model (figure 3.7) demonstrated that while this may reduce the proportion of antibiotic resistance within the slurry flow, the absence of the repeated bactericidal shockloading from excess metals results in an overall bacterial population that is 1000 time larger than the previous case,

and the oxytetracycline- and cefelexin-resistant *E.coli* populations being at a greater and more sustained concentration with the absence of the periodic oscillations created by the weekly emptyings.

These unexpected consequences also sit in addition to more practical issues around the removal of metal footbaths from the system. There is a significant question of how would the waste footwash be disposed of without emptying into the slurry system. It cannot be allowed to run-off into the environment due to environmental regulations as the elevated levels of copper can have a toxic impact on the environment potentially impacting on vegetation and wildlife. Similarly emptying footwash into local sewer systems is not an acceptable solution as this may lead to contamination of the public drinking water supply if wastewater treatment plants are unable to suitably remove the elevated heavy metal levels. In the UK it is possible to remove waste footbath through a licensed contractor but this solution is likely to be very expensive in the longterm. This may lead to the assumption that metal footbaths should not be used , but heavy metal footbaths are commonly used in dairy farms across the UK to prevent digital dermatitis, an issue that causes 20-25% of lameness in cattle [41], so an alternative option would need to be explored. Formalin footbaths are also available as an option, however, this may present other issues: for example formalin is listed as a Known Human Carcinogen (KHC) [42].

Another possible option would be to continue the usage of metal footwash and explore the possibility of removing copper and zinc from the the slurry system after the footbaths have been emptied via adsorbents [43], however, such a solution may not be practical or affordable on such a scale, and may have equally surprising consequences as observed in our counter-factual simulations.

While the model demonstrated the significant impact of the disposal of footbaths into the waste flow, analysis of the model also showed that the feedback loops in the farm slurry system due to recycling of muck heap effluent to clear scraper channels has a negligible impact on the AMR profile of the farm in the model. However, the importance of the muck heap and effluent run-off from it should not necessarily be discounted. Our understanding of the muck heap is far more limited due to a lack of study of the muck heap (compared to the slurry tank). Despite the limited study, antibiotic residues within the muck heap solids have been identified including some that have not been used on the farm for several years [21]. As farms may pivot away from the usage of antibiotics that have human-use, the long term retention of antibiotics within the muck heap, acting like an archive of antibiotics historically used on the farm, may be problematic and may lead to the co-selection and accumulation of resistances to different antibiotics. It is important to note that, in the interest of computational complexity, this model takes a simplified view of the muck heap by assuming the homogeneity of all factors (temperature, pH, COD, etc) throughout the entire compartment and neglects the possible effects of adsorption of metal ions, antibiotic residues and bacteria. An expanded model considering spatial inhomogeneities and adsorption processes within the muck heap could provide useful insight into the bacterial and resistance dynamics

within the muck heap, and further understand the possible AMR risks that usage of muck heap effluent and manure may pose.

Understanding how resistance is encoded in bacteria is important

In this study we have also shown the importance of considering where ARGs are located within bacteria. Observed spikes in ESBL resistance across different areas of the farm were not reflected in the slurry tank only model [21], and while time course simulations of our initial farm flow model (figure 3.2) showed variation in the concentration of cefelexin-resistance in the slurry tank, the maximum increase observed in the plasmid-encoded case was significantly lower than those observed experimentally in the slurry tank. However, when we alter the model to consider a scenario where cefelexin resistance genes are encoded chromosomally (figure 3.5), the model predicts spikes in the concentration of all resistant populations corresponding to the emptying of additional metal footbaths every 3 weeks, with magnitude more consistent with the concentrations of ESBLs observed in the presumptive *E. coli* counts of the slurry. This result presented an experimentally testable hypothesis for why we observe these sharp fluctuations in the levels of ESBLs across the farm that were previously unexplained by the model. Thus was backed up by whole genome sequencing data from *E. coli* isolates both from different areas of the farm, and from the slurry tank [21], identifying a chromosomally encoded ISEcp1 element containing *bla*CTX-M15 resistance genes, as well as tetracycline and quinolone resistances.

Most models of antimicrobial resistance consider the spread of resistance via conjugative plasmids [29, 33, 39, 12, 21], and while some models have considered other methods of HGT such as transduction [44, 30], these models still consider ARGs located on extra-chromosomal mobilisable elements, with an associated fitness cost of carriage. The fitness cost associated with carriage in these models are consistently seen as a highly sensitive parameter. When we explore further cases of the farm flow model where other resistances are chromosomally-encoded (e.g. copper, zinc, and oxytetracycline), we observe significantly changed dynamics: we see that all resistant populations become dominant with concentrations of $\approx 10^9$CFU L^{-1}, while the concentration of sensitive bacteria fluctuates. Hence an understanding of the way ARGs are encoded in bacteria is of great importance in understanding the dynamics of AMR in the wider environment.

Metagenomic analysis of samples from the slurry tank have revealed multiple metal resistance genes (MRGs) present: *cop*, *cus*, *pco/sil* which can confer copper resistance, *czc* which can confer resistance to zinc (as well as cadmium and cobalt), as well as *mer* (mercury), *ars* (arsenic & antimony), *pbr* (lead) and *cad* (cadmium) [21]. Both *pco/sil* and *czc* genes are typically plasmid-borne, hence our modelling assumption that both copper and zinc resistance are plamid-mediated is not unreasonable. However,

it should be noted this metagenomic only informs us that these *pco/sil* and *czc* genes are present in the slurry tank, does not confirm whether these genes are associated with *E.coli* plasmids in the slurry tank or other areas of the farm. Further experiments to select for CTX and zinc resistant strains of *E.coli* sampled from the farm could be completed to evaluate this hypothesis. The usage of long-read metagenomic sequencing could be of great advantage in future work to give a better overall view of the resistance profile and types of resistance observed. This is of particular advantage in interdisciplinary studies involving modelling, since we have demonstrated that consideration of different resistance types can impact on the results of the model.

Whether ARGs are located on the chromosome or plasmid has significant consequences for the risk that the bacteria within the slurry may pose to environmental and human health. One of the biggest risk factors of AMR within dairy slurry is transmission of ARGs into the environment in slurry spreading: the potential for ARGs to transfer cross-species, to potentially pathogenic bacteria, provides indirect pathways to impact on human health. Plasmid-borne resistance genes therefore present a greater threat within this context given the possibility of transmission via conjugation, while chromosomally-encoded resistances present less risk in this regard as ARGs are unable to be transferred horizontally to other bacteria.

3.5 Conclusion

We have developed a hybrid discrete-continuous multiscale mathematical model of the dynamics of antimicrobial resistant bacteria within the flow of slurry around a typical high performance UK dairy farm and evaluated the impact of farm management practices on the emergence and spread of AMR around the farm.

Disposal of copper sulphate / zinc oxide footbaths into the waste flow is predicted to have a significant effect on AMR within bacterial communities of the slurry tank. Weekly emptying of the footbaths provide periodic bactericidal inputs (particularly due to copper concentrations well in excess of MIC) which gives rise to high magnitude fluctuations across all bacterial sub-populations modelled. When considered alongside chromosomally-encoded cefelexin-resistance, the peak concentrations of these oscillations are concurrent with observed spikes in the presence of ESBL-producing *E.coli* in the slurry tank, offering a valid hypothesis for the reason for these observed spikes.

Acknowledgements

NERC grant. Nigel Armstrong and farm staff. Other EVAL-FARMS staff and advisory board members.

References

[1] Jim O'Neill. Tackling drug resistant infections globally: final report and recommendations. Technical report, The Review on Antimicrobial Resistance, 2016.

[2] T. P. Van Boeckel, E. E. Glennon, D. Chen, M. Gilbert, T. P. Robinson, B. T. renfell, S. A. Levin, S. Bonhoeffer, and R. Laxminarayan. Reducing antimicrobial use in food animals. *Science*, 357:1350–1352, 2017.

[3] Raymond Ruimy, Anne Brisabois, Claire Bernede, David Skurnik, Saïda Barnat, Guillaume Arlet, Sonia Momcilovic, Sandrine Elbaz, Frédérique Moury, Marie-Anne Vibet, Patrice Courvalin, Didier Guillemot, and Antoine Andremont. Organic and conventional fruits and vegetables contain equivalent counts of gram-negative bacteria expressing resistance to antibacterial agents. *Environmental Microbiology*, 12(3):608–615, 2010.

[4] Samantha L. Lammie and James M. Hughes. Antimicrobial resistance, food safety, and one health: The need for convergence. *Annual Review of Food Science and Technology*, 7(1):287–312, 2016. PMID: 26772408.

[5] R. Hummel, H. Tschape, and M. Witte. Spread of plasmid-mediated nourseothricin resistance due to antibiotic use in animal husbandry. *Journal of Basic Microbiology*, 26(8):461–466, 1986.

[6] Yi-Yun Liu, Yang Wang, Timothy R Walsh, Ling-Xian Yi, Rong Zhang, James Spencer, Yohei Doi, Guobao Tian, Baolei Dong, Xianhui Huang, Lin-Feng Yu, Danxia Gu, Hongwei Ren, Xiaojie Chen, Luchao Lv, Dandan He, Hongwei Zhou, Zisen Liang, Jian-Hua Liu, and Jianzhong Shen. Emergence of plasmid-mediated colistin resistance mechanism mcr-1 in animals and human beings in china: a microbiological and molecular biological study. *The Lancet Infectious Diseases*, 16(2):161 – 168, 2016.

[7] Rongsui Gao, Yongfei Hu, Zhencui Li, Jian Sun, Qingjing Wang, Jingxia Lin, Huiyan Ye, Fei Liu, Swaminath Srinivas, Defeng Li, Baoli Zhu, Ya-Hong Liu, Guo-Bao Tian, and Youjun Feng. Dissemination and mechanism for the mcr-1 colistin resistance. *PLOS Pathogens*, 12(11):1–19, 11 2016.

[8] World Health Organisation. Antimicrobial resistance: global report on surveillance. Technical report, World Health Organisation, 2014.

[9] UK-VARSS. Veterinary Antibiotic Resistance and Sales Surveillance Report (UK-VARSS 2019). Technical report, Veterinary Medicines Directorate, New Haw, Addlestone, 2020.

[10] Veterinary Medicines Directorate. UK One Health Report - Joint report on antibiotic use and antibiotic resistance, 2013–2017. Technical report, Veterinary Medicines Directorate, New Haw, Addlestone, 2019.

[11] Bethany Griffiths, Dai White, and Georgios Oikonomou. A cross-sectional study into the prevalence of dairy cattle lameness and associated herd-level risk factors in england and wales. *Frontiers in Veterinary Science*, 5:65, 04 2018.

[12] Sankalp Arya, Alexander Williams, Saul Vazquez Reina, Charles W. Knapp, Jan-Ulrich Kreft, Jon L. Hobman, and Dov J. Stekel. Towards a general model for predicting minimal metal concentrations co-selecting for antibiotic resistance plasmids. *Environmental Pollution*, 275, 2021.

[13] Craig Baker-Austin, Meredith S. Wright, Ramunas Stepanauskas, and J.V. McArthur. Co-selection of antibiotic and metal resistance. *Trends in Microbiology*, 14(4):176–182, 2006.

[14] Julius J Medardus, Bayleyegn Z Molla, Matthew Nicol, W Morgan Morrow, Paivi J Rajala-Schultz, Rudovick Kazwala, and Wondwossen A Gebreyes. In-feed use of heavy metal micronutrients in U.S. swine production systems and its role in persistence of multidrug-resistant salmonellae. *Applied and environmental microbiology*, 80(7):2317–2325, 2014.

[15] Jon L. Hobman and Lisa C. Crossman. Bacterial antimicrobial metal ion resistance. *Journal of Medical Microbiology*, 64(5):471–497, 2015.

[16] Chandan Pal, Karishma Asiani, Sankalp Arya, Christopher Rensing, Dov J. Stekel, D.G. Joakim Larsson, and Jon L. Hobman. Metal resistance and Its association with antibiotic resistance. *Advances in microbial physiology*, 70:261–313, 2017.

[17] Keith Poole. At the Nexus of Antibiotics and Metals: The Impact of Cu and Zn on Antibiotic Activity and Resistance. *Trends in Microbiology*, 25(10):820–832, 2017.

[18] Robert Davies and Andrew Wales. Antimicrobial resistance on farms: A review including biosecurity and the potential role of disinfectants in resistance selection. *Comprehensive Reviews in Food Science and Food Safety*, 18(3):753–774, 2019.

[19] K. A. Smith and A. G. Williams. Production and management of cattle manure in the uk and implications for land application practice. *Soil Use and Management*, 32(S1):73–82, 2016.

[20] Delveen R. Ibrahim, Christine E. R. Dodd, Dov J. Stekel, Stephen J. Ramsden, and Jon L. Hobman. Multidrug resistant, extended spectrum beta-lactamase (ESBL)-producing Escherichia coli isolated from a dairy farm. *FEMS Microbiology Ecology*, 92(4), 02 2016.

[21] Michelle Baker, Alexander D. Williams, Steven P.T. Hooton, Richard Helliwell, Elizabeth King, Thomas Dodsworth, Rosa María Baena-Nogueras, Andrew Warry, Catherine A. Ortori, Henry Todman, Charlotte J. Gray-Hammerton, Alexander C.W. Pritchard, Ethan Iles, Ryan Cook, Richard D. Emes, Michael A. Jones, Theodore Kypraios, Helen West, David A. Barrett, Stephen J. Ramsden, Rachel L. Gomes, Chris Hudson, Andrew D. Millard, Sujatha Raman, Carol Morris, Christine E.R. Dodd, Jan-Ulrich Kreft, Jon L. Hobman, and Dov J. Stekel. Antimicrobial resistance in dairy slurry tanks: A critical point for measurement and control. *Environment International*, 169:107516, 2022.

[22] W.-Y. Xie, Q. Shen, and F. J. Zhao. Antibiotics and antibiotic resistance from animal manures to soil: a review. *European Journal of Soil Science*, 69(1):181–195, 2018.

[23] Holger Heuer, Heike Schmitt, and Kornelia Smalla. Antibiotic resistance gene spread due to manure application on agricultural fields. *Current Opinion In Microbiology*, 14:236–243, 2011.

[24] Sven Jechalke, Holger Heuer, Jan Siemens, Wulf Amelung, and Kornelia Smalla. Fate and effects of veterinary antibiotics in soil. *Trends in Microbiology*, 22(9):536 – 545, 2014.

[25] Hiie Nõlvak, Marika Truu, Kärt Kanger, Mailiis Tampere, Mikk Espenberg, Evelin Loit, Henn Raave, and Jaak Truu. Inorganic and organic fertilizers impact the abundance and proportion of antibiotic resistance and integron-integrase genes in agricultural grassland soil. *Science of The Total Environment*, 562:678 – 689, 2016.

[26] Yuan-Ching Tien, Bing Li, Tong Zhang, Andrew Scott, Roger Murray, Lyne Sabourin, Romain Marti, and Edward Topp. Impact of dairy manure pre-application treatment on manure composition, soil dynamics of antibiotic resistance genes, and abundance of antibiotic-resistance genes on vegetables at harvest. *Science of The Total Environment*, 581-582:32 – 39, 2017.

[27] Yu-Jing Zhang, Hang-Wei Hu, Qing-Lin Chen, Brajesh K. Singh, Hui Yan, Deli Chen, and Ji-Zheng He. Transfer of antibiotic resistance from manure-amended soils to vegetable microbiomes. *Environment International*, 130:104912, 2019.

[28] Xiang Zhao, Jinhua Wang, Lusheng Zhu, and Jun Wang. Field-based evidence for enrichment of antibiotic resistance genes and mobile genetic elements in manure-amended vegetable soils. *Science of The Total Environment*, 654:906 – 913, 2019.

[29] Michelle Baker, Jon L. Hobman, Christine E. R. Dodd, Stephen J. Ramsden, and Dov J. Stekel. Mathematical modelling of antimicrobial resistance in agricultural waste highlights importance of gene transfer rate. *FEMS Microbiology Ecology*, 92(4), 2016.

[30] Sankalp Arya, Henry Todman, Michelle Baker, Steven Hooton, Andrew Millard, Jan-Ulrich Kreft, Jon L Hobman, and Dov J Stekel. A generalised model for generalised transduction: the importance of co-evolution and stochasticity in phage mediated antimicrobial resistance transfer. *FEMS Microbiology Ecology*, 96(7), 06 2020.

[31] C.W. Lanyon, J.R King, D.J. Stekel, and R.L. Gomes. A Model to Investigate the Impact of Farm Practice on Antimicrobial Resistance in UK Dairy Farms. *Bulletin Of Mathematical Biology*, 83(36), 2021.

[32] B. A. D. van Bunnik and M. E. J. Woolhouse. Modelling the impact of curtailing antibiotic usage in food animals on antibiotic resistance in humans. *Royal Society Open Science*, 4(4):161067, 2017.

[33] Victoriya V. Volkova, Cristina Lanzas, Zhao Lu, and Yrjö Tapio Gröhn. Mathematical Model of Plasmid-Mediated Resistance to Ceftiofur in Commensal Enteric Escherichia coli of Cattle. *PLoS ONE*, 7(5), 2012.

[34] A. Hughes, C. Morris, and S Seymour. Introduction. In *Ethnography and rural research*, pages 1–27. The Countryside and Community Press, 2000.

[35] R. Helliwell, C. Morris, and S. Raman. Can resistant infections be perceptible in UK dairy farming? *Palgrave Communications*, 5(1):1–9, 2019.

[36] R. Helliwell, C. Morris, and S. Raman. Antibiotic stewardship and its implications for agricultural animal-human relationships: Insights from an intensive dairy farm in England. *Journal Of Rural Studies*, 78:441–456, 2020.

[37] National Research Council. *Nutrient Requirements of Dairy Cattle: Seventh Revised Edition, 2001.* The National Academies Press, Washington, DC, 2001.

[38] MATLAB. *version 9.9.0 (R2020b).* The MathWorks Inc., Natick, Massachusetts, 2020.

[39] Casey L. Cazer, Lucas Ducrot, Victoriya V. Volkova, and Yrjö T. Gröhn. Monte carlo simulations suggest current chlortetracycline drug-residue based withdrawal periods would not control antimicrobial resistance dissemination from feedlot to slaughterhouse. *Frontiers in Microbiology*, 8, 2017.

[40] P Ayscue, C Lanzas, R Ivanek, and Y Gröhn. Modelling on-farm escherichia coli O157:H7 population dynamics. *Foodborne Pathogens And Disease*, 6(4):461–470, 2009.

[41] M.H.M. Speijers, L.G. Baird, G.A. Finney, J. McBride, D.J. Kilpatrick, D.N. Logue, and N.E. O'Connell. Effectiveness of different footbath solutions in the treatment of digital dermatitis in dairy cows. *Journal of Dairy Science*, 93(12):5782–5791, 2010.

[42] Jmes A. Swenberg, Benjamin C. Moeller, Kun Lu, Julia E. Rager, Rebecca C. Fry, and Thomas B. Starr. Formaldehyde carcinogenicity research: 30 years and counting for mode of action, epidemiology, and cancer risk assessment. *Toxicologic Pathology*, 41(2):181–189, 2013.

[43] Orla Williams, Ian Clark, Rachel L. Gomes, Tania Perehinec, Jon L. Hobman, Dov J. Stekel, Robert Hyde, Chris Dodds, and Edward Lester. Removal of copper from cattle footbath wastewater with layered double hydroxide adsorbents as a route to antimicrobial resistance mitigation on dairy farms. *Science of The Total Environment*, 655:1139–1149, 2019.

[44] Victoriya V Volkova, Zhao Lu, Thomas Besser, and Y. T. Gröhn. Modeling the infection dynamics of bacteriophages in enteric Escherichia coli: estimating the contribution of transduction to antimicrobial gene spread. *Applied and environmental microbiology*, 80(14):4350–62, 2014.

A Model Equations

We have developed a mathematical model describing the interactions between antimicrobial resistant and sensitive bacterial populations within the flow of slurry across a typical high-performance dairy farm in the UK. This model considers 6 different areas of the farm (the main dairy shed, bulling heifer shed, underground reservoir (UR), muck heap, effluent tank and slurry tank), and in each different area we model the volume of slurry ((A1)-(A6)), the mass of metals within the slurry ((A7)-(A12)), the mass of antibiotics within the slurry ((A13)-(A18)) and the populations of sensitive and resistant *E.coli* ((A19)-(A40)), giving a system of 126 ordinary differential equations.

Volume Flow

(A1)-(A6)

$$\begin{aligned}\frac{dV_{\text{dairy}}}{dt} = a - \rho V_{\text{dairy}} + \frac{\sigma V_{\text{UR}}}{2} + \Theta\left(T_{\text{footbath}}\right) V_{\text{footbath}} \\ + \Theta\left(T_{\text{extra foot.}}\right) V_{\text{extra foot.}} + \Theta\left(T_{\text{Eff. flush}}\right) \frac{\left(1-\epsilon_{\text{eff}}\right) V_{\text{eff}}}{2} \ ,\end{aligned} \tag{A1}$$

$$\frac{dV_{\text{heifer}}}{dt} = b - \rho V_{\text{heifer}} + \frac{\sigma V_{\text{UR}}}{2} + \Theta\left(T_{\text{Eff. flush}}\right) \frac{\left(1-\epsilon_{\text{eff}}\right) V_{\text{eff}}}{2} \ , \tag{A2}$$

$$\frac{dV_{\text{UR}}}{dt} = \rho\left(V_{\text{dairy}} + V_{\text{heifer}}\right) - \sigma V_{\text{UR}} - \gamma V_{\text{UR}} \ , \tag{A3}$$

$$\frac{dV_{\text{muck}}}{dt} = (1-\varepsilon)\,\gamma V_{\text{UR}} - \eta V_{\text{muck}} - \kappa_{\text{muck}} V_{\text{muck}} \ , \tag{A4}$$

$$\frac{dV_{\text{eff}}}{dt} = \eta V_{\text{muck}} + \iota_{\text{silage}} - \Theta\left(T_{\text{Eff. flush}}\right)\left(1-\epsilon_{\text{eff}}\right) V_{\text{eff}} \ , \tag{A5}$$

$$\frac{dV_{\text{tank}}}{dt} = \varepsilon\gamma V_{\text{UR}} - \Theta\left(T_{\text{Tank empty}}\right)\left(1-\epsilon_{\text{Tank}}\right) V_{\text{tank}} \ , \tag{A6}$$

where $\Theta(T) = \begin{cases} 1 & t \in T \\ 0 & \text{otherwise} \end{cases}$.

Metal Mass Flow

$$\begin{aligned}\frac{dM^{[j]}_{\text{dairy}}}{dt} = a^{[j]}_{\text{feed}} - \rho M^{[j]}_{\text{dairy}} + \frac{\sigma M^{[j]}_{\text{UR}}}{2} + \Theta\left(T_{\text{footbath}}\right) a^{[j]}_{\text{footbath}} \\ + \Theta\left(T_{\text{extra foot.}}\right) a^{[j]}_{\text{extra foot.}} + \Theta\left(T_{\text{Eff. flush}}\right) \frac{\left(1-\epsilon_{\text{eff}}\right) M^{[j]}_{\text{eff}}}{2} \ ,\end{aligned} \tag{A7}$$

$$\frac{dM^{[j]}_{\text{heifer}}}{dt} = b^{[j]}_{\text{feed}} - \rho M^{[j]}_{\text{heifer}} + \frac{\sigma M^{[j]}_{\text{UR}}}{2} + \Theta\left(T_{\text{Eff. flush}}\right) \frac{\left(1-\epsilon_{\text{eff}}\right) M^{[j]}_{\text{eff}}}{2} \ , \tag{A8}$$

$$\frac{dM^{[j]}_{\text{UR}}}{dt} = \rho\left(M^{[j]}_{\text{dairy}} + M^{[j]}_{\text{heifer}}\right) - \sigma M^{[j]}_{\text{UR}} - \gamma M^{[j]}_{\text{UR}}, \tag{A9}$$

$$\frac{dM^{[j]}_{\text{muck}}}{dt} = \left(1-\varepsilon\right)\gamma M^{[j]}_{\text{UR}} - \eta M^{[j]}_{\text{muck}} - \kappa_{\text{muck}} M^{[j]}_{\text{muck}}, \tag{A10}$$

$$\frac{dM^{[j]}_{\text{eff}}}{dt} = \eta M^{[j]}_{\text{muck}} - \Theta\left(T_{\text{Effluent}}\right)\left(1-\epsilon_{\text{eff}}\right) M^{[j]}_{\text{eff}} \ , \ , \tag{A11}$$

$$\frac{dM^{[j]}_{\text{tank}}}{dt} = \varepsilon\gamma M^{[j]}_{\text{UR}} - \Theta\left(T_{\text{Tank empty}}\right)\left(1-\epsilon_{\text{Tank}}\right) M^{[j]}_{\text{tank}} \ , \tag{A12}$$

where $j \in \{\text{Cu}, \text{Zn}\}$.

Antibiotic Mass Flow

$$\frac{dA^{[j]}_{\text{dairy}}}{dt} = \ a^{[j]}\left(t\right) - \rho A^{[j]}_{\text{dairy}} + \frac{\sigma A^{[j]}_{\text{UR}}}{2} - \delta_{[j]} A^{[j]}_{\text{dairy}} + \Theta\left(T_{\text{Eff. flush}}\right) \frac{\left(1-\epsilon_{\text{eff}}\right) A^{[j]}_{\text{eff}}}{2} \ , \tag{A13}$$

$$\frac{dA^{[j]}_{\text{heifer}}}{dt} = -\rho A^{[j]}_{\text{heifer}} + \frac{\sigma A^{[j]}_{\text{UR}}}{2} - \delta_{[j]} A^{[j]}_{\text{heifer}} + \Theta\left(T_{\text{Eff. flush}}\right) \frac{\left(1-\epsilon_{\text{eff}}\right) A^{[j]}_{\text{eff}}}{2} \ , \tag{A14}$$

$$\frac{dA^{[j]}_{\text{UR}}}{dt} = \rho\left(A^{[j]}_{\text{dairy}} + A^{[j]}_{\text{heifer}}\right) - \sigma A^{[j]}_{\text{UR}} - \gamma A^{[j]}_{\text{UR}} - \delta_{[j]} A^{[j]}_{\text{UR}}, \tag{A15}$$

$$\frac{dA^{[j]}_{\text{muck}}}{dt} = \left(1-\varepsilon\right)\gamma A^{[j]}_{\text{UR}} - \eta A^{[j]}_{\text{muck}} - \kappa_{\text{muck}} A^{[j]}_{\text{muck}} - \delta_{[j]} A^{[j]}_{\text{muck}}, \tag{A16}$$

$$\frac{dA^{[j]}_{\text{eff}}}{dt} = \eta A^{[j]}_{\text{muck}} - \delta_{[j]} A^{[j]}_{\text{eff}} - \Theta\left(T_{\text{Effluent}}\right)\left(1-\epsilon_{\text{eff}}\right) A^{[j]}_{\text{eff}} \ , \tag{A17}$$

$$\frac{dA^{[j]}_{\text{tank}}}{dt} = \varepsilon\gamma A^{[j]}_{\text{UR}} - \delta_{[j]} A^{[j]}_{\text{tank}} - \Theta\left(T_{\text{Tank empty}}\right)\left(1-\epsilon_{\text{Tank}}\right) A^{[j]}_{\text{tank}} \ , \tag{A18}$$

where $j \in \{\text{Oxy}, \text{Cex}\}$.

Bacteria

In each compartment $i \in \{\text{dairy, heifer, UR, muck, eff., tank}\}$, we shall denote bacterial populations by $R_i^{[x_1,x_2,x_3,x_4]}$, where $[x_1, x_2, x_3, x_4] \in \{0,1\}^4$ such that $x_1 = 1$ if the population is resistant to copper, while $x_1 = 0$ if it is sensitive to copper, and similarly x_2, x_3 and x_4 reflect zinc, oxytetracycline and cefalexin resistance or sensitivity respectively. We shall denote the bacterial population sensitive to all antimicrobial agents as S_i (i.e. $S_i = R_i^{[0,0,0,0]}$)

We define Ω_i as the set of all bacterial populations within the compartment i:

$$\Omega_i = \left\{ S_i, R_i^{[1,0,0,0]}, R_i^{[0,1,0,0]}, \ldots, R_i^{[1,1,1,1]} \right\},$$

We shall also define Ω_i^* as the set of all bacterial populations carrying at least one resistance within the compartment i, i.e. $\Omega_i^* = \Omega_i \ / \{S_i\}$.

We shall also describe the flow of each bacterial population, $R_i^{[x_1,x_2,x_3,x_4]}$, between the different farm areas by the function $\mathscr{F} : \Omega_i \to \mathbb{R}$ such that:

$$\mathscr{F}(R_i^{[x_1,x_2,x_3,x_4]}) = \begin{cases} a\nu_{[x_1,x_2,x_3,x_4]}\psi_{\text{E.coli}} - \rho R_{\text{dairy}}^{[x_1,x_2,x_3,x_4]} + \frac{\sigma R_{\text{UR}}^{[x_1,x_2,x_3,x_4]}}{2}, & \text{for } i = \text{dairy} \\ b\nu_{[x_1,x_2,x_3,x_4]}\psi_{\text{E.coli}} - \rho R_{\text{heifer}}^{[x_1,x_2,x_3,x_4]} + \frac{\sigma R_{\text{UR}}^{[x_1,x_2,x_3,x_4]}}{2}, & \text{for } i = \text{heifer} \\ \rho\left(R_{\text{dairy}}^{[x_1,x_2,x_3,x_4]} + R_{\text{heifer}}^{[x_1,x_2,x_3,x_4]}\right) - \sigma R_{\text{UR}}^{[x_1,x_2,x_3,x_4]} - \gamma R_{\text{UR}}^{[x_1,x_2,x_3,x_4]}, & \text{for } i = \text{UR} \\ (1-\varepsilon)\,\gamma R_{\text{UR}}^{[x_1,x_2,x_3,x_4]} - \eta R_{\text{muck}}^{[x_1,x_2,x_3,x_4]} - \kappa_{\text{muck}} R_{\text{muck}}^{[x_1,x_2,x_3,x_4]}, & \text{for } i = \text{muck} \\ \eta R_{\text{muck}}^{[x_1,x_2,x_3,x_4]}, & \text{for } i = \text{eff} \\ \varepsilon\gamma R_{\text{UR}}^{[x_1,x_2,x_3,x_4]}, & \text{for } i = \text{tank} \end{cases} \tag{A19}$$

We shall also define the effect of the discrete farm processes on each bacterial population, $R_i^{[x_1,x_2,x_3,x_4]}$, by the function $\mathscr{D} : \Omega_i \to \mathbb{R}$ such that:

$$\mathscr{D}(R_i^{[x_1,x_2,x_3,x_4]}) = \begin{cases} \Theta\left(T_{\text{Eff. flush}}\right) \frac{(1-\epsilon_{\text{eff}}) R_{\text{eff}}^{[x_1,x_2,x_3,x_4]}}{2}, & \text{for } i = \text{dairy, heifer} \\ 0, & \text{for } i = \text{UR, muck} \\ -\Theta\left(T_{\text{Eff. flush}}\right)(1-\epsilon_{\text{eff}})\, R_{\text{eff}}^{[x_1,x_2,x_3,x_4]}, & \text{for } i = \text{eff} \\ -\Theta\left(T_{\text{Tank empty}}\right)(1-\epsilon_{\text{tank}})\, R_{\text{tank}}^{[x_1,x_2,x_3,x_4]}, & \text{for } i = \text{tank} \end{cases} \tag{A20}$$

Similarly, we describe the growth and death of each bacterial population, $R_i^{[x_1,x_2,x_3,x_4]}$, by the function $\mathscr{G} : \Omega_i \to \mathbb{R}$ such that:

$$\begin{aligned}\mathscr{G}(R_i^{[x_1,x_2,x_3,x_4]}) =& rR_i^{[x_1,x_2,x_3,x_4]}) \left(1 - x_1\alpha_{[\mathrm{Cu}]} - x_2\alpha_{[\mathrm{Zn}]} - x_3\alpha_{[\mathrm{Oxy}]} - x_4\alpha_{[\mathrm{Cex}]}\right) \left(1 - \frac{N_{\mathrm{i}}}{N_{\max}}\right) \\ & \left(1 - (1 - x_3)ES_{[\mathrm{Oxy}]}\right) - \left((1 - x_1)ES_{[\mathrm{Cu}]} - (1 - x_2)ES_{[\mathrm{Zn}]} - (1 - x_4)ES_{[\mathrm{Cex}]}\right. \\ & \left. - \delta\right) R_i^{[x_1,x_2,x_3,x_4]}\end{aligned} \tag{A21}$$

Where N_{i} denotes the total bacterial population in the compartment $i \in \{$dairy, heifer, UR, muck, eff, tank$\}$, such that:

$$N_{\mathrm{i}} = \sum_{\mathscr{R}_i \in \Omega_i} \left(\mathscr{R}_i\right), \tag{A22}$$

and $E_{\mathrm{i}}^{[j]}$ (for $i \in \{$dairy, heifer, UR, muck, eff, tank$\}$ and $j \in \{$Cu, Zn, Oxy, Cex$\}$) denotes the antimicrobial effect on the bacterial growth rate in the case of bacteriostatic antibiotics (e.g. oxytetracycline), or the antimicrobial effect on the bacterial death rate in the case of bacteriocidal antimicrobials (e.g. copper, zinc or cefalexin).

$$E_{\mathrm{i}}^{[j]} = \frac{E_{\max}^{[j]} \left(A_i/V_i\right)^{H_{[j]}}}{{MIC_{[j]}}^{H_{[j]}} + \left(A_i/V_i\right)^{H_{[j]}}} \tag{A23}$$

We shall also describe the horizontal transfer of resistance between bacterial populations by the function $\mathscr{H} : \Omega_i \to \mathbb{R}$ such that:

$$\begin{aligned}\mathscr{H}\left(S_i\right) = & -\beta S_i \left(\frac{R_i^{[1,0,0,0]}}{S_i + R_i^{[1,0,0,0]}} + \frac{R_i^{[0,1,0,0]}}{S_i + R_i^{[0,1,0,0]}} + \frac{R_i^{[0,0,1,0]}}{S_i + R_i^{[0,0,1,0]}} + \frac{R_i^{[0,0,0,1]}}{S_i + R_i^{[0,0,0,1]}} + \right. \\ & \frac{R_i^{[1,1,0,0]}}{S_i + R_i^{[1,1,0,0]}} + \frac{R_i^{[1,0,1,0]}}{S_i + R_i^{[1,0,1,0]}} + \frac{R_i^{[1,0,0,1]}}{S_i + R_i^{[1,0,0,1]}} + \frac{R_i^{[0,1,1,0]}}{S_i + R_i^{[0,1,1,0]}} + \\ & \frac{R_i^{[0,1,0,1]}}{S_i + R_i^{[0,1,0,1]}} + \frac{R_i^{[0,0,1,1]}}{S_i + R_i^{[0,0,1,1]}} + \frac{R_i^{[1,1,1,0]}}{S_i + R_i^{[1,1,1,0]}} + \frac{R_i^{[1,1,0,1]}}{S_i + R_i^{[1,1,0,1]}} + \\ & \left. \frac{R_i^{[1,0,1,1]}}{S_i + R_i^{[1,0,1,1]}} + \frac{R_i^{[0,1,1,1]}}{S_i + R_i^{[0,1,1,1]}} + \frac{R_i^{[1,1,1,1]}}{S_i + R_i^{[1,1,1,1]}} \right),\end{aligned} \tag{A24}$$

$$\mathscr{H}\left(R_i^{[1,0,0,0]}\right) = \frac{\beta S_i R_i^{[1,0,0,0]}}{S_i + R_i^{[1,0,0,0]}} - \beta R_i^{[1,0,0,0]} \left(\frac{R_i^{[0,1,0,0]}}{R_i^{[1,0,0,0]} + R_i^{[0,1,0,0]}} + \frac{R_i^{[0,0,1,0]}}{R_i^{[1,0,0,0]} + R_i^{[0,0,1,0]}} + \right.$$
$$\frac{R_i^{[0,0,0,1]}}{R_i^{[1,0,0,0]} + R_i^{[0,0,0,1]}} + \frac{R_i^{[1,1,0,0]}}{R_i^{[1,0,0,0]} + R_i^{[1,1,0,0]}} + \frac{R_i^{[1,0,1,0]}}{R_i^{[1,0,0,0]} + R_i^{[1,0,1,0]}} +$$
$$\frac{R_i^{[1,0,0,1]}}{R_i^{[1,0,0,0]} + R_i^{[1,0,0,1]}} + \frac{R_i^{[0,1,1,0]}}{R_i^{[1,0,0,0]} + R_i^{[0,1,1,0]}} + \frac{R_i^{[0,1,0,1]}}{R_i^{[1,0,0,0]} + R_i^{[0,1,0,1]}} + \tag{A25}$$
$$\frac{R_i^{[0,0,1,1]}}{R_i^{[1,0,0,0]} + R_i^{[0,0,1,1]}} + \frac{R_i^{[1,1,1,0]}}{R_i^{[1,0,0,0]} + R_i^{[1,1,1,0]}} + \frac{R_i^{[1,1,0,1]}}{R_i^{[1,0,0,0]} + R_i^{[1,1,0,1]}} +$$
$$\left. \frac{R_i^{[1,0,1,1]}}{R_i^{[1,0,0,0]} + R_i^{[1,0,1,1]}} + \frac{R_i^{[0,1,1,1]}}{R_i^{[1,0,0,0]} + R_i^{[0,1,1,1]}} + \frac{R_i^{[1,1,1,1]}}{R_i^{[1,0,0,0]} + R_i^{[1,1,1,1]}} \right),$$

$$\mathscr{H}\left(R_i^{[0,1,0,0]}\right) = \frac{\beta S_i R_i^{[0,1,0,0]}}{S_i + R_i^{[0,1,0,0]}} - \beta R_i^{[0,1,0,0]} \left(\frac{R_i^{[1,0,0,0]}}{R_i^{[0,1,0,0]} + R_i^{[1,0,0,0]}} + \frac{R_i^{[0,0,1,0]}}{R_i^{[0,1,0,0]} + R_i^{[0,0,1,0]}} + \right.$$
$$\frac{R_i^{[0,0,0,1]}}{R_i^{[0,1,0,0]} + R_i^{[0,0,0,1]}} + \frac{R_i^{[1,1,0,0]}}{R_i^{[0,1,0,0]} + R_i^{[1,1,0,0]}} + \frac{R_i^{[1,0,1,0]}}{R_i^{[0,1,0,0]} + R_i^{[1,0,1,0]}} +$$
$$\frac{R_i^{[1,0,0,1]}}{R_i^{[0,1,0,0]} + R_i^{[1,0,0,1]}} + \frac{R_i^{[0,1,1,0]}}{R_i^{[0,1,0,0]} + R_i^{[0,1,1,0]}} + \frac{R_i^{[0,1,0,1]}}{R_i^{[0,1,0,0]} + R_i^{[0,1,0,1]}} + \tag{A26}$$
$$\frac{R_i^{[0,0,1,1]}}{R_i^{[0,1,0,0]} + R_i^{[0,0,1,1]}} + \frac{R_i^{[1,1,1,0]}}{R_i^{[0,1,0,0]} + R_i^{[1,1,1,0]}} + \frac{R_i^{[1,1,0,1]}}{R_i^{[0,1,0,0]} + R_i^{[1,1,0,1]}} +$$
$$\left. \frac{R_i^{[1,0,1,1]}}{R_i^{[0,1,0,0]} + R_i^{[1,0,1,1]}} + \frac{R_i^{[0,1,1,1]}}{R_i^{[0,1,0,0]} + R_i^{[0,1,1,1]}} + \frac{R_i^{[1,1,1,1]}}{R_i^{[0,1,0,0]} + R_i^{[1,1,1,1]}} \right),$$

$$\mathscr{H}\left(R_i^{[0,0,1,0]}\right) = \frac{\beta S_i R_i^{[0,0,1,0]}}{S_i + R_i^{[0,0,1,0]}} - \beta R_i^{[0,0,1,0]} \left(\frac{R_i^{[1,0,0,0]}}{R_i^{[0,0,1,0]} + R_i^{[1,0,0,0]}} + \frac{R_i^{[0,1,0,0]}}{R_i^{[0,0,1,0]} + R_i^{[0,1,0,0]}} + \right.$$
$$\frac{R_i^{[0,0,0,1]}}{R_i^{[0,0,1,0]} + R_i^{[0,0,0,1]}} + \frac{R_i^{[1,1,0,0]}}{R_i^{[0,0,1,0]} + R_i^{[1,1,0,0]}} + \frac{R_i^{[1,0,1,0]}}{R_i^{[0,0,1,0]} + R_i^{[1,0,1,0]}} +$$
$$\frac{R_i^{[1,0,0,1]}}{R_i^{[0,0,1,0]} + R_i^{[1,0,0,1]}} + \frac{R_i^{[0,1,1,0]}}{R_i^{[0,0,1,0]} + R_i^{[0,1,1,0]}} + \frac{R_i^{[0,1,0,1]}}{R_i^{[0,0,1,0]} + R_i^{[0,1,0,1]}} + \tag{A27}$$
$$\frac{R_i^{[0,0,1,1]}}{R_i^{[0,0,1,0]} + R_i^{[0,0,1,1]}} + \frac{R_i^{[1,1,1,0]}}{R_i^{[0,0,1,0]} + R_i^{[1,1,1,0]}} + \frac{R_i^{[1,1,0,1]}}{R_i^{[0,0,1,0]} + R_i^{[1,1,0,1]}} +$$
$$\left. \frac{R_i^{[1,0,1,1]}}{R_i^{[0,0,1,0]} + R_i^{[1,0,1,1]}} + \frac{R_i^{[0,1,1,1]}}{R_i^{[0,0,1,0]} + R_i^{[0,1,1,1]}} + \frac{R_i^{[1,1,1,1]}}{R_i^{[0,0,1,0]} + R_i^{[1,1,1,1]}} \right),$$

$$\mathscr{H}\left(R_i^{[0,0,0,1]}\right) = \frac{\beta S_i R_i^{[0,0,0,1]}}{S_i + R_i^{[0,0,0,1]}} - \beta R_i^{[0,0,0,1]} \left(\frac{R_i^{[1,0,0,0]}}{R_i^{[0,0,0,1]} + R_i^{[1,0,0,0]}} + \frac{R_i^{[0,1,0,0]}}{R_i^{[0,0,0,1]} + R_i^{[0,1,0,0]}} + \right.$$
$$\frac{R_i^{[0,0,1,0]}}{R_i^{[0,0,0,1]} + R_i^{[0,0,1,0]}} + \frac{R_i^{[1,1,0,0]}}{R_i^{[0,0,0,1]} + R_i^{[1,1,0,0]}} + \frac{R_i^{[1,0,1,0]}}{R_i^{[0,0,0,1]} + R_i^{[1,0,1,0]}} +$$
$$\frac{R_i^{[1,0,0,1]}}{R_i^{[0,0,0,1]} + R_i^{[1,0,0,1]}} + \frac{R_i^{[0,1,1,0]}}{R_i^{[0,0,0,1]} + R_i^{[0,1,1,0]}} + \frac{R_i^{[0,1,0,1]}}{R_i^{[0,0,0,1]} + R_i^{[0,1,0,1]}} +$$
$$\frac{R_i^{[0,0,1,1]}}{R_i^{[0,0,0,1]} + R_i^{[0,0,1,1]}} + \frac{R_i^{[1,1,1,0]}}{R_i^{[0,0,0,1]} + R_i^{[1,1,1,0]}} + \frac{R_i^{[1,1,0,1]}}{R_i^{[0,0,0,1]} + R_i^{[1,1,0,1]}} +$$
$$\left. \frac{R_i^{[1,0,1,1]}}{R_i^{[0,0,0,1]} + R_i^{[1,0,1,1]}} + \frac{R_i^{[0,1,1,1]}}{R_i^{[0,0,0,1]} + R_i^{[0,1,1,1]}} + \frac{R_i^{[1,1,1,1]}}{R_i^{[0,0,0,1]} + R_i^{[1,1,1,1]}} \right), \tag{A28}$$

$$\mathscr{H}\left(R_i^{[1,1,0,0]}\right) = \beta R_i^{[1,1,0,0]} \left(\frac{S_i}{S_i + R_i^{[1,1,0,0]}} + \frac{R_i^{[1,0,0,0]}}{R_i^{[1,0,0,0]} + R_i^{[1,1,0,0]}} + \frac{R_i^{[0,1,0,0]}}{R_i^{[0,1,0,0]} + R_i^{[1,1,0,0]}} \right) +$$
$$2\frac{\beta R_i^{[1,0,0,0]} R_i^{[0,1,0,0]}}{R_i^{[1,0,0,0]} + R_i^{[0,1,0,0]}} - \beta R_i^{[1,1,0,0]} \left(\frac{R_i^{[0,0,1,0]}}{R_i^{[1,1,0,0]} + R_i^{[0,0,1,0]}} + \right.$$
$$\frac{R_i^{[0,0,0,1]}}{R_i^{[1,1,0,0]} + R_i^{[0,0,0,1]}} + \frac{R_i^{[1,0,1,0]}}{R_i^{[1,1,0,0]} + R_i^{[1,0,1,0]}} + \frac{R_i^{[1,0,0,1]}}{R_i^{[1,1,0,0]} + R_i^{[1,0,0,1]}} +$$
$$\frac{R_i^{[0,1,1,0]}}{R_i^{[1,1,0,0]} + R_i^{[0,1,1,0]}} + \frac{R_i^{[0,1,0,1]}}{R_i^{[1,1,0,0]} + R_i^{[0,1,0,1]}} + \frac{R_i^{[0,0,1,1]}}{R_i^{[1,1,0,0]} + R_i^{[0,0,1,1]}} +$$
$$\frac{R_i^{[1,1,1,0]}}{R_i^{[1,1,0,0]} + R_i^{[1,1,1,0]}} + \frac{R_i^{[1,1,0,1]}}{R_i^{[1,1,0,0]} + R_i^{[1,1,0,1]}} + \frac{R_i^{[1,0,1,1]}}{R_i^{[1,1,0,0]} + R_i^{[1,0,1,1]}} +$$
$$\left. \frac{R_i^{[0,1,1,1]}}{R_i^{[1,1,0,0]} + R_i^{[0,1,1,1]}} + \frac{R_i^{[1,1,1,1]}}{R_i^{[1,1,0,0]} + R_i^{[1,1,1,1]}} \right), \tag{A29}$$

$$\mathscr{H}\left(R_i^{[1,0,1,0]}\right) = \beta R_i^{[1,0,1,0]} \left(\frac{S_i}{S_i + R_i^{[1,0,1,0]}} + \frac{R_i^{[1,0,0,0]}}{R_i^{[1,0,0,0]} + R_i^{[1,0,1,0]}} + \frac{R_i^{[0,0,1,0]}}{R_i^{[0,0,1,0]} + R_i^{[1,0,1,0]}} \right) +$$
$$2\frac{\beta R_i^{[1,0,0,0]} R_i^{[0,0,1,0]}}{R_i^{[1,0,0,0]} + R_i^{[0,0,1,0]}} - \beta R_i^{[1,0,1,0]} \left(\frac{R_i^{[0,1,0,0]}}{R_i^{[1,0,1,0]} + R_i^{[0,1,0,0]}} + \right.$$
$$\frac{R_i^{[0,0,0,1]}}{R_i^{[1,0,1,0]} + R_i^{[0,0,0,1]}} + \frac{R_i^{[1,1,0,0]}}{R_i^{[1,0,1,0]} + R_i^{[1,1,0,0]}} + \frac{R_i^{[1,0,0,1]}}{R_i^{[1,0,1,0]} + R_i^{[1,0,0,1]}} +$$
$$\frac{R_i^{[0,1,1,0]}}{R_i^{[1,0,1,0]} + R_i^{[0,1,1,0]}} + \frac{R_i^{[0,1,0,1]}}{R_i^{[1,0,1,0]} + R_i^{[0,1,0,1]}} + \frac{R_i^{[0,0,1,1]}}{R_i^{[1,0,1,0]} + R_i^{[0,0,1,1]}} +$$
$$\frac{R_i^{[1,1,1,0]}}{R_i^{[1,0,1,0]} + R_i^{[1,1,1,0]}} + \frac{R_i^{[1,1,0,1]}}{R_i^{[1,0,1,0]} + R_i^{[1,1,0,1]}} + \frac{R_i^{[1,0,1,1]}}{R_i^{[1,0,1,0]} + R_i^{[1,0,1,1]}} +$$
$$\left. \frac{R_i^{[0,1,1,1]}}{R_i^{[1,0,1,0]} + R_i^{[0,1,1,1]}} + \frac{R_i^{[1,1,1,1]}}{R_i^{[1,0,1,0]} + R_i^{[1,1,1,1]}} \right), \tag{A30}$$

$$\mathscr{H}\left(R_i^{[1,0,0,1]}\right) = \beta R_i^{[1,0,0,1]}\left(\frac{S_i}{S_i+R_i^{[1,0,0,1]}}+\frac{R_i^{[1,0,0,0]}}{R_i^{[1,0,0,0]}+R_i^{[1,0,0,1]}}+\frac{R_i^{[0,0,0,1]}}{R_i^{[0,0,1,0]}+R_i^{[1,0,0,1]}}\right)+$$
$$2\frac{\beta R_i^{[1,0,0,0]}R_i^{[0,0,0,1]}}{R_i^{[1,0,0,0]}+R_i^{[0,0,0,1]}}-\beta R_i^{[1,0,0,1]}\left(\frac{R_i^{[0,1,0,0]}}{R_i^{[1,0,0,1]}+R_i^{[0,1,0,0]}}+\right.$$
$$\frac{R_i^{[0,0,1,0]}}{R_i^{[1,0,0,1]}+R_i^{[0,0,1,0]}}+\frac{R_i^{[1,1,0,0]}}{R_i^{[1,0,0,1]}+R_i^{[1,1,0,0]}}+\frac{R_i^{[1,0,1,0]}}{R_i^{[1,0,0,1]}+R_i^{[1,0,1,0]}}+$$
$$\frac{R_i^{[0,1,1,0]}}{R_i^{[1,0,0,1]}+R_i^{[0,1,1,0]}}+\frac{R_i^{[0,1,0,1]}}{R_i^{[1,0,0,1]}+R_i^{[0,1,0,1]}}+\frac{R_i^{[0,0,1,1]}}{R_i^{[1,0,0,1]}+R_i^{[0,0,1,1]}}+$$
$$\frac{R_i^{[1,1,1,0]}}{R_i^{[1,0,0,1]}+R_i^{[1,1,1,0]}}+\frac{R_i^{[1,1,0,1]}}{R_i^{[1,0,0,1]}+R_i^{[1,1,0,1]}}+\frac{R_i^{[1,0,1,1]}}{R_i^{[1,0,0,1]}+R_i^{[1,0,1,1]}}+$$
$$\left.\frac{R_i^{[0,1,1,1]}}{R_i^{[1,0,0,1]}+R_i^{[0,1,1,1]}}+\frac{R_i^{[1,1,1,1]}}{R_i^{[1,0,0,1]}+R_i^{[1,1,1,1]}}\right), \tag{A31}$$

$$\mathscr{H}\left(R_i^{[0,1,1,0]}\right) = \beta R_i^{[0,1,1,0]}\left(\frac{S_i}{S_i+R_i^{[0,1,1,0]}}+\frac{R_i^{[0,1,0,0]}}{R_i^{[0,1,0,0]}+R_i^{[0,1,1,0]}}+\frac{R_i^{[0,0,1,0]}}{R_i^{[0,0,1,0]}+R_i^{[0,1,1,0]}}\right)+$$
$$2\frac{\beta R_i^{[0,1,0,0]}R_i^{[0,0,1,0]}}{R_i^{[0,1,0,0]}+R_i^{[0,0,1,0]}}-\beta R_i^{[0,1,1,0]}\left(\frac{R_i^{[1,0,0,0]}}{R_i^{[0,1,1,0]}+R_i^{[1,0,0,0]}}+\right.$$
$$\frac{R_i^{[0,0,0,1]}}{R_i^{[0,1,1,0]}+R_i^{[0,0,0,1]}}+\frac{R_i^{[1,1,0,0]}}{R_i^{[0,1,1,0]}+R_i^{[1,1,0,0]}}+\frac{R_i^{[1,0,1,0]}}{R_i^{[0,1,1,0]}+R_i^{[1,0,1,0]}}+$$
$$\frac{R_i^{[1,0,0,1]}}{R_i^{[0,1,1,0]}+R_i^{[1,0,0,1]}}+\frac{R_i^{[0,1,0,1]}}{R_i^{[0,1,1,0]}+R_i^{[0,1,0,1]}}+\frac{R_i^{[0,0,1,1]}}{R_i^{[0,1,1,0]}+R_i^{[0,0,1,1]}}+$$
$$\frac{R_i^{[1,1,1,0]}}{R_i^{[0,1,1,0]}+R_i^{[1,1,1,0]}}+\frac{R_i^{[1,1,0,1]}}{R_i^{[0,1,1,0]}+R_i^{[1,1,0,1]}}+\frac{R_i^{[1,0,1,1]}}{R_i^{[0,1,1,0]}+R_i^{[1,0,1,1]}}+$$
$$\left.\frac{R_i^{[0,1,1,1]}}{R_i^{[0,1,1,0]}+R_i^{[0,1,1,1]}}+\frac{R_i^{[1,1,1,1]}}{R_i^{[0,1,1,0]}+R_i^{[1,1,1,1]}}\right), \tag{A32}$$

$$\mathscr{H}\left(R_i^{[0,1,0,1]}\right) = \beta R_i^{[0,1,0,1]}\left(\frac{S_i}{S_i+R_i^{[0,1,0,1]}}+\frac{R_i^{[0,1,0,0]}}{R_i^{[0,1,0,0]}+R_i^{[0,1,0,1]}}+\frac{R_i^{[0,0,0,1]}}{R_i^{[0,0,1,0]}+R_i^{[0,1,0,1]}}\right)+$$
$$2\frac{\beta R_i^{[0,1,0,0]}R_i^{[0,0,0,1]}}{R_i^{[0,1,0,0]}+R_i^{[0,0,0,1]}}-\beta R_i^{[0,1,0,1]}\left(\frac{R_i^{[1,0,0,0]}}{R_i^{[0,1,0,1]}+R_i^{[1,0,0,0]}}+\right.$$
$$\frac{R_i^{[0,0,1,0]}}{R_i^{[0,1,0,1]}+R_i^{[0,0,1,0]}}+\frac{R_i^{[1,1,0,0]}}{R_i^{[0,1,0,1]}+R_i^{[1,1,0,0]}}+\frac{R_i^{[1,0,1,0]}}{R_i^{[0,1,0,1]}+R_i^{[1,0,1,0]}}+$$
$$\frac{R_i^{[1,0,0,1]}}{R_i^{[0,1,0,1]}+R_i^{[1,0,0,1]}}+\frac{R_i^{[0,1,1,0]}}{R_i^{[0,1,0,1]}+R_i^{[0,1,1,0]}}+\frac{R_i^{[0,0,1,1]}}{R_i^{[0,1,0,1]}+R_i^{[0,0,1,1]}}+$$
$$\frac{R_i^{[1,1,1,0]}}{R_i^{[0,1,0,1]}+R_i^{[1,1,1,0]}}+\frac{R_i^{[1,1,0,1]}}{R_i^{[0,1,0,1]}+R_i^{[1,1,0,1]}}+\frac{R_i^{[1,0,1,1]}}{R_i^{[0,1,0,1]}+R_i^{[1,0,1,1]}}+$$
$$\left.\frac{R_i^{[0,1,1,1]}}{R_i^{[0,1,0,1]}+R_i^{[0,1,1,1]}}+\frac{R_i^{[1,1,1,1]}}{R_i^{[0,1,0,1]}+R_i^{[1,1,1,1]}}\right), \tag{A33}$$

$$\mathscr{H}\left(R_i^{[0,0,1,1]}\right) = \beta R_i^{[0,0,1,1]}\left(\frac{S_i}{S_i+R_i^{[0,0,1,1]}}+\frac{R_i^{[0,0,1,0]}}{R_i^{[0,0,1,0]}+R_i^{[0,0,1,1]}}+\frac{R_i^{[0,0,0,1]}}{R_i^{[0,0,1,0]}+R_i^{[0,0,1,1]}}\right)+$$
$$2\frac{\beta R_i^{[0,0,1,0]}R_i^{[0,0,0,1]}}{R_i^{[0,0,1,0]}+R_i^{[0,0,0,1]}}-\beta R_i^{[0,0,1,1]}\left(\frac{R_i^{[1,0,0,0]}}{R_i^{[0,0,1,1]}+R_i^{[1,0,0,0]}}+\right.$$
$$\frac{R_i^{[0,1,0,0]}}{R_i^{[0,0,1,1]}+R_i^{[0,1,0,0]}}+\frac{R_i^{[1,1,0,0]}}{R_i^{[0,0,1,1]}+R_i^{[1,1,0,0]}}+\frac{R_i^{[1,0,1,0]}}{R_i^{[0,0,1,1]}+R_i^{[1,0,1,0]}}+$$
$$\frac{R_i^{[1,0,0,1]}}{R_i^{[0,0,1,1]}+R_i^{[1,0,0,1]}}+\frac{R_i^{[0,1,1,0]}}{R_i^{[0,0,1,1]}+R_i^{[0,1,1,0]}}+\frac{R_i^{[0,1,0,1]}}{R_i^{[0,0,1,1]}+R_i^{[0,1,0,1]}}+$$
$$\frac{R_i^{[1,1,1,0]}}{R_i^{[0,0,1,1]}+R_i^{[1,1,1,0]}}+\frac{R_i^{[1,1,0,1]}}{R_i^{[0,0,1,1]}+R_i^{[1,1,0,1]}}+\frac{R_i^{[1,0,1,1]}}{R_i^{[0,0,1,1]}+R_i^{[1,0,1,1]}}+$$
$$\left.\frac{R_i^{[0,1,1,1]}}{R_i^{[0,0,1,1]}+R_i^{[0,1,1,1]}}+\frac{R_i^{[1,1,1,1]}}{R_i^{[0,0,1,1]}+R_i^{[1,1,1,1]}}\right), \tag{A34}$$

$$\mathscr{H}\left(R_i^{[1,1,1,0]}\right) = \beta R_i^{[1,1,1,0]}\left(\frac{S_i}{S_i+R_i^{[1,1,1,0]}}+\frac{R_i^{[1,0,0,0]}}{R_i^{[1,0,0,0]}+R_i^{[1,1,1,0]}}+\frac{R_i^{[0,1,0,0]}}{R_i^{[0,1,0,0]}+R_i^{[1,1,1,0]}}+\right.$$
$$\frac{R_i^{[0,0,1,0]}}{R_i^{[0,0,1,0]}+R_i^{[1,1,1,0]}}+\frac{R_i^{[1,1,0,0]}}{R_i^{[1,1,0,0]}+R_i^{[1,1,1,0]}}+\frac{R_i^{[1,0,1,0]}}{R_i^{[1,0,1,0]}+R_i^{[1,1,1,0]}}+$$
$$\left.\frac{R_i^{[0,1,1,0]}}{R_i^{[0,1,1,0]}+R_i^{[1,1,1,0]}}\right)+$$
$$\beta R_i^{[1,1,0,0]}\left(\frac{R_i^{[0,0,1,0]}}{R_i^{[0,0,1,0]}+R_i^{[1,1,0,0]}}+\frac{R_i^{[1,0,1,0]}}{R_i^{[1,0,1,0]}+R_i^{[1,1,0,0]}}+\frac{R_i^{[0,1,1,0]}}{R_i^{[1,0,1,0]}+R_i^{[1,1,0,0]}}\right)+$$
$$\beta R_i^{[1,0,1,0]}\left(\frac{R_i^{[0,1,0,0]}}{R_i^{[0,1,0,0]}+R_i^{[1,0,1,0]}}+\frac{R_i^{[1,1,0,0]}}{R_i^{[1,1,0,0]}+R_i^{[1,0,1,0]}}+\frac{R_i^{[0,1,1,0]}}{R_i^{[0,1,1,0]}+R_i^{[1,0,1,0]}}\right)+$$
$$\beta R_i^{[0,1,1,0]}\left(\frac{R_i^{[1,0,0,0]}}{R_i^{[1,0,0,0]}+R_i^{[0,1,1,0]}}+\frac{R_i^{[1,1,0,0]}}{R_i^{[1,1,0,0]}+R_i^{[0,1,1,0]}}+\frac{R_i^{[1,0,1,0]}}{R_i^{[1,0,1,0]}+R_i^{[0,1,1,0]}}\right)+$$
$$\frac{\beta R_i^{[1,0,0,0]}R_i^{[0,1,1,0]}}{R_i^{[1,0,0,0]}+R_i^{[0,1,1,0]}}+\frac{\beta R_i^{[0,1,0,0]}R_i^{[1,0,1,0]}}{R_i^{[0,1,0,0]}+R_i^{[1,0,1,0]}}+\frac{\beta R_i^{[0,0,1,0]}R_i^{[1,1,0,0]}}{R_i^{[0,0,1,0]}+R_i^{[1,1,0,0]}}-$$
$$\beta R_i^{[1,1,1,0]}\left(\frac{R_i^{[0,0,0,1]}}{R_i^{[0,0,0,1]}+R_i^{[1,1,1,0]}}+\frac{R_i^{[1,0,0,1]}}{R_i^{[1,0,0,1]}+R_i^{[1,1,1,0]}}+\frac{R_i^{[0,1,0,1]}}{R_i^{[0,1,0,1]}+R_i^{[1,1,1,0]}}+\right.$$
$$\frac{R_i^{[0,0,1,1]}}{R_i^{[0,0,1,1]}+R_i^{[1,1,1,0]}}+\frac{R_i^{[1,1,0,1]}}{R_i^{[1,1,0,1]}+R_i^{[1,1,1,0]}}+\frac{R_i^{[1,0,1,1]}}{R_i^{[1,0,1,1]}+R_i^{[1,1,1,0]}}+$$
$$\left.\frac{R_i^{[0,1,1,1]}}{R_i^{[0,1,1,1]}+R_i^{[1,1,1,0]}}+\frac{R_i^{[1,1,1,1]}}{R_i^{[1,1,1,1]}+R_i^{[1,1,1,0]}}\right), \tag{A35}$$

$$
\begin{aligned}
\mathscr{H}\left(R_i^{[1,1,0,1]}\right) = \beta R_i^{[1,1,0,1]} \Bigg(& \frac{S_i}{S_i + R_i^{[1,1,0,1]}} + \frac{R_i^{[1,0,0,0]}}{R_i^{[1,0,0,0]} + R_i^{[1,1,0,1]}} + \frac{R_i^{[0,1,0,0]}}{R_i^{[0,1,0,0]} + R_i^{[1,1,0,1]}} + \\
& \frac{R_i^{[0,0,0,1]}}{R_i^{[0,0,0,1]} + R_i^{[1,1,0,1]}} + \frac{R_i^{[1,1,0,0]}}{R_i^{[1,1,0,0]} + R_i^{[1,1,0,1]}} + \frac{R_i^{[1,0,0,1]}}{R_i^{[1,0,0,1]} + R_i^{[1,1,0,1]}} + \\
& \frac{R_i^{[0,1,0,1]}}{R_i^{[0,1,0,1]} + R_i^{[1,1,0,1]}} \Bigg) + \\
\beta R_i^{[1,1,0,0]} & \left(\frac{R_i^{[0,0,0,1]}}{R_i^{[0,0,0,1]} + R_i^{[1,1,0,0]}} + \frac{R_i^{[1,0,0,1]}}{R_i^{[1,0,0,1]} + R_i^{[1,1,0,0]}} + \frac{R_i^{[0,1,0,1]}}{R_i^{[0,1,0,1]} + R_i^{[1,1,0,0]}} \right) + \\
\beta R_i^{[1,0,0,1]} & \left(\frac{R_i^{[0,1,0,0]}}{R_i^{[0,1,0,0]} + R_i^{[1,0,0,1]}} + \frac{R_i^{[1,1,0,0]}}{R_i^{[1,1,0,0]} + R_i^{[1,0,0,1]}} + \frac{R_i^{[0,1,0,1]}}{R_i^{[0,1,0,1]} + R_i^{[1,0,0,1]}} \right) + \\
\beta R_i^{[0,1,0,1]} & \left(\frac{R_i^{[1,0,0,0]}}{R_i^{[1,0,0,0]} + R_i^{[0,1,0,1]}} + \frac{R_i^{[1,1,0,0]}}{R_i^{[1,1,0,0]} + R_i^{[0,1,0,1]}} + \frac{R_i^{[1,0,0,1]}}{R_i^{[1,0,0,1]} + R_i^{[0,1,0,1]}} \right) + \\
& \frac{\beta R_i^{[1,0,0,0]} R_i^{[0,1,0,1]}}{R_i^{[1,0,0,0]} + R_i^{[0,1,0,1]}} + \frac{\beta R_i^{[0,1,0,0]} R_i^{[1,0,0,1]}}{R_i^{[0,1,0,0]} + R_i^{[1,0,0,1]}} + \frac{\beta R_i^{[0,0,0,1]} R_i^{[1,1,0,0]}}{R_i^{[0,0,0,1]} + R_i^{[1,1,0,0]}} - \\
\beta R_i^{[1,1,0,1]} & \Bigg(\frac{R_i^{[0,0,1,0]}}{R_i^{[0,0,1,0]} + R_i^{[1,1,0,1]}} + \frac{R_i^{[1,0,1,0]}}{R_i^{[1,0,1,0]} + R_i^{[1,1,0,1]}} + \frac{R_i^{[0,1,1,0]}}{R_i^{[0,1,1,0]} + R_i^{[1,1,0,1]}} + \\
& \frac{R_i^{[0,0,1,1]}}{R_i^{[0,0,1,1]} + R_i^{[1,1,0,1]}} + \frac{R_i^{[1,1,1,0]}}{R_i^{[1,1,1,0]} + R_i^{[1,1,0,1]}} + \frac{R_i^{[1,0,1,1]}}{R_i^{[1,0,1,1]} + R_i^{[1,1,0,1]}} + \\
& \frac{R_i^{[0,1,1,1]}}{R_i^{[0,1,1,1]} + R_i^{[1,1,0,1]}} + \frac{R_i^{[1,1,1,1]}}{R_i^{[1,1,1,1]} + R_i^{[1,1,0,1]}} \Bigg),
\end{aligned}
\tag{A36}
$$

$$\mathscr{H}\left(R_i^{[1,0,1,1]}\right) = \beta R_i^{[1,0,1,1]}\left(\frac{S_i}{S_i+R_i^{[1,0,1,1]}}+\frac{R_i^{[1,0,0,0]}}{R_i^{[1,0,0,0]}+R_i^{[1,0,1,1]}}+\frac{R_i^{[0,0,1,0]}}{R_i^{[0,0,1,0]}+R_i^{[1,0,1,1]}}+\right.$$
$$\frac{R_i^{[0,0,0,1]}}{R_i^{[0,0,0,1]}+R_i^{[1,0,1,1]}}+\frac{R_i^{[1,0,1,0]}}{R_i^{[1,0,1,0]}+R_i^{[1,0,1,1]}}+\frac{R_i^{[1,0,0,1]}}{R_i^{[1,0,0,1]}+R_i^{[1,0,1,1]}}+$$
$$\left.\frac{R_i^{[0,0,1,1]}}{R_i^{[0,0,1,1]}+R_i^{[1,0,1,1]}}\right)+$$
$$\beta R_i^{[1,0,1,0]}\left(\frac{R_i^{[0,0,0,1]}}{R_i^{[0,0,0,1]}+R_i^{[1,0,1,0]}}+\frac{R_i^{[1,0,0,1]}}{R_i^{[1,0,0,1]}+R_i^{[1,0,1,0]}}+\frac{R_i^{[0,0,1,1]}}{R_i^{[0,0,1,1]}+R_i^{[1,0,1,0]}}\right)+$$
$$\beta R_i^{[1,0,0,1]}\left(\frac{R_i^{[0,0,1,0]}}{R_i^{[0,0,1,0]}+R_i^{[1,0,0,1]}}+\frac{R_i^{[1,0,1,0]}}{R_i^{[1,0,1,0]}+R_i^{[1,0,0,1]}}+\frac{R_i^{[0,0,1,1]}}{R_i^{[0,0,1,1]}+R_i^{[1,0,0,1]}}\right)+$$
$$\beta R_i^{[0,0,1,1]}\left(\frac{R_i^{[1,0,0,0]}}{R_i^{[1,0,0,0]}+R_i^{[0,0,1,1]}}+\frac{R_i^{[1,0,1,0]}}{R_i^{[1,0,1,0]}+R_i^{[0,0,1,1]}}+\frac{R_i^{[1,0,0,1]}}{R_i^{[1,0,0,1]}+R_i^{[0,0,1,1]}}\right)+$$
$$\frac{\beta R_i^{[1,0,0,0]}R_i^{[0,0,1,1]}}{R_i^{[1,0,0,0]}+R_i^{[0,0,1,1]}}+\frac{\beta R_i^{[0,0,1,0]}R_i^{[1,0,0,1]}}{R_i^{[0,0,1,0]}+R_i^{[1,0,0,1]}}+\frac{\beta R_i^{[0,0,0,1]}R_i^{[1,0,1,0]}}{R_i^{[0,0,0,1]}+R_i^{[1,0,1,0]}}-$$
$$\beta R_i^{[1,0,1,1]}\left(\frac{R_i^{[0,1,0,0]}}{R_i^{[0,1,0,0]}+R_i^{[1,0,1,1]}}+\frac{R_i^{[1,1,0,0]}}{R_i^{[1,1,0,0]}+R_i^{[1,0,1,1]}}+\frac{R_i^{[0,1,1,0]}}{R_i^{[0,1,1,0]}+R_i^{[1,0,1,1]}}+\right.$$
$$\frac{R_i^{[0,1,0,1]}}{R_i^{[0,1,0,1]}+R_i^{[1,0,1,1]}}+\frac{R_i^{[1,1,1,0]}}{R_i^{[1,1,1,0]}+R_i^{[1,0,1,1]}}+\frac{R_i^{[1,1,0,1]}}{R_i^{[1,1,0,1]}+R_i^{[1,0,1,1]}}+$$
$$\left.\frac{R_i^{[0,1,1,1]}}{R_i^{[0,1,1,1]}+R_i^{[1,0,1,1]}}+\frac{R_i^{[1,1,1,1]}}{R_i^{[1,1,1,1]}+R_i^{[1,0,1,1]}}\right), \tag{A37}$$

$$
\begin{aligned}
\mathscr{H}\left(R_i^{[0,1,1,1]}\right) = \beta R_i^{[0,1,1,1]} \Bigg(& \frac{S_i}{S_i + R_i^{[0,1,1,1]}} + \frac{R_i^{[0,1,0,0]}}{R_i^{[0,1,0,0]} + R_i^{[0,1,1,1]}} + \frac{R_i^{[0,0,1,0]}}{R_i^{[0,0,1,0]} + R_i^{[0,1,1,1]}} + \\
& \frac{R_i^{[0,0,0,1]}}{R_i^{[0,0,0,1]} + R_i^{[0,1,1,1]}} + \frac{R_i^{[0,1,1,0]}}{R_i^{[0,1,1,0]} + R_i^{[0,1,1,1]}} + \frac{R_i^{[0,1,0,1]}}{R_i^{[0,1,0,1]} + R_i^{[0,1,1,1]}} + \\
& \frac{R_i^{[0,0,1,1]}}{R_i^{[0,0,1,1]} + R_i^{[0,1,1,1]}} \Bigg) + \\
\beta R_i^{[0,1,1,0]} & \left(\frac{R_i^{[0,0,0,1]}}{R_i^{[0,0,0,1]} + R_i^{[0,1,1,0]}} + \frac{R_i^{[0,1,0,1]}}{R_i^{[0,1,0,1]} + R_i^{[0,1,1,0]}} + \frac{R_i^{[0,0,1,1]}}{R_i^{[0,0,1,1]} + R_i^{[0,1,1,0]}} \right) + \\
\beta R_i^{[0,1,0,1]} & \left(\frac{R_i^{[0,0,1,0]}}{R_i^{[0,0,1,0]} + R_i^{[0,1,0,1]}} + \frac{R_i^{[0,1,1,0]}}{R_i^{[0,1,1,0]} + R_i^{[0,1,0,1]}} + \frac{R_i^{[0,0,1,1]}}{R_i^{[0,0,1,1]} + R_i^{[0,1,0,1]}} \right) + \\
\beta R_i^{[0,0,1,1]} & \left(\frac{R_i^{[0,1,0,0]}}{R_i^{[0,1,0,0]} + R_i^{[0,0,1,1]}} + \frac{R_i^{[0,1,1,0]}}{R_i^{[0,1,1,0]} + R_i^{[0,0,1,1]}} + \frac{R_i^{[0,1,0,1]}}{R_i^{[0,1,0,1]} + R_i^{[0,0,1,1]}} \right) + \\
& \frac{\beta R_i^{[0,1,0,0]} R_i^{[0,0,1,1]}}{R_i^{[0,1,0,0]} + R_i^{[0,0,1,1]}} + \frac{\beta R_i^{[0,0,1,0]} R_i^{[0,1,0,1]}}{R_i^{[0,0,1,0]} + R_i^{[0,1,0,1]}} + \frac{\beta R_i^{[0,0,0,1]} R_i^{[0,1,1,0]}}{R_i^{[0,0,0,1]} + R_i^{[0,1,1,0]}} - \\
\beta R_i^{[0,1,1,1]} \Bigg(& \frac{R_i^{[1,0,0,0]}}{R_i^{[1,0,0,0]} + R_i^{[0,1,1,1]}} + \frac{R_i^{[1,1,0,0]}}{R_i^{[1,1,0,0]} + R_i^{[0,1,1,1]}} + \frac{R_i^{[1,0,1,0]}}{R_i^{[1,0,1,0]} + R_i^{[0,1,1,1]}} + \\
& \frac{R_i^{[1,0,0,1]}}{R_i^{[1,0,0,1]} + R_i^{[0,1,1,1]}} + \frac{R_i^{[1,1,1,0]}}{R_i^{[1,1,1,0]} + R_i^{[0,1,1,1]}} + \frac{R_i^{[1,1,0,1]}}{R_i^{[1,1,0,1]} + R_i^{[0,1,1,1]}} + \\
& \frac{R_i^{[1,0,1,1]}}{R_i^{[1,0,1,1]} + R_i^{[0,1,1,1]}} + \frac{R_i^{[1,1,1,1]}}{R_i^{[1,1,1,1]} + R_i^{[0,1,1,1]}} \Bigg),
\end{aligned}
\tag{A38}
$$

$$\mathscr{H}\left(R_i^{[1,1,1,1]}\right) = \frac{\beta S_i R_i^{[1,1,1,1]}}{S_i + R_i^{[1,1,1,1]}} + \beta R_i^{[1,0,0,0]}\left(\frac{R_i^{[1,1,1,1]}}{R_i^{[1,0,0,0]} + R_i^{[1,1,1,1]}} + \frac{R_i^{[0,1,1,1]}}{R_i^{[1,0,0,0]} + R_i^{[0,1,1,1]}}\right) + \beta R_i^{[0,1,0,0]}\left(\frac{R_i^{[1,1,1,1]}}{R_i^{[0,1,0,0]} + R_i^{[1,1,1,1]}} + \frac{R_i^{[1,0,1,1]}}{R_i^{[0,1,0,0]} + R_i^{[1,0,1,1]}}\right) + \beta R_i^{[0,0,1,0]}\left(\frac{R_i^{[1,1,1,1]}}{R_i^{[0,0,1,0]} + R_i^{[1,1,1,1]}} + \frac{R_i^{[1,1,0,1]}}{R_i^{[0,0,1,0]} + R_i^{[1,1,0,1]}}\right) + \beta R_i^{[0,0,0,1]}\left(\frac{R_i^{[1,1,1,1]}}{R_i^{[0,0,0,1]} + R_i^{[1,1,1,1]}} + \frac{R_i^{[1,1,1,0]}}{R_i^{[0,0,0,1]} + R_i^{[1,1,1,0]}}\right) + \beta R_i^{[1,1,0,0]}\left(\frac{R_i^{[1,1,1,1]}}{R_i^{[1,1,0,0]} + R_i^{[1,1,1,1]}} + \frac{R_i^{[1,0,1,1]}}{R_i^{[1,1,0,0]} + R_i^{[1,0,1,1]}} + \frac{R_i^{[0,1,1,1]}}{R_i^{[1,1,0,0]} + R_i^{[0,1,1,1]}} + \frac{R_i^{[0,0,1,1]}}{R_i^{[1,1,0,0]} + R_i^{[0,0,1,1]}}\right) + \beta R_i^{[1,0,1,0]}\left(\frac{R_i^{[1,1,1,1]}}{R_i^{[1,0,1,0]} + R_i^{[1,1,1,1]}} + \frac{R_i^{[1,1,0,1]}}{R_i^{[1,0,1,0]} + R_i^{[1,1,0,1]}} + \frac{R_i^{[0,1,1,1]}}{R_i^{[1,0,1,0]} + R_i^{[0,1,1,1]}} + \frac{R_i^{[0,1,0,1]}}{R_i^{[1,0,1,0]} + R_i^{[0,1,0,1]}}\right) + \beta R_i^{[1,0,0,1]}\left(\frac{R_i^{[1,1,1,1]}}{R_i^{[1,0,0,1]} + R_i^{[1,1,1,1]}} + \frac{R_i^{[1,1,1,0]}}{R_i^{[1,0,0,1]} + R_i^{[1,1,1,0]}} + \frac{R_i^{[0,1,1,1]}}{R_i^{[1,0,0,1]} + R_i^{[0,1,1,1]}} + \frac{R_i^{[0,1,1,0]}}{R_i^{[1,0,0,1]} + R_i^{[0,1,1,0]}}\right) + \beta R_i^{[0,1,1,0]}\left(\frac{R_i^{[1,1,1,1]}}{R_i^{[0,1,1,0]} + R_i^{[1,1,1,1]}} + \frac{R_i^{[1,1,0,1]}}{R_i^{[0,1,1,0]} + R_i^{[1,1,0,1]}} + \frac{R_i^{[1,0,1,1]}}{R_i^{[0,1,1,0]} + R_i^{[1,0,1,1]}} + \frac{R_i^{[1,00,1]}}{R_i^{[0,1,1,0]} + R_i^{[1,0,0,1]}}\right) + \beta R_i^{[0,1,0,1]}\left(\frac{R_i^{[1,1,1,1]}}{R_i^{[0,1,0,1]} + R_i^{[1,1,1,1]}} + \frac{R_i^{[1,1,1,0]}}{R_i^{[0,1,0,1]} + R_i^{[1,1,1,0]}} + \frac{R_i^{[1,0,1,1]}}{R_i^{[0,1,0,1]} + R_i^{[1,0,1,1]}} + \frac{R_i^{[1,0,1,0]}}{R_i^{[0,1,0,1]} + R_i^{[1,0,1,0]}}\right) + \beta R_i^{[0,0,1,1]}\left(\frac{R_i^{[1,1,1,1]}}{R_i^{[0,0,1,1]} + R_i^{[1,1,1,1]}} + \frac{R_i^{[1,1,1,0]}}{R_i^{[0,0,1,1]} + R_i^{[1,1,1,0]}} + \frac{R_i^{[1,1,0,1]}}{R_i^{[0,0,1,1]} + R_i^{[1,1,0,1]}} + \frac{R_i^{[1,1,0,0]}}{R_i^{[0,0,1,1]} + R_i^{[1,1,0,0]}}\right) + \beta R_i^{[1,1,1,0]}\left(\frac{R_i^{[1,1,1,1]}}{R_i^{[1,1,1,0]} + R_i^{[1,1,1,1]}} + \frac{R_i^{[1,1,0,1]}}{R_i^{[1,1,1,0]} + R_i^{[1,1,0,1]}} + \frac{R_i^{[1,0,1,1]}}{R_i^{[1,1,1,0]} + R_i^{[1,0,1,1]}} + \frac{R_i^{[0,1,1,1]}}{R_i^{[1,1,1,0]} + R_i^{[0,1,1,1]}} + \frac{R_i^{[1,0,0,1]}}{R_i^{[1,1,1,0]} + R_i^{[1,0,0,1]}} + \frac{R_i^{[0,1,0,1]}}{R_i^{[1,1,1,0]} + R_i^{[0,1,0,1]}} + \frac{R_i^{[0,0,1,1]}}{R_i^{[1,1,1,0]} + R_i^{[0,0,1,1]}} + \frac{R_i^{[0,0,0,1]}}{R_i^{[1,1,1,0]} + R_i^{[0,0,0,1]}}\right) + \beta R_i^{[1,1,0,1]}\left(\frac{R_i^{[1,1,1,1]}}{R_i^{[1,1,0,1]} + R_i^{[1,1,1,1]}} + \frac{R_i^{[1,1,1,0]}}{R_i^{[1,1,0,1]} + R_i^{[1,1,1,0]}} + \frac{R_i^{[1,0,1,1]}}{R_i^{[1,1,0,1]} + R_i^{[1,0,1,1]}} + \frac{R_i^{[0,1,1,1]}}{R_i^{[1,1,0,1]} + R_i^{[0,1,1,1]}} + \frac{R_i^{[1,0,1,0]}}{R_i^{[1,1,0,1]} + R_i^{[1,0,1,0]}} + \frac{R_i^{[0,1,1,0]}}{R_i^{[1,1,0,1]} + R_i^{[0,1,1,0]}} + \frac{R_i^{[0,0,1,1]}}{R_i^{[1,1,0,1]} + R_i^{[0,0,1,1]}} + \frac{R_i^{[0,0,1,0]}}{R_i^{[1,1,0,1]} + R_i^{[0,0,1,0]}}\right) + \beta R_i^{[1,0,1,1]}\left(\frac{R_i^{[1,1,1,1]}}{R_i^{[1,0,1,1]} + R_i^{[1,1,1,1]}} + \frac{R_i^{[1,1,1,0]}}{R_i^{[1,0,1,1]} + R_i^{[1,1,1,0]}} + \frac{R_i^{[1,1,0,1]}}{R_i^{[1,0,1,1]} + R_i^{[1,1,0,1]}} + \frac{R_i^{[0,1,1,1]}}{R_i^{[1,0,1,1]} + R_i^{[0,1,1,1]}} + \frac{R_i^{[1,1,0,0]}}{R_i^{[1,0,1,1]} + R_i^{[1,1,0,0]}} + \frac{R_i^{[0,1,1,0]}}{R_i^{[1,0,1,1]} + R_i^{[0,1,1,0]}} + \frac{R_i^{[0,1,0,1]}}{R_i^{[1,0,1,1]} + R_i^{[0,1,0,1]}} + \frac{R_i^{[0,1,0,0]}}{R_i^{[1,0,1,1]} + R_i^{[0,1,0,0]}}\right) + \beta R_i^{[0,1,1,1]}\left(\frac{R_i^{[1,1,1,1]}}{R_i^{[0,1,1,1]} + R_i^{[1,1,1,1]}} + \frac{R_i^{[1,1,1,0]}}{R_i^{[0,1,1,1]} + R_i^{[1,1,1,0]}} + \frac{R_i^{[1,1,0,1]}}{R_i^{[0,1,1,1]} + R_i^{[1,1,0,1]}} + \frac{R_i^{[1,0,1,1]}}{R_i^{[0,1,1,1]} + R_i^{[1,0,1,1]}} + \frac{R_i^{[1,1,0,0]}}{R_i^{[0,1,1,1]} + R_i^{[1,1,0,0]}} + \frac{R_i^{[1,0,1,0]}}{R_i^{[0,1,1,1]} + R_i^{[1,0,1,0]}} + \frac{R_i^{[1,0,0,1]}}{R_i^{[0,1,1,1]} + R_i^{[1,0,0,1]}} + \frac{R_i^{[1,0,0,0]}}{R_i^{[0,1,1,1]} + R_i^{[1,0,0,0]}}\right). \tag{A39}$$

The dynamics of each bacterial population in the farm flow system can then be described by the system of equations defined by:

$$\frac{dR_i^{[x_1,x_2,x_3,x_4]}}{dt} = \mathscr{F}(R_i^{[x_1,x_2,x_3,x_4]}) + \mathscr{D}(R_i^{[x_1,x_2,x_3,x_4]}) + \mathscr{G}(R_i^{[x_1,x_2,x_3,x_4]}) + \mathscr{H}(R_i^{[x_1,x_2,x_3,x_4]}), \tag{A40}$$

where $i \in \{\text{dairy, heifer, UR, muck, eff., tank}\}$ & $[x_1, x_2, x_3, x_4] \in \{0, 1\}^4$.

Model Parameters

Parameter	Parameter Name	Parameter Values	Units	Source
	Volume Flow Parameters			
a	Main dairy shed waste volume input	1.238×10^{3}	L h^{-1}	farm observations, [8]
b	Bulling heifer shed waste volume input	1.358×10^{2}	L h^{-1}	farm observations, [8]
ρ	Scraper channel natural outflow rate	4.167×10^{-2}	h^{-1}	Assumed
γ	Pump rate from UR to slurry tank	9.625×10^{-2}	h^{-1}	farm observations, [7]
σ	Pump rate from UR to scraper channels	4.010×10^{-3}	h^{-1}	farm observations, [7]
ε	Fraction of slurry separated as liquid	0.950	-	farm observations
κ_{muck}	Muck heap emptying rate	7.500×10^{-5}	h^{-1}	farm observations
η	Muck heap effluent run off rate	2.083×10^{-5}	h^{-1}	farm observations
ι_{silage}	Volume of effluent run off from the silage clamp	2.382	L h^{-1}	farm observations

Table A1:

Parameter	Parameter Name	Parameter Values	Units	Source
Metal Parameters				
$a_{\text{feed}}^{[Cu]}$	Copper input from daily cow feed in main dairy shed	2.985×10^3	mg h^{-1}	farm observations, [1, 5]
$a_{\text{feed}}^{[Zn]}$	Zinc input from daily cow feed in main dairy shed	1.090×10^4	mg h^{-1}	farm observations, [2, 5]
$b_{\text{feed}}^{[Cu]}$	Copper input from daily cow feed in bulling heifer shed	8.954×10^2	mg h^{-1}	farm observations, [1, 5]
$b_{\text{feed}}^{[Zn]}$	Zinc input from daily cow feed in bulling heifer shed	3.269×10^3	mg h^{-1}	farm observations, [2, 5]

Table A2:

Parameter	Parameter Name	Parameter Values	Units	Source
Antibiotic Parameters				
$\delta^{[Oxy]}$	Oxytetracycline degradation rate	2.888×10^3	h^{-1}	[4]
$\delta^{[Cex]}$	Cefalexin degradation rate	1.764×10^3	h^{-1}	[4]

Table A3:

Parameter	Parameter Name	Parameter Values	Units	Source
Bacterial Parameters				
r	Specific growth rate	8.000×10^{-2}	h^{-1}	[4]
β	Horizontal gene transfer rate	1.000×10^{-6}	h^{-1}	[4]
N_{Max}	Carrying capacity	1.000×10^{10}	CFU L^{-1}	[4]
δ	Natural death rate of bacteria	4.684×10^{-2}	h^{-1}	Estimated, [4]
$\psi_{E.coli}$	Concentration of bacteria in slurry inflow	4.479×10^{7}	CFU L^{-1} h^{-1}	[4]
ν	Proportion of resistant bacteria in slurry inflow	3.178×10^{-4}	-	Estimated, [4]
$\alpha^{[Cu]}$	Fitness cost of copper resistance carried on plasmid	2.921×10^{-1}	-	Estimated, [4]
$\alpha^{[Zn]}$	Fitness cost of zinc resistance carried on plasmid	2.921×10^{-1}	-	Estimated, [4]
$\alpha^{[Oxy]}$	Fitness cost of Oxytetracycline resistance carried on plasmid	3.000×10^{-3}	-	[4]
$\alpha^{[Cex]}$	Fitness cost of Cefalexin resistance carried on plasmid	1.561×10^{-1}	-	Estimated, [4]

Table A4:

Parameter	Parameter Name	Parameter Values	Units	Source
Pharmacodynamic Parameters				
$MIC^{[Cu]}$	Minimum inhibitory concentration of copper	212.79	mg L^{-1}	[6, 3, 4]
$MIC^{[Zn]}$	Minimum inhibitory concentration of zinc	2760.31	mg L^{-1}	[6, 3, 4]
$MIC^{[Oxy]}$	Minimum inhibitory concentration of Oxytetracycline	1	mg L^{-1}	[4]
$MIC^{[Cex]}$	Minimum inhibitory concentration of Cefalexin	8	mg L^{-1}	[4]
$E_{\text{Max}}^{[Cu]}$	Maximum death rate due to copper	1.74	h^{-1}	[6, 3, 4]
$E_{\text{Max}}^{[Zn]}$	Maximum death rate due to zinc	1.37	h^{-1}	[6, 3, 4]
$E_{\text{Max}}^{[Oxy]}$	Maximum death rate due to Oxytetracycline	1	h^{-1}	[4]
$E_{\text{Max}}^{[Cex]}$	Maximum death rate due to Cefalexin	1	h^{-1}	[4]
$H^{[Cu]}$	Hill coefficient for copper	1.54	-	[6, 3, 4]
$H^{[Zn]}$	Hill coefficient for zinc	0.72	-	[6, 3, 4]
$H^{[Oxy]}$	Hill coefficient for Oxytetracycline	2	-	[4]
$H^{[Cex]}$	Hill coefficient for Cefalexin	2	-	[4]

Table A5:

Parameter	Parameter Name	Parameter Values	Units	Source
Discrete Farm Parameters				
T_{footbath}	Days on which metal footbaths are emptied into the main dairy shed scraper channels	$\{7, 14, 21, \ldots, 364\}$	days	Assumed
$T_{\text{extra foot.}}$	Days on which additional metal footbaths are emptied into the main dairy shed scraper channels	$\{21, 42, 63, \ldots, 357\}$	days	Assumed
$T_{\text{eff. flushing}}$	Days on which MHE is used to flush out the main dairy shed and bulling heifer shed scraper channels	$\{28, 56, 74, \ldots, 364\}$	days	Assumed
$T_{\text{Empty Tank}}$	Days on which the slurry tank is emptied	$\{50, 110, 170, \ldots, 350\}$	days	Assumed, [4]

Table A6:

B Sensitivity Analysis Parameter Space

Parameter	Parameter Name	Parameter Value	Reasonable Parameter Space
$\alpha^{[metal]}$	Fitness cost of metal resistance	2.921×10^{-1}	$[0, 1]$
$\alpha^{[Oxy]}$	Fitness cost of oxytetracycline resistance	3.000×10^{-3}	$[0, 1]$
$\delta^{[Oxy]}$	Degradation rate of oxytetracycline	2.888×10^{-3}	$\left[1 \times 10^{-5}, 1 \times 10^{-1}\right]$
$\alpha^{[Cex]}$	Fitness cost of cefelexin resistance	1.561×10^{-1}	$[0, 1]$
$\delta^{[Cex]}$	Degradation rate of cefelexin	1.764×10^{-3}	$\left[1 \times 10^{-5}, 1 \times 10^{-1}\right]$
ν	Proportion of resistant bacteria in waste inflow	3.178×10^{-4}	$[0, 0.3]$
r	Bacterial growth rate	8.000×10^{-2}	$[0, 0.9]$
β	Horizontal gene transfer rate	1.000×10^{-6}	$\left[1 \times 10^{-9}, 1 \times 10^{-2}\right]$
δ	Bacterial environmental death rate	4.684×10^{-2}	$\left[1.250 \times 10^{-2}, 3.360 \times 10^{-1}\right]$

Table B7: This table shows the farm flow model bacterial and antimicrobial parameters that we have explored in our parameter sensitivity analysis, Fig 3.3, and gives the parameter space which the parameters were sampled from in this analysis.

Parameter	Parameter Name	Parameter Value	Reasonable Parameter Space
τ_{tank}	Frequency of emptying of the slurry tank	60	$[0, 365]$
τ_{footbath}	Frequency of emptying of the main dairy shed metal footbaths	7	$[0, 100]$
$V^{[footbath]}$	Volume of main dairy shed metal footbaths	800	$[50, 5000]$
$\tau_{\text{eff. flushing}}$	Frequency of muck heap effluent flushing of the main dairy shed and bulling heifer shed scraper channels	28	$[0, 365]$
ω	Volume of muck heap effluent used in flushing of scraper channels	1.182×10^4	$\left[1 \times 10^2, 1 \times 10^5\right]$

Table B8: This table shows the farm flow model discrete farm management parameters that we have explored in our parameter sensitivity analysis, Fig 3.5, and gives the parameter space from which the parameters were sampled.

C Chromosomally-Encoded Resistance Model Equations

In the case where cefelexin-resistance is chromosomally encoded, the volume, metal and antibiotic model equations remain the same ((A1)-(A18)), however, the model equations describing the bacterial dynamics are different: since they are now located on the chromosome, cefelexin-resistance genes no longer bear a fitness cost (i.e. $\alpha_{[\text{Cex.}]} = 0$) and also cannot be passed on to other cells via HGT. The function $\mathscr{H}^{[0,0,0,1]} : \Omega_i \to \mathbb{R}$ describes the horizontal gene transfer processes in this case and is defined by the set of equations (C1)-(C16).

$$\begin{aligned}\mathscr{H}^{[0,0,0,1]}(S_i) = -\beta S_i \Bigg(&\frac{R_i^{[1,0,0,0]}}{S_i + R_i^{[1,0,0,0]}} + \frac{R_i^{[0,1,0,0]}}{S_i + R_i^{[0,1,0,0]}} + \frac{R_i^{[0,0,1,0]}}{S_i + R_i^{[0,0,1,0]}} + \frac{R_i^{[1,1,0,0]}}{S_i + R_i^{[1,1,0,0]}} + \\ &\frac{R_i^{[1,0,1,0]}}{S_i + R_i^{[1,0,1,0]}} + \frac{R_i^{[1,0,0,1]}}{S_i + R_i^{[1,0,0,1]}} + \frac{R_i^{[0,1,1,0]}}{S_i + R_i^{[0,1,1,0]}} + \frac{R_i^{[0,1,0,1]}}{S_i + R_i^{[0,1,0,1]}} + \\ &\frac{R_i^{[0,0,1,1]}}{S_i + R_i^{[0,0,1,1]}} + \frac{R_i^{[1,1,0,1]}}{S_i + R_i^{[1,1,0,1]}} + \frac{R_i^{[1,0,1,1]}}{S_i + R_i^{[1,0,1,1]}} + \\ &\frac{R_i^{[0,1,1,1]}}{S_i + R_i^{[0,1,1,1]}} + \frac{R_i^{[1,1,1,1]}}{S_i + R_i^{[1,1,1,1]}} \Bigg)\end{aligned}, \tag{C1}$$

$$\begin{aligned}\mathscr{H}^{[0,0,0,1]}\left(R_i^{[1,0,0,0]}\right) = &\frac{\beta S_i R_i^{[1,0,0,0]}}{S_i + R_i^{[1,0,0,0]}} + \frac{\beta S_i R_i^{[1,0,0,1]}}{S_i + R_i^{[1,0,0,1]}} - \beta R_i^{[1,0,0,0]} \Bigg(\frac{R_i^{[0,1,0,0]}}{R_i^{[1,0,0,0]} + R_i^{[0,1,0,0]}} + \\ &\frac{R_i^{[0,0,1,0]}}{R_i^{[1,0,0,0]} + R_i^{[0,0,1,0]}} + \frac{R_i^{[1,1,0,0]}}{R_i^{[1,0,0,0]} + R_i^{[1,1,0,0]}} + \frac{R_i^{[1,0,1,0]}}{R_i^{[1,0,0,0]} + R_i^{[1,0,1,0]}} + \\ &\frac{R_i^{[0,1,1,0]}}{R_i^{[1,0,0,0]} + R_i^{[0,1,1,0]}} + \frac{R_i^{[0,1,0,1]}}{R_i^{[1,0,0,0]} + R_i^{[0,1,0,1]}} + \frac{R_i^{[0,0,1,1]}}{R_i^{[1,0,0,0]} + R_i^{[0,0,1,1]}} + \\ &\frac{R_i^{[1,1,1,0]}}{R_i^{[1,0,0,0]} + R_i^{[1,1,1,0]}} + \frac{R_i^{[1,1,0,1]}}{R_i^{[1,0,0,0]} + R_i^{[1,1,0,1]}} + \frac{R_i^{[1,0,1,1]}}{R_i^{[1,0,0,0]} + R_i^{[1,0,1,1]}} + \\ &\frac{R_i^{[0,1,1,1]}}{R_i^{[1,0,0,0]} + R_i^{[0,1,1,1]}} + \frac{R_i^{[1,1,1,1]}}{R_i^{[1,0,0,0]} + R_i^{[1,1,1,1]}} \Bigg),\end{aligned} \tag{C2}$$

$$\mathscr{H}^{[0,0,0,1]}\left(R_i^{[0,1,0,0]}\right) = \frac{\beta S_i R_i^{[0,1,0,0]}}{S_i + R_i^{[0,1,0,0]}} + \frac{\beta S_i R_i^{[0,1,0,1]}}{S_i + R_i^{[0,1,0,1]}} - \beta R_i^{[0,1,0,0]} \left(\frac{R_i^{[1,0,0,0]}}{R_i^{[1,0,0,0]} + R_i^{[0,1,0,0]}} + \right.$$
$$\frac{R_i^{[0,0,1,0]}}{R_i^{[0,1,0,0]} + R_i^{[0,0,1,0]}} + \frac{R_i^{[1,1,0,0]}}{R_i^{[0,1,0,0]} + R_i^{[1,1,0,0]}} + \frac{R_i^{[1,0,1,0]}}{R_i^{[0,1,0,0]} + R_i^{[1,0,1,0]}} +$$
$$\frac{R_i^{[1,0,0,1]}}{R_i^{[0,1,0,0]} + R^{[1,0,0,1]}} + \frac{R_i^{[0,1,1,0]}}{R_i^{[0,1,0,0]} + R_i^{[0,1,1,0]}} + \frac{R_i^{[0,0,1,1]}}{R_i^{[0,1,0,0]} + R_i^{[0,0,1,1]}} + \tag{C3}$$
$$\frac{R_i^{[1,1,1,0]}}{R_i^{[0,1,0,0]} + R_i^{[1,1,1,0]}} + \frac{R_i^{[1,1,0,1]}}{R_i^{[0,1,0,0]} + R_i^{[1,1,0,1]}} + \frac{R_i^{[1,0,1,1]}}{R_i^{[0,1,0,0]} + R_i^{[1,0,1,1]}} +$$
$$\left. \frac{R_i^{[0,1,1,1]}}{R_i^{[0,1,0,0]} + R_i^{[0,1,1,1]}} + \frac{R_i^{[1,1,1,1]}}{R_i^{[0,1,0,0]} + R_i^{[1,1,1,1]}} \right),$$

$$\mathscr{H}^{[0,0,0,1]}\left(R_i^{[0,0,1,0]}\right) = \frac{\beta S_i R_i^{[0,0,1,0]}}{S_i + R_i^{[0,0,1,0]}} + \frac{\beta S_i R_i^{[0,0,1,1]}}{S_i + R_i^{[0,0,1,1]}} - \beta R_i^{[0,0,1,0]} \left(\frac{R_i^{[1,0,0,0]}}{R_i^{[1,0,0,0]} + R_i^{[0,0,1,0]}} + \right.$$
$$\frac{R_i^{[0,1,0,0]}}{R_i^{[0,1,0,0]} + R_i^{[0,0,1,0]}} + \frac{R_i^{[1,1,0,0]}}{R_i^{[0,0,1,0]} + R_i^{[1,1,0,0]}} + \frac{R_i^{[1,0,1,0]}}{R_i^{[0,0,1,0]} + R_i^{[1,0,1,0]}} +$$
$$\frac{R_i^{[1,0,0,1]}}{R_i^{[0,0,1,0]} + R_i^{[1,0,0,1]}} + \frac{R_i^{[0,1,1,0]}}{R_i^{[0,0,1,0]} + R_i^{[0,1,1,0]}} + \frac{R_i^{[0,1,0,1]}}{R_i^{[0,0,1,0]} + R_i^{[0,1,0,1]}} + \tag{C4}$$
$$\frac{R_i^{[1,1,1,0]}}{R_i^{[0,0,1,0]} + R_i^{[1,1,1,0]}} + \frac{R_i^{[1,1,0,1]}}{R_i^{[0,0,1,0]} + R_i^{[1,1,0,1]}} + \frac{R_i^{[1,0,1,1]}}{R_i^{[0,0,1,0]} + R_i^{[1,0,1,1]}} +$$
$$\left. \frac{R_i^{[0,1,1,1]}}{R_i^{[0,0,1,0]} + R_i^{[0,1,1,1]}} + \frac{R_i^{[1,1,1,1]}}{R_i^{[0,0,1,0]} + R_i^{[1,1,1,1]}} \right),$$

$$\mathscr{H}^{[0,0,0,1]}\left(R_i^{[0,0,0,1]}\right) = -\beta R_i^{[0,0,0,1]} \left(\frac{R_i^{[1,0,0,0]}}{R_i^{[0,0,0,1]} + R_i^{[1,0,0,0]}} + \frac{R_i^{[0,1,0,0]}}{R_i^{[0,0,0,1]} + R_i^{[0,1,0,0]}} + \right.$$
$$\frac{R_i^{[0,0,1,0]}}{R_i^{[0,0,0,1]} + R_i^{[0,0,1,0]}} + \frac{R_i^{[1,1,0,0]}}{R_i^{[0,0,0,1]} + R_i^{[1,1,0,0]}} + \frac{R_i^{[1,0,1,0]}}{R_i^{[0,0,0,1]} + R_i^{[1,0,1,0]}} +$$
$$\frac{R_i^{[1,0,0,1]}}{R_i^{[0,0,0,1]} + R_i^{[1,0,0,1]}} + \frac{R_i^{[0,1,1,0]}}{R_i^{[0,0,0,1]} + R_i^{[0,1,1,0]}} + \frac{R_i^{[0,1,0,1]}}{R_i^{[0,0,0,1]} + R_i^{[0,1,0,1]}} + \tag{C5}$$
$$\frac{R_i^{[0,0,1,1]}}{R_i^{[0,0,0,1]} + R_i^{[0,0,1,1]}} + \frac{R_i^{[1,1,1,0]}}{R_i^{[0,0,0,1]} + R_i^{[1,1,1,0]}} + \frac{R_i^{[1,1,0,1]}}{R_i^{[0,0,0,1]} + R_i^{[1,1,0,1]}} +$$
$$\left. \frac{R_i^{[1,0,1,1]}}{R_i^{[0,0,0,1]} + R_i^{[1,0,1,1]}} + \frac{R_i^{[0,1,1,1]}}{R_i^{[0,0,0,1]} + R_i^{[0,1,1,1]}} + \frac{R_i^{[1,1,1,1]}}{R_i^{[0,0,0,1]} + R_i^{[1,1,1,1]}} \right),$$

$$\mathscr{H}^{[0,0,0,1]}\left(R_i^{[1,1,0,0]}\right) = \frac{\beta S_i R_i^{[1,1,0,0]}}{S_i + R_i^{[1,1,0,0]}} + \frac{\beta S_i R_i^{[1,1,0,1]}}{S_i + R_i^{[1,1,0,1]}} + 2\frac{\beta R^{[1,0,0,0]} R_i^{[0,1,0,0]}}{R^{[1,0,0,0]} + R_i^{[0,1,0,0]}} +$$
$$\frac{\beta R^{[1,0,0,0]} R_i^{[1,1,0,0]}}{R^{[1,0,0,0]} + R_i^{[1,1,0,0]}} + \frac{\beta R^{[0,1,0,0]} R_i^{[1,1,0,0]}}{R^{[0,1,0,0]} + R_i^{[1,1,0,0]}} + \frac{\beta R^{[1,0,0,0]} R_i^{[0,1,0,1]}}{R^{[1,0,0,0]} + R_i^{[0,1,0,1]}} +$$
$$\frac{\beta R^{[0,1,0,0]} R_i^{[1,0,0,1]}}{R^{[0,1,0,0]} + R_i^{[1,0,0,1]}} + \frac{\beta R^{[1,0,0,0]} R_i^{[1,1,0,1]}}{R^{[1,0,0,0]} + R_i^{[1,1,0,1]}} + \frac{\beta R^{[0,1,0,0]} R_i^{[1,1,0,1]}}{R^{[0,1,0,0]} + R_i^{[1,1,0,1]}} -$$
$$\beta R_i^{[1,1,0,0]} \left(\frac{R_i^{[0,0,1,0]}}{R_i^{[0,0,1,0]} + R^{[1,1,0,0]}} + \frac{R_i^{[1,0,1,0]}}{R_i^{[1,1,0,0]} + R_i^{[1,0,1,0]}} + \right.$$
$$\frac{R_i^{[0,1,1,0]}}{R_i^{[1,1,0,0]} + R_i^{[0,1,1,0]}} + \frac{R_i^{[0,0,1,1]}}{R_i^{[1,1,0,0]} + R_i^{[0,0,1,1]}} + \frac{R_i^{[1,1,1,0]}}{R_i^{[1,1,0,0]} + R_i^{[1,1,1,0]}} +$$
$$\left. \frac{R_i^{[1,0,1,1]}}{R_i^{[1,1,0,0]} + R_i^{[1,0,1,1]}} + \frac{R_i^{[0,1,1,1]}}{R_i^{[1,1,0,0]} + R_i^{[0,1,1,1]}} + \frac{R_i^{[1,1,1,1]}}{R_i^{[1,1,0,0]} + R_i^{[1,1,1,1]}} \right), \tag{C6}$$

$$\mathscr{H}^{[0,0,0,1]}\left(R_i^{[1,0,1,0]}\right) = \frac{\beta S_i R_i^{[1,0,1,0]}}{S_i + R_i^{[1,0,1,0]}} + \frac{\beta S_i R_i^{[1,0,1,1]}}{S_i + R_i^{[1,0,1,1]}} + 2\frac{\beta R^{[1,0,0,0]} R_i^{[0,0,1,0]}}{R^{[1,0,0,0]} + R_i^{[0,0,1,0]}} +$$
$$\frac{\beta R^{[1,0,0,0]} R_i^{[1,0,1,0]}}{R^{[1,0,0,0]} + R_i^{[1,0,1,0]}} + \frac{\beta R^{[0,0,1,0]} R_i^{[1,0,1,0]}}{R^{[0,0,1,0]} + R_i^{[1,0,1,0]}} + \frac{\beta R^{[1,0,0,0]} R_i^{[0,0,1,1]}}{R^{[1,0,0,0]} + R_i^{[0,0,1,1]}} +$$
$$\frac{\beta R^{[0,0,1,0]} R_i^{[1,0,0,1]}}{R^{[0,0,1,0]} + R_i^{[1,0,0,1]}} + \frac{\beta R^{[1,0,0,0]} R_i^{[1,0,1,1]}}{R^{[1,0,0,0]} + R_i^{[1,0,1,1]}} + \frac{\beta R^{[0,0,1,0]} R_i^{[1,1,0,1]}}{R^{[0,0,1,0]} + R_i^{[1,1,0,1]}} -$$
$$\beta R_i^{[1,0,1,0]} \left(\frac{R_i^{[0,1,0,0]}}{R_i^{[0,1,0,0]} + R^{[1,0,1,0]}} + \frac{R_i^{[1,1,0,0]}}{R_i^{[1,1,0,0]} + R_i^{[1,0,1,0]}} + \right.$$
$$\frac{R_i^{[0,1,1,0]}}{R_i^{[1,0,1,0]} + R_i^{[0,1,1,0]}} + \frac{R_i^{[0,1,0,1]}}{R_i^{[1,0,1,0]} + R_i^{[0,1,0,1]}} + \frac{R_i^{[1,1,1,0]}}{R_i^{[1,0,1,0]} + R_i^{[1,1,1,0]}} +$$
$$\left. \frac{R_i^{[1,1,0,1]}}{R_i^{[1,0,1,0]} + R_i^{[1,1,0,1]}} + \frac{R_i^{[0,1,1,1]}}{R_i^{[1,0,1,0]} + R_i^{[0,1,1,1]}} + \frac{R_i^{[1,1,1,1]}}{R_i^{[1,0,1,0]} + R_i^{[1,1,1,1]}} \right) \tag{C7}$$

$$\mathscr{H}^{[0,0,0,1]}\left(R_i^{[1,0,01]}\right) = \frac{\beta R_i^{[1,0,0,0]} R_i^{[0,0,0,1]}}{R_i^{[1,0,0,0]} + R_i^{[0,0,0,1]}} + \frac{\beta R_i^{[0,0,0,1]} R_i^{[1,0,0,1]}}{R_i^{[0,0,0,1]} + R_i^{[1,0,0,1]}} - \beta R_i^{[1,0,0,1]} \left(\frac{R_i^{[0,1,0,0]}}{R_i^{[1,0,0,1]} + R_i^{[0,1,0,0]}} + \right.$$
$$\frac{R_i^{[0,0,1,0]}}{R_i^{[1,0,0,1]} + R_i^{[0,0,1,0]}} + \frac{R_i^{[1,1,0,0]}}{R_i^{[1,0,0,1]} + R_i^{[1,1,0,0]}} + \frac{R_i^{[1,0,1,0]}}{R_i^{[1,0,0,1]} + R_i^{[1,0,1,0]}} +$$
$$\frac{R_i^{[0,1,1,0]}}{R_i^{[1,0,0,1]} + R_i^{[0,1,1,0]}} + \frac{R_i^{[0,1,0,1]}}{R_i^{[1,0,0,1]} + R_i^{[0,1,0,1]}} + \frac{R_i^{[0,0,1,1]}}{R_i^{[1,0,0,1]} + R_i^{[0,0,1,1]}} +$$
$$\frac{R_i^{[1,1,1,0]}}{R_i^{[1,0,0,1]} + R_i^{[1,1,1,0]}} + \frac{R_i^{[1,1,0,1]}}{R_i^{[1,0,0,1]} + R_i^{[1,1,0,1]}} + \frac{R_i^{[1,0,1,1]}}{R_i^{[1,0,0,1]} + R_i^{[1,0,1,1]}} +$$
$$\left. \frac{R_i^{[0,1,1,1]}}{R_i^{[1,0,0,1]} + R_i^{[0,1,1,1]}} + \frac{R_i^{[1,1,1,1]}}{R_i^{[1,0,0,1]} + R_i^{[1,1,1,1]}} \right), \tag{C8}$$

$$\mathscr{H}^{[0,0,0,1]}\left(R_i^{[0,1,1,0]}\right) = \frac{\beta S_i R_i^{[0,1,1,0]}}{S_i + R_i^{[0,1,1,0]}} + \frac{\beta S_i R_i^{[0,1,1,1]}}{S_i + R_i^{[0,1,1,1]}} + 2\frac{\beta R^{[0,1,0,0]} R_i^{[0,0,1,0]}}{R^{[0,1,0,0]} + R_i^{[0,0,1,0]}} +$$
$$\frac{\beta R^{[0,1,0,0]} R_i^{[0,1,1,0]}}{R^{[0,1,0,0]} + R_i^{[0,1,1,0]}} + \frac{\beta R^{[0,0,1,0]} R_i^{[0,1,1,0]}}{R^{[0,0,1,0]} + R_i^{[0,1,1,0]}} + \frac{\beta R^{[0,1,0,0]} R_i^{[0,0,1,1]}}{R^{[0,1,0,0]} + R_i^{[0,0,1,1]}} +$$
$$\frac{\beta R^{[0,0,1,0]} R_i^{[0,1,0,1]}}{R^{[0,0,1,0]} + R_i^{[0,1,0,1]}} + \frac{\beta R^{[0,1,0,0]} R_i^{[0,1,1,1]}}{R^{[0,1,0,0]} + R_i^{[0,1,1,1]}} + \frac{\beta R^{[0,0,1,0]} R_i^{[0,1,1,1]}}{R^{[0,0,1,0]} + R_i^{[0,1,1,1]}} -$$
$$\beta R_i^{[0,1,1,0]} \left(\frac{R_i^{[1,0,0,0]}}{R_i^{[1,0,0,0]} + R^{[0,1,1,0]}} + \frac{R_i^{[1,1,0,0]}}{R_i^{[1,1,0,0]} + R_i^{[0,1,1,0]}} + \right.$$
$$\frac{R_i^{[1,0,1,0]}}{R_i^{[1,0,1,0]} + R_i^{[0,1,1,0]}} + \frac{R_i^{[1,0,0,1]}}{R_i^{[1,0,0,1]} + R_i^{[0,1,1,0]}} + \frac{R_i^{[1,1,1,0]}}{R_i^{[0,1,1,0]} + R_i^{[1,1,1,0]}} +$$
$$\left. \frac{R_i^{[1,0,1,1]}}{R_i^{[0,1,1,0]} + R_i^{[0,1,1,1]}} + \frac{R_i^{[1,1,0,1]}}{R_i^{[0,1,1,0]} + R_i^{[1,1,0,1]}} + \frac{R_i^{[1,1,1,1]}}{R_i^{[0,1,1,0]} + R_i^{[1,1,1,1]}} \right), \tag{C9}$$

$$\mathscr{H}^{[0,0,0,1]}\left(R_i^{[0,1,0,1]}\right) = \frac{\beta R_i^{[0,1,0,0]} R_i^{[0,0,0,1]}}{R_i^{[0,1,0,0]} + R_i^{[0,0,0,1]}} + \frac{\beta R_i^{[0,0,0,1]} R_i^{[0,1,0,1]}}{R_i^{[0,0,0,1]} + R_i^{[0,1,0,1]}} - \beta R_i^{[0,1,0,1]} \left(\frac{R_i^{[1,0,0,0]}}{R_i^{[1,0,0,0]} + R_i^{[0,1,0,1]}} + \right.$$
$$\frac{R_i^{[0,0,1,0]}}{R_i^{[0,0,1,0]} + R_i^{[0,1,0,1]}} + \frac{R_i^{[1,1,0,0]}}{R_i^{[1,1,0,0]} + R_i^{[0,1,0,1]}} + \frac{R_i^{[1,0,1,0]}}{R_i^{[1,0,1,0]} + R_i^{[0,1,0,1]}} +$$
$$\frac{R_i^{[1,0,0,1]}}{R^{[1,0,0,1]} + R_i^{[0,1,0,1]}} + \frac{R_i^{[0,1,1,0]}}{R_i^{[0,1,1,0]} R_i^{[0,1,0,1]}} + \frac{R_i^{[0,0,1,1]}}{R_i^{[0,1,0,1]} + R_i^{[0,0,1,1]}} +$$
$$\frac{R_i^{[1,1,1,0]}}{R_i^{[0,1,0,1]} + R_i^{[1,1,1,0]}} + \frac{R_i^{[1,1,0,1]}}{R_i^{[0,1,0,1]} + R_i^{[1,1,0,1]}} + \frac{R_i^{[1,0,1,1]}}{R_i^{[0,1,0,1]} + R_i^{[1,0,1,1]}} +$$
$$\left. \frac{R_i^{[0,1,1,1]}}{R_i^{[0,1,0,1]} + R_i^{[0,1,1,1]}} + \frac{R_i^{[1,1,1,1]}}{R_i^{[0,1,0,1]} + R_i^{[1,1,1,1]}} \right), \tag{C10}$$

$$\mathscr{H}^{[0,0,0,1]}\left(R_i^{[0,0,1,1]}\right) = \frac{\beta R_i^{[0,0,1,0]} R_i^{[0,0,0,1]}}{R_i^{[0,0,1,0]} + R_i^{[0,0,0,1]}} + \frac{\beta R_i^{[0,0,0,1]} R_i^{[0,0,1,1]}}{R_i^{[0,0,0,1]} + R_i^{[0,0,1,1]}} - \beta R_i^{[0,0,1,1]} \left(\frac{R_i^{[1,0,0,0]}}{R_i^{[1,0,0,0]} + R_i^{[0,0,1,1]}} + \right.$$
$$\frac{R_i^{[0,1,0,0]}}{R_i^{[0,1,0,0]} + R_i^{[0,0,1,1]}} + \frac{R_i^{[1,1,0,0]}}{R_i^{[1,1,0,0]} + R_i^{[0,0,1,1]}} + \frac{R_i^{[1,0,1,0]}}{R_i^{[1,0,1,0]} + R_i^{[0,0,1,1]}} +$$
$$\frac{R_i^{[1,0,0,1]}}{R_i^{[1,0,0,1]} + R_i^{[0,0,1,1]}} + \frac{R_i^{[0,1,1,0]}}{R_i^{[0,1,1,0]} + R_i^{[0,0,1,1]}} + \frac{R_i^{[0,1,0,1]}}{R_i^{[0,1,0,1]} + R_i^{[0,0,1,1]}} +$$
$$\frac{R_i^{[1,1,1,0]}}{R_i^{[0,0,1,1]} + R_i^{[1,1,1,0]}} + \frac{R_i^{[1,1,0,1]}}{R_i^{[0,0,1,1]} + R_i^{[1,1,0,1]}} + \frac{R_i^{[1,0,1,1]}}{R_i^{[0,0,1,1]} + R_i^{[1,0,1,1]}} +$$
$$\left. \frac{R_i^{[0,1,1,1]}}{R_i^{[0,0,1,1]} + R_i^{[0,1,1,1]}} + \frac{R_i^{[1,1,1,1]}}{R_i^{[0,0,1,1]} + R_i^{[1,1,1,1]}} \right), \tag{C11}$$

$$
\begin{aligned}
\mathscr{H}^{[0,0,0,1]}\left(R_i^{[1,1,1,0]}\right) = {} & \beta R_i^{[1,1,1,0]}\left(\frac{S_i}{S_i+R_i^{[1,1,1,0]}}+\frac{R_i^{[1,0,0,0]}}{R_i^{[1,0,0,0]}+R_i^{[1,1,1,0]}}+\frac{R_i^{[0,1,0,0]}}{R_i^{[0,1,0,0]}+R_i^{[1,1,1,0]}}+\right.\\
& \frac{R_i^{[0,0,1,0]}}{R_i^{[0,0,1,0]}+R_i^{[1,1,1,0]}}+\frac{R_i^{[1,1,0,0]}}{R_i^{[1,1,0,0]}+R_i^{[1,1,1,0]}}+\frac{R_i^{[1,0,1,0]}}{R_i^{[1,0,1,0]}+R_i^{[1,1,1,0]}}+\\
& \left.\frac{R_i^{[0,1,1,0]}}{R_i^{[0,1,1,0]}+R_i^{[1,1,1,0]}}\right)+\\
& \beta R_i^{[1,1,0,0]}\left(\frac{R_i^{[0,0,1,0]}}{R_i^{[0,0,1,0]}+R_i^{[1,1,0,0]}}+\frac{R_i^{[1,0,1,0]}}{R_i^{[1,0,1,0]}+R_i^{[1,1,0,0]}}+\frac{R_i^{[0,1,1,0]}}{R_i^{[0,1,1,0]}+R_i^{[1,1,0,0]}}\right)+\\
& \beta R_i^{[1,0,1,0]}\left(\frac{R_i^{[0,1,0,0]}}{R_i^{[0,0,1,0]}+R_i^{[1,0,1,0]}}+\frac{R_i^{[1,1,0,0]}}{R_i^{[1,1,0,0]}+R_i^{[1,0,1,0]}}+\frac{R_i^{[0,1,1,0]}}{R_i^{[0,1,1,0]}+R_i^{[1,0,1,0]}}\right)+\\
& \beta R_i^{[0,1,1,0]}\left(\frac{R_i^{[1,0,0,0]}}{R_i^{[1,0,0,0]}+R_i^{[0,1,1,0]}}+\frac{R_i^{[1,1,0,0]}}{R_i^{[1,1,0,0]}+R_i^{[0,1,1,0]}}+\frac{R_i^{[1,0,1,0]}}{R_i^{[1,0,1,0]}+R_i^{[0,1,1,0]}}\right)+\\
& \frac{\beta R_i^{[1,0,0,0]}R_i^{[0,1,1,0]}}{R_i^{[1,0,0,0]}+R_i^{[0,1,1,0]}}+\frac{\beta R_i^{[0,1,0,0]}R_i^{[1,0,1,0]}}{R_i^{[0,1,0,0]}+R_i^{[1,0,1,0]}}+\frac{\beta R_i^{[0,0,1,0]}R_i^{[1,1,0,0]}}{R_i^{[0,0,1,0]}+R_i^{[1,1,0,0]}}+\\
& \beta R_i^{[1,1,1,1]}\left(\frac{S_i}{S_i+R_i^{[1,1,1,1]}}+\frac{R_i^{[1,0,0,0]}}{R_i^{[1,0,0,0]}+R_i^{[1,1,1,1]}}+\frac{R_i^{[0,1,0,0]}}{R_i^{[0,1,0,0]}+R_i^{[1,1,1,1]}}+\right.\\
& \frac{R_i^{[0,0,1,0]}}{R_i^{[0,0,1,0]}+R_i^{[1,1,1,0]}}+\frac{R_i^{[1,1,0,0]}}{R_i^{[1,1,0,0]}+R_i^{[1,1,1,0]}}+\frac{R_i^{[1,0,1,0]}}{R_i^{[1,0,1,0]}+R_i^{[1,1,1,0]}}+\\
& \left.\frac{R_i^{[0,1,1,0]}}{R_i^{[0,1,1,0]}+R_i^{[1,1,1,0]}}\right)+\\
& \beta R_i^{[1,1,0,1]}\left(\frac{R_i^{[0,0,1,0]}}{R_i^{[0,0,1,0]}+R_i^{[1,1,0,1]}}+\frac{R_i^{[1,0,1,0]}}{R_i^{[1,0,1,0]}+R_i^{[1,1,0,1]}}+\frac{R_i^{[0,1,1,0]}}{R_i^{[0,1,1,0]}+R_i^{[1,1,0,1]}}\right)+\\
& \beta R_i^{[1,0,1,1]}\left(\frac{R_i^{[0,1,0,0]}}{R_i^{[0,0,1,0]}+R_i^{[1,0,1,1]}}+\frac{R_i^{[1,1,0,0]}}{R_i^{[1,1,0,0]}+R_i^{[1,0,1,1]}}+\frac{R_i^{[0,1,1,0]}}{R_i^{[0,1,1,0]}+R_i^{[1,0,1,1]}}\right)+\\
& \beta R_i^{[0,1,1,1]}\left(\frac{R_i^{[1,0,0,0]}}{R_i^{[1,0,0,0]}+R_i^{[0,1,1,1]}}+\frac{R_i^{[1,1,0,0]}}{R_i^{[1,1,0,0]}+R_i^{[0,1,1,1]}}+\frac{R_i^{[1,0,1,0]}}{R_i^{[1,0,1,0]}+R_i^{[0,1,1,1]}}\right)+\\
& \frac{\beta R_i^{[1,0,0,1]}R_i^{[0,1,1,0]}}{R_i^{[1,0,0,1]}+R_i^{[0,1,1,0]}}+\frac{\beta R_i^{[0,1,0,1]}R_i^{[1,0,1,0]}}{R_i^{[0,1,0,1]}+R_i^{[1,0,1,0]}}+\frac{\beta R_i^{[0,0,1,1]}R_i^{[1,1,0,0]}}{R_i^{[0,0,1,1]}+R_i^{[1,1,0,0]}},
\end{aligned}
\tag{C12}
$$

$$\mathscr{H}^{[0,0,0,1]}\left(R_i^{[1,1,0,1]}\right) = \beta R_i^{[0,0,0,1]}\left(\frac{R_i^{[1,1,0,1]}}{R_i^{[0,0,0,1]}+R_i^{[1,1,0,1]}}+\frac{R_i^{[1,1,0,0]}}{R_i^{[0,0,0,1]}+R_i^{[1,1,0,0]}}\right)+$$
$$\beta R_i^{[1,0,0,1]}\left(\frac{R_i^{[1,1,0,1]}}{R_i^{[1,0,0,1]}+R_i^{[1,1,0,1]}}+\frac{R_i^{[0,1,0,1]}}{R_i^{[1,0,0,1]}+R_i^{[0,1,0,1]}}+\frac{R_i^{[0,1,0,0]}}{R_i^{[1,0,0,1]}+R_i^{[0,1,0,0]}}\right)+$$
$$\beta R_i^{[0,1,0,1]}\left(\frac{R_i^{[1,1,0,1]}}{R_i^{[0,1,0,1]}+R_i^{[1,1,0,1]}}+\frac{R_i^{[1,0,0,1]}}{R_i^{[0,1,0,1]}+R_i^{[1,0,0,1]}}+\frac{R_i^{[1,0,0,0]}}{R_i^{[0,1,0,1]}+R_i^{[1,0,0,0]}}\right)-$$
$$\beta R_i^{[1,1,0,1]}\left(\frac{R_i^{[0,0,1,0]}}{R_i^{[0,0,1,0]}+R_i^{[1,1,0,1]}}+\frac{R_i^{[1,0,1,0]}}{R_i^{[1,0,1,0]}+R_i^{[1,1,0,1]}}+\frac{R_i^{[0,1,1,0]}}{R_i^{[0,1,1,0]}+R_i^{[1,1,0,1]}}+\right.$$
$$\frac{R_i^{[0,0,1,1]}}{R_i^{[0,0,1,1]}+R_i^{[1,1,0,1]}}+\frac{R_i^{[1,1,1,0]}}{R_i^{[1,1,1,0]}+R_i^{[1,1,0,1]}}+\frac{R_i^{[1,0,1,1]}}{R_i^{[1,0,1,1]}+R_i^{[1,1,0,1]}}+$$
$$\left.\frac{R_i^{[0,1,1,1]}}{R_i^{[0,1,1,1]}+R_i^{[1,1,0,1]}}+\frac{R_i^{[1,1,1,1]}}{R_i^{[1,1,1,1]}+R_i^{[1,1,0,1]}}\right), \tag{C13}$$

$$\mathscr{H}^{[0,0,0,1]}\left(R_i^{[1,0,1,1]}\right) = \beta R_i^{[0,0,0,1]}\left(\frac{R_i^{[1,0,1,1]}}{R_i^{[0,0,0,1]}+R_i^{[1,0,1,1]}}+\frac{R_i^{[1,0,1,0]}}{R_i^{[0,0,0,1]}+R_i^{[1,0,1,0]}}\right)+$$
$$\beta R_i^{[1,0,0,1]}\left(\frac{R_i^{[1,0,1,1]}}{R_i^{[1,0,0,1]}+R_i^{[1,0,1,1]}}+\frac{R_i^{[0,0,1,1]}}{R_i^{[1,0,0,1]}+R_i^{[0,0,1,1]}}+\frac{R_i^{[0,0,1,0]}}{R_i^{[1,0,0,1]}+R_i^{[0,0,1,0]}}\right)+$$
$$\beta R_i^{[0,0,1,1]}\left(\frac{R_i^{[1,0,1,1]}}{R_i^{[0,0,1,1]}+R_i^{[1,0,1,1]}}+\frac{R_i^{[1,0,0,1]}}{R_i^{[0,0,1,1]}+R_i^{[1,0,0,1]}}+\frac{R_i^{[1,0,0,0]}}{R_i^{[0,0,1,1]}+R_i^{[1,0,0,0]}}\right)-$$
$$\beta R_i^{[1,0,1,1]}\left(\frac{R_i^{[0,1,0,0]}}{R_i^{[0,1,0,0]}+R_i^{[1,0,1,1]}}+\frac{R_i^{[1,1,0,0]}}{R_i^{[1,1,0,0]}+R_i^{[1,0,1,1]}}+\frac{R_i^{[0,1,1,0]}}{R_i^{[0,1,1,0]}+R_i^{[1,0,1,1]}}+\right.$$
$$\frac{R_i^{[0,1,0,1]}}{R_i^{[0,1,0,1]}+R_i^{[1,0,1,1]}}+\frac{R_i^{[1,1,1,0]}}{R_i^{[1,1,1,0]}+R_i^{[1,0,1,1]}}+\frac{R_i^{[1,1,0,1]}}{R_i^{[1,1,0,1]}+R_i^{[1,0,1,1]}}+$$
$$\left.\frac{R_i^{[0,1,1,1]}}{R_i^{[0,1,1,1]}+R_i^{[1,0,1,1]}}+\frac{R_i^{[1,1,1,1]}}{R_i^{[1,1,1,1]}+R_i^{[1,0,1,1]}}\right), \tag{C14}$$

$$
\begin{aligned}
\mathscr{H}^{[0,0,0,1]}\left(R_i^{[0,1,1,1]}\right) = {} & \beta R_i^{[0,0,0,1]}\left(\frac{R_i^{[0,1,1,1]}}{R_i^{[0,0,0,1]}+R_i^{[0,1,1,1]}}+\frac{R_i^{[0,1,1,0]}}{R_i^{[0,0,0,1]}+R_i^{[0,1,1,0]}}\right)+ \\
& \beta R_i^{[0,1,0,1]}\left(\frac{R_i^{[0,1,1,1]}}{R_i^{[0,1,0,1]}+R_i^{[0,1,1,1]}}+\frac{R_i^{[0,0,1,1]}}{R_i^{[0,1,0,1]}+R_i^{[0,0,1,1]}}+\frac{R_i^{[0,0,1,0]}}{R_i^{[0,1,0,1]}+R_i^{[0,0,1,0]}}\right)+ \\
& \beta R_i^{[0,0,1,1]}\left(\frac{R_i^{[0,1,1,1]}}{R_i^{[0,0,1,1]}+R_i^{[0,1,1,1]}}+\frac{R_i^{[0,1,0,1]}}{R_i^{[0,0,1,1]}+R_i^{[0,1,0,1]}}+\frac{R_i^{[0,1,0,0]}}{R_i^{[0,0,1,1]}+R_i^{[0,1,0,0]}}\right)- \\
& \beta R_i^{[0,1,1,1]}\left(\frac{R_i^{[1,0,0,0]}}{R_i^{[1,0,0,0]}+R_i^{[0,1,1,1]}}+\frac{R_i^{[1,1,0,0]}}{R_i^{[1,1,0,0]}+R_i^{[0,1,1,1]}}+\frac{R_i^{[1,0,1,0]}}{R_i^{[1,0,1,0]}+R_i^{[0,1,1,1]}}+\right. \\
& \frac{R_i^{[1,0,0,1]}}{R_i^{[1,0,0,1]}+R_i^{[0,1,1,1]}}+\frac{R_i^{[1,1,1,0]}}{R_i^{[1,1,1,0]}+R_i^{[0,1,1,1]}}+\frac{R_i^{[1,1,0,1]}}{R_i^{[1,1,0,1]}+R_i^{[0,1,1,1]}}+ \\
& \left.\frac{R_i^{[1,0,1,1]}}{R_i^{[1,0,1,1]}+R_i^{[0,1,1,1]}}+\frac{R_i^{[1,1,1,1]}}{R_i^{[1,1,1,1]}+R_i^{[0,1,1,1]}}\right),
\end{aligned}
\tag{C15}
$$

$$
\begin{aligned}
\mathscr{H}^{[0,0,0,1]}\left(R_i^{[1,1,1,1]}\right) = \\
&\beta R_i^{[0,0,0,1]}\left(\frac{R_i^{[1,1,1,0]}}{R_i^{[0,0,0,1]}+R_i^{[1,1,1,0]}}+\frac{R_i^{[1,1,1,1]}}{R_i^{[0,0,0,1]}+R_i^{[1,1,1,1]}}\right)+\\
&\beta R_i^{[1,0,0,1]}\left(\frac{R_i^{[0,1,1,0]}}{R_i^{[1,0,0,1]}+R_i^{[0,1,1,0]}}+\frac{R_i^{[1,1,1,0]}}{R_i^{[1,0,0,1]}+R_i^{[1,1,1,0]}}+\frac{R_i^{[0,1,1,1]}}{R_i^{[1,0,0,1]}+R_i^{[0,1,1,1]}}+\right.\\
&\left.\frac{R_i^{[1,1,1,1]}}{R_i^{[1,0,0,1]}+R_i^{[1,1,1,1]}}\right)+\\
&\beta R_i^{[0,1,0,1]}\left(\frac{R_i^{[1,0,1,0]}}{R_i^{[0,1,0,1]}+R_i^{[1,0,1,0]}}+\frac{R_i^{[1,1,1,0]}}{R_i^{[1,0,0,1]}+R_i^{[1,1,1,0]}}+\frac{R_i^{[1,0,1,1]}}{R_i^{[1,0,0,1]}+R_i^{[1,0,1,1]}}+\right.\\
&\left.\frac{R_i^{[1,1,1,1]}}{R_i^{[0,1,0,1]}+R_i^{[1,1,1,1]}}\right)+\\
&\beta R_i^{[0,0,1,1]}\left(\frac{R_i^{[1,1,0,0]}}{R_i^{[0,0,1,1]}+R_i^{[1,1,00]}}+\frac{R_i^{[1,1,1,0]}}{R_i^{[0,0,1,1]}+R_i^{[1,1,1,0]}}+\frac{R_i^{[1,1,0,1]}}{R_i^{[0,0,0,1]}+R_i^{[1,1,0,1]}}+\right.\\
&\left.\frac{R_i^{[1,1,1,1]}}{R_i^{[0,0,1,1]}+R_i^{[1,1,1,1]}}\right)+\\
&\beta R_i^{[1,1,0,1]}\left(\frac{R_i^{[0,0,1,0]}}{R_i^{[0,0,1,0]}+R_i^{[1,1,0,1]}}+\frac{R_i^{[1,0,1,0]}}{R_i^{[1,0,1,0]}+R_i^{[1,1,0,1]}}+\frac{R_i^{[0,1,1,0]}}{R_i^{[0,1,1,0]}+R_i^{[1,1,0,1]}}+\right.\\
&\frac{R_i^{[0,0,1,1]}}{R_i^{[0,0,1,1]}+R_i^{[1,1,0,1]}}+\frac{R_i^{[1,1,1,0]}}{R_i^{[1,1,1,0]}+R_i^{[1,1,0,1]}}+\frac{R_i^{[1,0,1,1]}}{R_i^{[1,0,1,1]}+R_i^{[1,1,0,1]}}+\\
&\left.\frac{R_i^{[0,1,1,1]}}{R_i^{[1,1,0,1]}+R_i^{[0,1,1,1]}}+\frac{R_i^{[1,1,1,1]}}{R_i^{[1,1,1,1]}+R_i^{[1,1,0,1]}}\right)+\\
&\beta R_i^{[1,0,1,1]}\left(\frac{R_i^{[0,1,0,0]}}{R_i^{[0,1,0,0]}+R_i^{[1,0,1,1]}}+\frac{R_i^{[1,1,0,0]}}{R_i^{[1,1,0,0]}+R_i^{[1,0,1,1]}}+\frac{R_i^{[0,1,1,0]}}{R_i^{[0,1,1,0]}+R_i^{[1,0,1,1]}}+\right.\\
&\frac{R_i^{[0,1,0,1]}}{R_i^{[0,1,0,1]}+R_i^{[1,0,1,1]}}+\frac{R_i^{[1,1,1,0]}}{R_i^{[1,1,1,0]}+R_i^{[1,0,1,1]}}+\frac{R_i^{[1,1,0,1]}}{R_i^{[1,1,0,1]}+R_i^{[1,0,1,1]}}+\\
&\left.\frac{R_i^{[0,1,1,1]}}{R_i^{[1,0,1,1]}+R_i^{[0,1,1,1]}}+\frac{R_i^{[1,1,1,1]}}{R_i^{[1,1,1,1]}+R_i^{[1,0,1,1]}}\right)+\\
&\beta R_i^{[0,1,1,1]}\left(\frac{R_i^{[1,0,0,0]}}{R_i^{[1,0,0,0]}+R_i^{[0,1,1,1]}}+\frac{R_i^{[1,1,0,0]}}{R_i^{[1,1,0,0]}+R_i^{[0,1,1,1]}}+\frac{R_i^{[1,0,1,0]}}{R_i^{[1,0,1,0]}+R_i^{[0,1,1,1]}}+\right.\\
&\frac{R_i^{[1,0,0,1]}}{R_i^{[1,0,0,1]}+R_i^{[0,1,1,1]}}+\frac{R_i^{[1,1,1,0]}}{R_i^{[1,1,1,0]}+R_i^{[0,1,1,1]}}+\frac{R_i^{[1,1,0,1]}}{R_i^{[1,1,0,1]}+R_i^{[0,1,1,1]}}+\\
&\left.\frac{R_i^{[1,0,1,1]}}{R_i^{[1,0,1,1]}+R_i^{[0,1,1,1]}}+\frac{R_i^{[1,1,1,1]}}{R_i^{[1,1,1,1]}+R_i^{[0,1,1,1]}}\right).
\end{aligned}
\tag{C16}
$$

Therefore the farm flow model when cefelexin resistance is chromosomally encoded is defined by the system of equations given by (A1)-(A21), (C1)-(C17).

$$\frac{dR_i^{[x_1,x_2,x_3,x_4]}}{dt} = \mathscr{F}(R_i^{[x_1,x_2,x_3,x_4]}) + \mathscr{D}(R_i^{[x_1,x_2,x_3,x_4]}) + \mathscr{G}(R_i^{[x_1,x_2,x_3,x_4]}) + \mathscr{H}^{[0,0,0,1]}(R_i^{[x_1,x_2,x_3,x_4]}),$$

where $i \in \{\text{dairy, heifer, UR, muck, eff., tank}\}$ & $[x_1, x_2, x_3, x_4] \in \{0, 1\}^4$. (C17)

where $\mathscr{F}(R_i^{[x_1,x_2,x_3,x_4]})$, $\mathscr{D}(R_i^{[x_1,x_2,x_3,x_4]})$, $\mathscr{G}(R_i^{[x_1,x_2,x_3,x_4]})$ are defined by (A19), (A20) and (A21) respectively.

References

[1] EFSA Panel on Additives and Products or Substances used in Animal Feed (FEEDAP) . Scientific opinion on the safety and efficacy of copper compounds (e4) as feed additives for all animal species (cupric acetate, monohydrate; basic cupric carbonate, monohydrate; cupric chloride, dihydrate; cupric oxide; cupric sulphate, pentahydrate; cupric chelate of amino acids, hydrate; cupric chelate of glycine, hydrate), based on a dossier submitted by fefana asbl. *EFSA Journal*, 13(4), 2015.

[2] EFSA Panel on Additives and Products or Substances used in Animal Feed (FEEDAP) . Scientific opinion on the safety and efficacy of zinc compounds (e6) as feed additives for all animal species (zinc acetate, dihydrate; zinc chloride, anhydrous; zinc oxide; zinc sulphate, heptahydrate; zinc sulphate, monohydrate; zinc chelate of amino acids, hydrate; zinc chelate of glycine, hydrate), based on a dossier submitted by fefana asbl. *EFSA Journal*, 13(4), 2015.

[3] Sankalp Arya, Alexander Williams, Saul Vazquez Reina, Charles W. Knapp, Jan-Ulrich Kreft, Jon L. Hobman, and Dov J. Stekel. Towards a general model for predicting minimal metal concentrations co-selecting for antibiotic resistance plasmids. *Environmental Pollution*, 275, 2021.

[4] Michelle Baker, Alexander D. Williams, Steven P.T. Hooton, Richard Helliwell, Elizabeth King, Thomas Dodsworth, Rosa María Baena-Nogueras, Andrew Warry, Catherine A. Ortori, Henry Todman, Charlotte J. Gray-Hammerton, Alexander C.W. Pritchard, Ethan Iles, Ryan Cook, Richard D. Emes, Michael A. Jones, Theodore Kypraios, Helen West, David A. Barrett, Stephen J. Ramsden, Rachel L. Gomes, Chris Hudson, Andrew D. Millard, Sujatha Raman, Carol Morris, Christine E.R. Dodd, Jan-Ulrich Kreft, Jon L. Hobman, and Dov J. Stekel. Antimicrobial resistance in dairy slurry tanks: A critical point for measurement and control. *Environment International*, 169:107516, 2022.

[5] INRA-CIRAD-AFZ. Feedtables: Tables of composition and nutritional values of feed materials. https://feedtables.com/, 2018. [Online; accessed 31-May-2019].

[6] A Ivask, T Rolova, and Kahru A. A suite of recombinant luminescent bacterial strains for the quantification of bioavailable heavy metals and toxicity testing. *BMC Biotechnology*, 9(1), 2009.

[7] Landia. *Submersible Slurry Pump DG*, n.d.

[8] American Society of Agricultural Engineers. Manure Production and Characteristics. Technical report, American Society of Agricultural Engineers, 2005.

Chapter 4

A model of antibiotic resistance genes accumulation through lifetime exposure from food intake and antibiotic treatment

Publication Note

The following work has now been published in PLOS ONE:

Todman H, Arya S, Baker M, Stekel DJ. A model of antibiotic resistance genes accumulation through lifetime exposure from food intake and antibiotic treatment. *PLOS ONE* 18(8), 2023: e0289941. https://doi.org/10.1371/journal.pone.0289941

Abstract

Antimicrobial resistant bacterial infections represent one of the most serious contemporary global healthcare crises [1]. Acquisition and spread of resistant infections can occur through community, hospitals, food, water or endogenous bacteria [2, 3]. Global efforts to reduce resistance have typically focussed on antibiotic use, hygiene and sanitation and drug discovery [4, 5, 6]. However, resistance in endogenous infections, e.g. many urinary tract infections, can result from life-long acquisition and persistence of resistance genes in commensal microbial flora of individual patients [7, 8], which is not normally considered. Here, using individual based Monte Carlo models calibrated using antibiotic use data [9] and human gut resistomes [10], we show that the long-term increase in resistance in human gut microbiomes can be substantially lowered by reducing exposure to resistance genes found in food and water, alongside reduced medical antibiotic use. Reduced dietary exposure is especially important during patient antibiotic treatment because of increased selection for resistance gene retention; inappropriate use of antibiotics can be directly harmful to the patient being treated for the same reason. We conclude that a One Health approach to antimicrobial resistance that additionally incorporates food production and diet considerations will be more effective in reducing resistant infections than a purely medical-based approach.

4.1 Introduction

The human gut is a diverse and dynamic environment playing host to a wide variety of bacteria, viruses, archaea and eukaryotes. Genomic studies have shown that the human gut microbiota contains more than 300 species of bacteria [11]. These commensal enteric bacteria are thought to be largely harmless and play an important role in maintaining the health of the host through various mechanisms: i.e. protection against colonisation by pathogens through competitive exclusion or production of antimicrobial chemicals [12, 13, 14], maintaining the host immune system [15, 13], and extracting energy and nutrients from food [13]). However, at lower levels there are pathogenic bacteria endogenous to the gut (in particular *Enterobacteriaceae* and *Enterococcaceae*) [16].

In addition to playing host to a diverse collection of bacteria and other micro-organism, the human gut represents a reservoir of antimicrobial resistance (AMR) as enteric bacteria hold antimicrobial resistance genes (ARGs) either on their chromosomes or on mobile genetic elements; it is thought that these ARGs predominantly reside within non-pathogenic unclassified species [17].

Antimicrobial resistances in the gut may become established after ingestion of contaminated food. Many studies have shown ARGs to be present in a range of high-risk food products: raw and cooked meats [18, 19, 20, 21, 22], fermented milk products [23, 24, 25], fermented meat products [26, 27] and vegetable products [28, 29, 30]. The ready-to-eat food market is particularly problematic due to a lack of cooking and washing before consumption [31, 32, 33, 34].

Several authors have identified systematic differences in ARG levels between individuals resident in different countries [9, 35]. One source of these differences is likely to result from differing levels of availability of antibiotic treatments. Governmental approaches to antibiotic availability are diverse and defined daily doses per inhabitant can vary widely [10, 36].

Ageing individuals are at higher risk of AMR infections because of increased exposure to ARGs, increased lifetime exposure to antibiotics and increased vulnerability to infection with age.

Recently, research has shown that the number of ARGs within an individual's intestinal tract is correlated with age[37, 38]. Work by Lu et al [37] showed that the number of resistances from faecal samples of four different age groups were positively correlated with increasing age. Further, cluster analysis suggested that resistances were being acquired and accumulated over time rather than being transient. Other research has also supported this view. Ghosh et al [17] profiled resistance genes of 275 gut flora samples sourced from multiple countries and found increasing ARG diversity with age.

Antimicrobial resistant bacterial infections in older age can often result from endogenous bacteria moving from the intestinal tract to other areas of the body, for example the urinary tract [7, 39].

In this work, we bring together these aspects of ARG establishment using a probabilistic mathematical

model of the accumulation of antimicrobial resistance over an individual lifetime. We consider four key model parameters: antibiotic use, ARG ingestion, and the probabilities of an ARG becoming established in the presence and absence of concurrent antibiotic use. Taking reported demographic data, we show how accumulation of resistances are likely to vary by country depending on antibiotic availability and use. We show that alterations to food intake during antibiotic treatment can reduce the overall antibiotic resistance level in an individual.

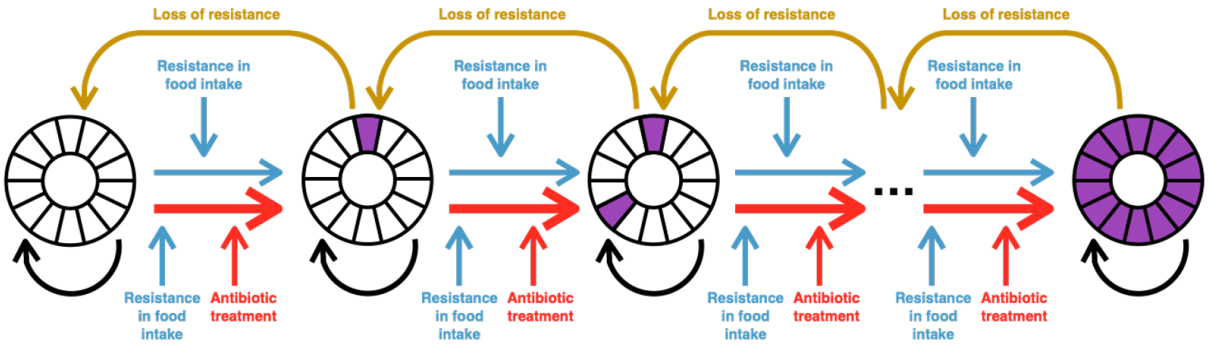

Figure 4.1: **Schematic diagram of the lifetime food model showing key model interactions.**

4.2 Methods

We have defined a probabilistic model to define the acquisition of ARGs in the enteric system of individuals (figure 4.1), which we have evaluated using Monte Carlo simulations.

We consider the acquisition of resistance genes to 14 different classes of antibiotics. It is important to note that this is an oversimplified view of resistance to different antibiotics: there is significant variation in resistance genes of antibiotics within the same class and indeed variation between ARGs conferring resistance to the same antibiotic (e.g. there are over 40 different genes divided into 11 different classes of action which encode resistance to tetracycline [40]). However, in order to reduce model complexity, we consider resistance to individual classes of antibiotics (e.g. beta lactams, carbapenems, cepholosporins, aminoglycosides, etc), rather than specific antibiotics.

For each antibiotic class, we consider the probability that an individual is exposed to resistance genes through ingestion of food, and the probability of these resistance genes becoming fixed in the individual's enteric bacterial communities. The probability of resistance becoming established in the gut microbiome is dependant on whether the individual may be undergoing antibiotic treatment (of the same class as the resistance genes), as the presence of antibiotic treatment provides selective pressure for these resistance genes.

Parameter	**Parameter Name**	**Parameter Values**	**Parameter Range**	Source
N	Number of antibiotic classes considered	14	-	[40]
n	Number of individuals simulated	1000	-	-
$P_{\text{Ab. Treat}}(A_i)$	Probability of an individual receiving antibiotic treatment for antibiotic class A_i	1.4×10^{-2} (low Ab usage) 2.1×10^{-2}(medium Ab usage) 5.0×10^{-2} (high Ab usage)	0 - 1	[9] [9] Assumed
β_{food}	Upper bound for uniform distribution of $P_{\text{food res.}}(A_i)$	0.5	0 - 1	[41, 42]
$P_{\text{food res.}}(A_i)$	Probability of resistance genes for antibiotic class A_i being present in an individual's food intake	$P_{\text{food res.}}(A_i) \sim \mathcal{U}(0, \beta_{\text{food}})$	0 - β_{food}	-
$P_{\text{Fix}}(A_i)$	Probability of resistance genes becoming established in an individuals resistome in absence of antibiotics	1.0×10^{-4}	0 - 1	[37]
$P_{\text{Ab. Fix}}(A_i)$	Probability of resistance genes for antibiotic class A_i becoming established in an individuals resistome in presence of antibiotics	5.0×10^{-2}	0 - 1	[37]
$P_{\text{Loss}}(A_i)$	Probability of resistance genes for antibiotic class A_i being lost	1.0×10^{-6}	0 - 1	[43]

Table 4.1: **A table giving the standard parameters used when simulating the lifetime resistance model.**

For each class of antibiotic, we consider the probability of exposure to resistance genes for that antibiotic via the food chain, as well as the probability of resistance becoming established in the gut microbiome in the presence and absence of selective pressures from concurrent antibiotic treatment. For simplicity, once acquired and established, we assume that the resistance will persist in the commensal flora of an individual throughout their lifetime; this is in accordance with metagenomics studies [37].

Throughout our analysis we considered three different levels of antibiotic use, which reflect different national levels of antibiotic availability. We ran different simulations of this model, with each scenario for 1000 individuals. We have based the parameter values for the probability of antibiotic use in areas with low and medium antibiotic usage from drug utilization figures for European countries [9], and then estimated high antibiotic use areas parameter values based on this.

We simulate individual lifetimes in the Monte Carlo model with time steps of one week. The probability of an individual being exposed to resistance via food intake each week ($P_{\text{FoodRes.}}$) is a random variable with a uniform distribution. Once exposed to resistance, there is a probability that this resistance shall establish in the microbial flora in the gut of the individual (P_{Fix}). Each week, there is an independent probability that the individual may undergo antibiotic treatment ($P_{\text{Ab. Treat.}}$). As the use of antibiotics can exert selective pressures on resistant bacterial populations, we assign a greater probability of establishment of ARGs in the presence of antibiotic treatment ($P_{\text{Ab. Fix.}}$). The probability that the individual acquires a new class of resistance in any given week is given by the transition probability (4.1).

$$\mu_i = P_{\text{food res.}}(A_i)\left((1 - P_{\text{Ab. treat}}(A_i))\, P_{Fix}(A_i) + P_{\text{Ab. treat}}(A_i) P_{Ab.Fix}(A_i)\right) \tag{4.1}$$

The parameters used for each scenario are given in the table 4.1. At each time step in the model, we sample the probability of resistance in food intake from a continuous uniform distribution $U(0, \beta_{\text{food}})$: this distribution is chosen to reflect intake of a varied diet from a variety of food sources, with the upper bound based on observed frequencies of resistance in E. coli isolates from food products [41, 42]. Then we estimate probabilities of resistance becoming established for this model based on metagenomic data for human gut microbiota in areas of different levels of antibiotic use [37].

We conducted a local sensitivity analysis for each of the model parameters. For each parameter, we take 1000 parameter values sampled from the feasible parameter space (table 4.1) and calculate the mean resistance load at the age of 70 over the corresponding 1000 simulations.

We then considered an alternative model which includes the possibility of acquired resistance genes to be lost. In order to simulate the possible loss of ARGs from the resistome through wash out, at the end of each time step in the Markov chain model there is a possibility that an acquired resistance, A_i, is lost with probability $P_{\text{Loss}}(A_i)$.

MATLAB R2020b was used to run time course simulations of the lifetime resistance model and to perform a local sensitivity parameter analysis of the model.

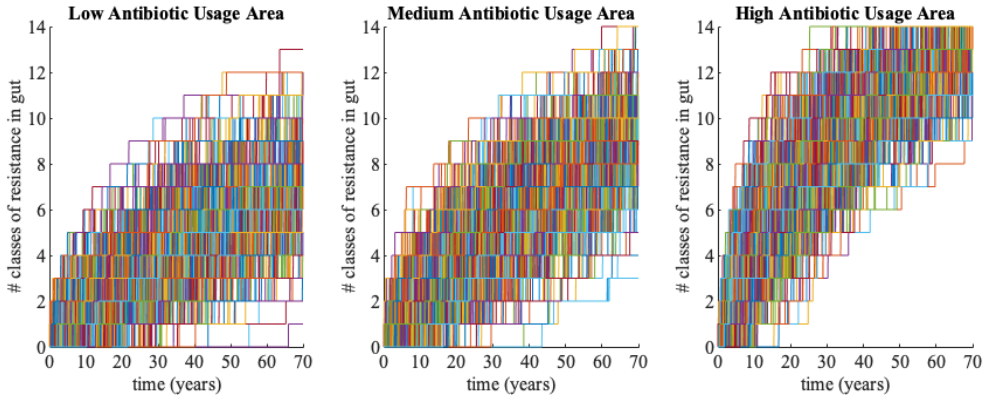

(a) Time course of lifetime resistance model

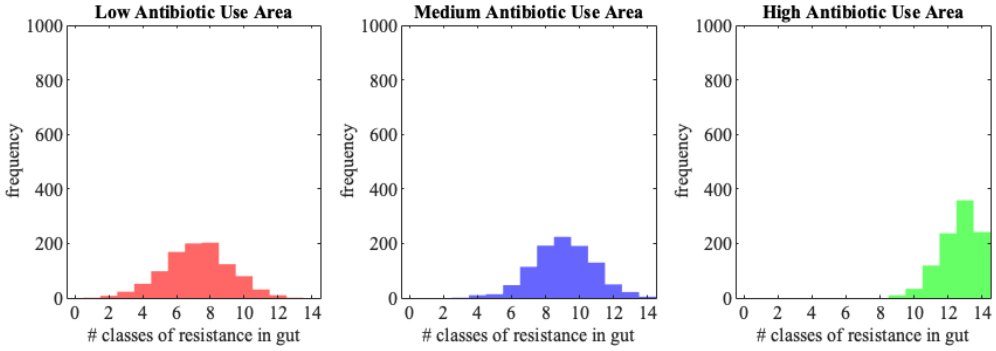

(b) Histogram showing the distribution of ARG load in individual's resistomes

Figure 4.2: **(a) Time course simulation of Lifetime resistance model for low, medium and high antibiotic use countries.** In each of the three antibiotic use scenarios (low, medium and high), we have run the lifetime resistance model using the standard parameter set (given in table 4.1) for 1000 individuals. Each line represents an individual simulated in the lifetime resistance model. We can clearly see that individuals acquire more ARGs more quickly in areas of higher antibiotic usage.

(b) Histogram showing the distribution of ARG load in individual's resistomes by age 70 for the lifetime resistance model. These histograms show the distribution of the number of resistance classes at the end of the time course simulations of 1000 individuals shown in (a) (i.e. at age 70). The mean and standard deviation, $(\mu,\ \sigma)$, for low, medium and high antimicrobial use areas are $(7.2120,\ 1.9475)$, $(9.0410,\ 1.7946)$ and $(12.6250,\ 1.1321)$ respectively.

4.3 Results & Discussion

Simulation of 1000 individuals in each of the 3 antibiotic usage scenaios (low, medium and high) for the standard parameter set (table 4.1) shows that higher antibiotic use increases ARG acquisition over time

by commensal bacteria (figure 4.2).

The average resistance load in individuals, at 70 years of age, from medium and high antibiotic use areas is 24.38% and 71.40% higher, respectively, than low antibiotic use areas. Thus our model concurs with many researchers and organisations including WHO [44], in advocating a reduction in antibiotic usage as a way to control the spread of antibiotic resistance, among other strategies. This strategy reduces opportunities for resistance genes to be the selected for in the gut over the lifetime of the individual.

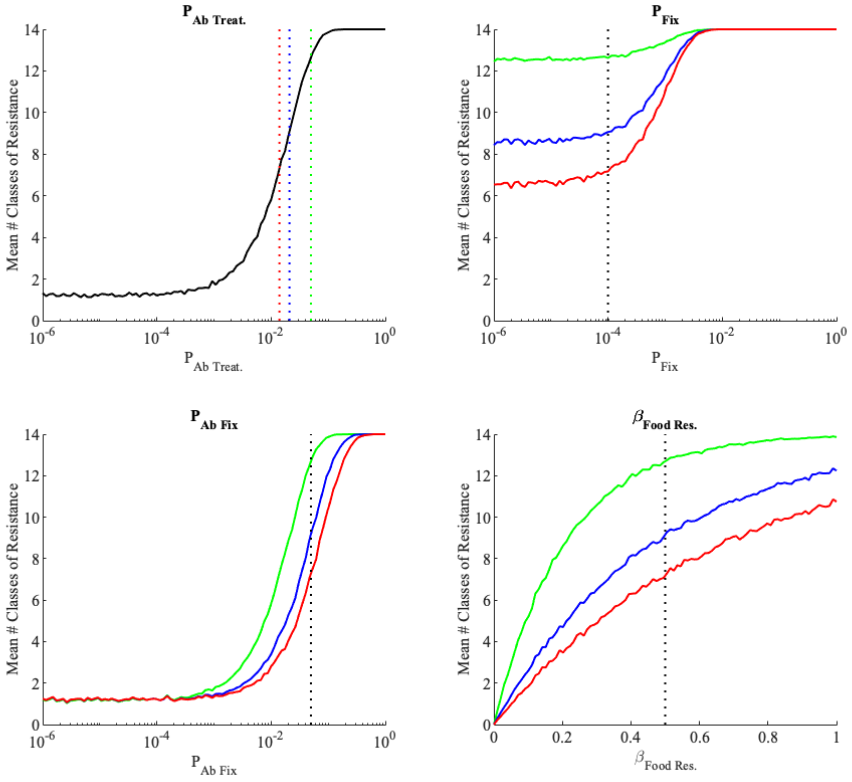

Figure 4.3: **Local sensitivity analysis of the lifetime resistance model parameters.** We vary the model parameters ($P_{\text{Ab. Treat.}}$, P_{Fix}, $P_{\text{Ab. Fix}}$, and β_{food}) across the possible parameter space (given in table 4.1) and then calculated the mean ARG load at age 70 of 1000 individuals for each of the different parameter values. For $P_{\text{Ab. Treat.}}$, the black line shows the mean resistance load as the probability of undergoing antibiotic treatment is varied across the parameter space, and the dashed red, blue and green lines indicate the parameter values used for $P_{\text{Ab. Treat.}}$in the low, medium and high antibiotic use areas respectively. For the local sensitivity analyses of P_{Fix}, $P_{\text{Ab. Fix}}$, and $\beta_{\text{food res.}}$, the red, blue and green lines represent the average resistance load as the parameter of interest is varied for low, medium and high antibiotic use areas respectively. The dashed black line in these subplots represents the values used for these parameters in the model simulations.

In order to frame analyses of potential interventions on long term accumulation of resistance, we carried out local sensitivity analyses of the key parameters from the model (Figure 4.3). The accumulation of resistance is most sensitive to the probability of antibiotic treatment, and the probability of resistance fixing during antibiotic use. This effect is greatest in low and medium use countries. This led us to investigate impact of those factors in greater detail

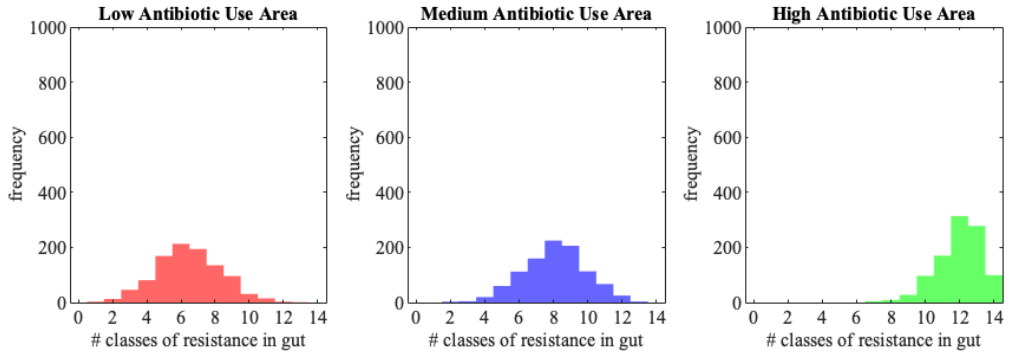

(a) 20% reduction in antibiotic usage

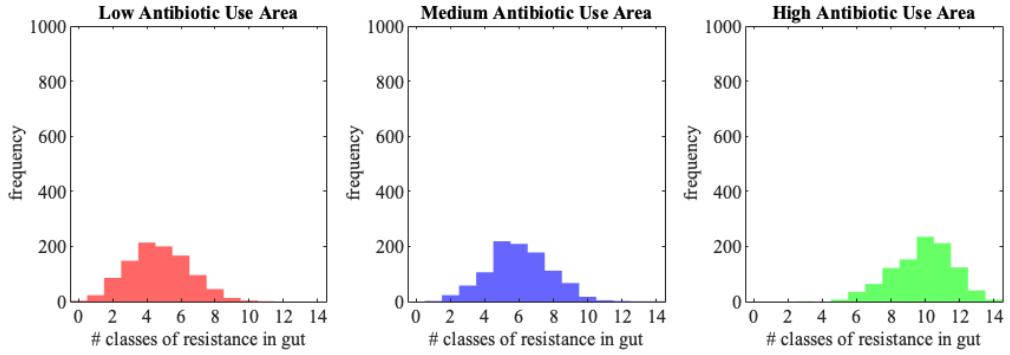

(b) 50% reduction in antibiotic usage

Figure 4.4: **Histograms showing distribution of ARG load in individual by age 70 when there is (a) 20% and (b) 50% reduction in the probability of antibiotic treatment.** The mean and standard deviation, (μ, σ), for the low antibiotic use area are (6.4400, 1.9042) and (4.6970, 1.7985) for the 20% and 50% reduction respectively. Similarly (μ, σ) for the medium and high antibiotic use areas is (8.0660, 1.8604) and (11.9670, 1.3243) respectively when antibiotic use is reduced by 20%, and (6.0160, 1.8160) and (9.8370, 1.7770) respectively when reduced by 50%.

The number of resistance genes acquired by an individual is dependent on the use of antibiotics over the individual's lifetime and can be meaningfully reduced by a reduction in an individual's intake of ARGs through food.

We explored the impact of a reduction in Ab usage by running simulations with a 20% and 50% reduction in the probability of an individual undergoing treatment in any given week (figure 4.4).

While mathematically this is no different from exploring the three different Ab usage areas as shown in figure 4.2, this analysis explores the practical effects of an Ab reduction policy in countries such as Denmark (low usage), Spain (medium usage) or China (high usage).

Another avenue of control is the reduction of ARG intake through food and water. We considered two possibilities: an overall reduction of ARGs in food, representative of a ONE Health approach that includes food and water; and a reduction only during antibiotic treatment, representing dietary change during such treatment, e.g. avoiding higher risk or raw foods. We considered two levels of reduction, 20% and 50% for both antibiotic usage and ARG levels in food. All scenarios were applied for low, medium and high antibiotic use countries.

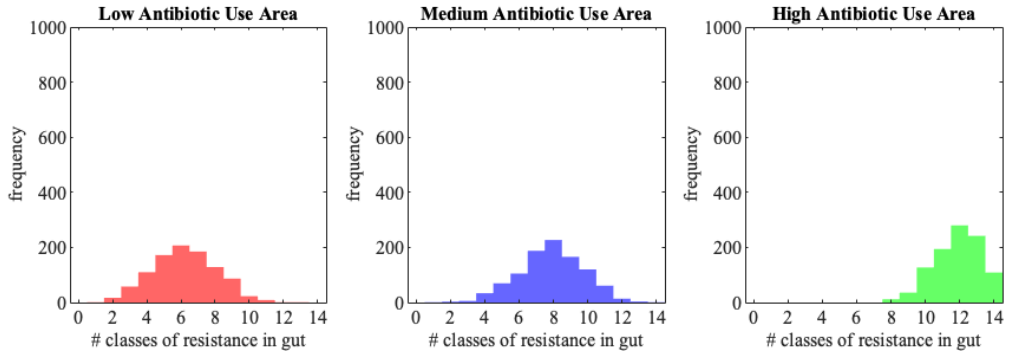

(a) 20% reduction in resistance genes in food intake

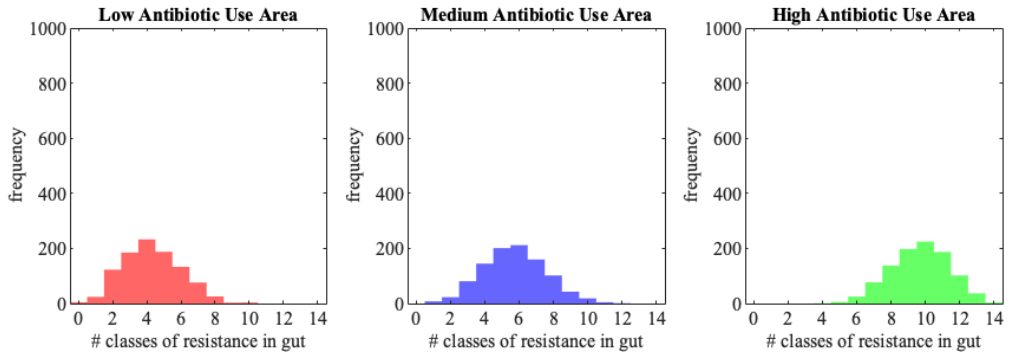

(b) 50% reduction in resistance genes in food intake

Figure 4.5: **Histograms showing distribution of ARG load in individual by age 70 under a 20% and 50% reduction in resistance genes in an individual's food intake.** Simulated using 1000 individuals in each of the case for each of the 3 Ab usage areas (low, medium & high). [Mean, Std, Max] for 20% food resistance reduction are [6.2150, 1.8842, 13], [7.8720, 1.9056, 14] and [11.8560, 1.7087, 14] in Low, Medium and High areas respectively. For 50% reduction [4.3020, 1.7099, 10], [5.7340, 1.8522, 12] and [9.677, 1.7087, 14] .

Figure 4.4 shows the effect of reducing the probability of undergoing antibiotic treatment alone and figure 4.5 the effect of reducing the probability of ARG in food alone. As expected, we observe that

both these approaches result in a reduction in ARG acquisition over a lifetime, and reducing either ARG intake or antibiotic consumption by 50% gives a greater effect than reducing by 20%.

Reducing the antibiotic consumption in areas that have a higher rate of antibiotic treatment is on average more effective at reducing the ARG load: a 20% reduction in Ab usage yields an average 5.98% and 11.33% reduction in resistance load by age 70 in high and medium use areas respectively, while a 50% reduces the mean resistance load by 21.21% and 32.92%. Comparatively a reduction in ARG intake via food is more effective at reducing ARG acquisition in low antibiotic usage areas with a 20% and 50% reduction in ARG intake giving a 13.11% and 35.23% reduction in the mean resistance load.

Reducing ARG intake via food during periods of antibiotic treatment is particularly effective at limiting acquisition of resistance genes.

The greatest reduction in the number of resistance classes acquired by 70 years comes for a combined approach. Here for even a modest 20% decrease in both actions we see a reduction of between 12.63% and 24.02%, depending upon the original level antibiotic usage. For a 50% decrease in both, we observe the number of resistance classes acquired by 70 years can be reduced significantly (by between 46.35% and 56.52%) reducing the likelihood that endogenous bacterial infections in older age will be resistant to treatment. For the case of reduction only at times of antibiotic use, we saw a similar reduction in ARG load as for the reduced probability of ARG in food in general (Figure 4.6, 4.A1 & 4.A2).

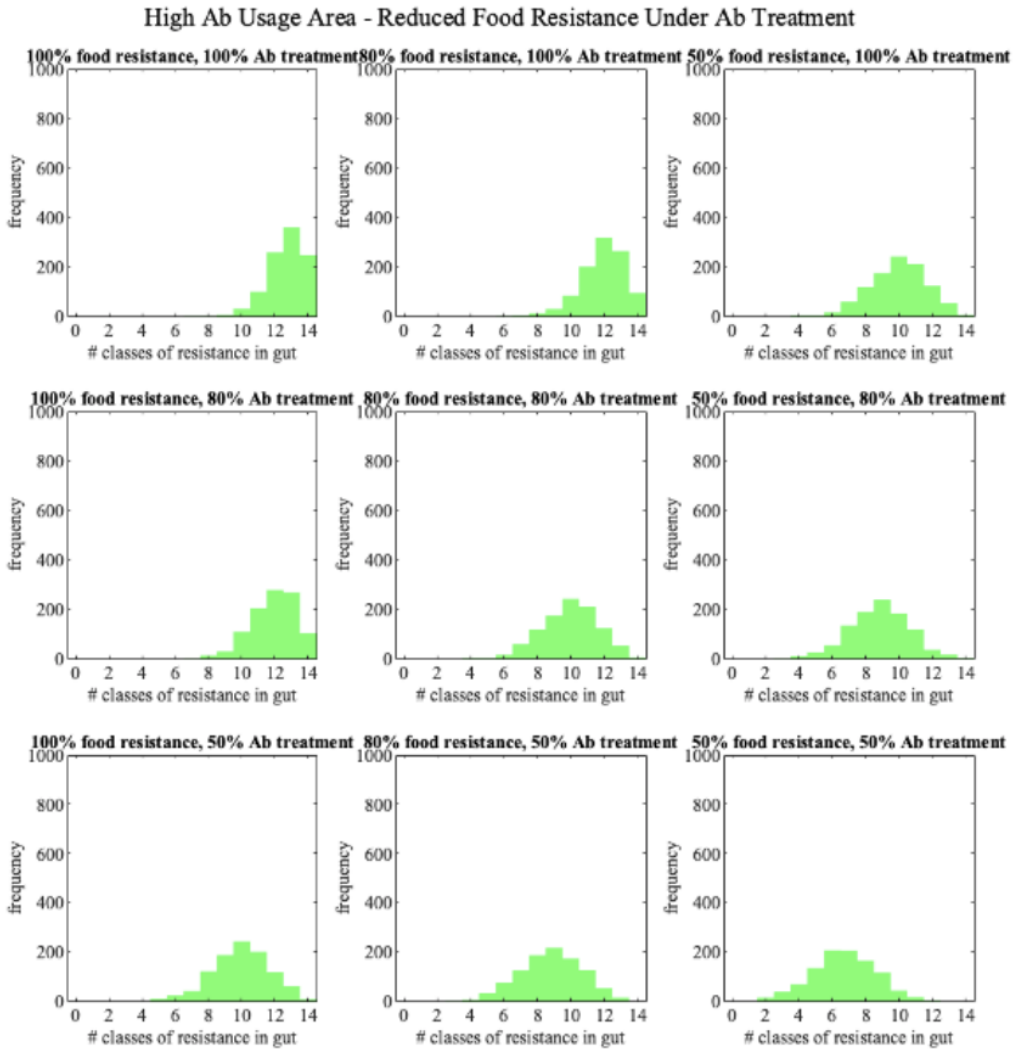

Figure 4.6: **Distributions of ARG load in resistome for different levels of intervention strategies in high antibiotic usage area.** Simulated using 1000 individuals in each intervention case. In each of these simulations the reduction in food resistance is assumed to only occur while the individual in undergoing antibiotic treatment, i.e. we assume a dietary change whilst under treatment.

Inclusion of ARG loss from resistome does not significantly impact lifetime resistance model simulations for realistic values of P_{Loss}.

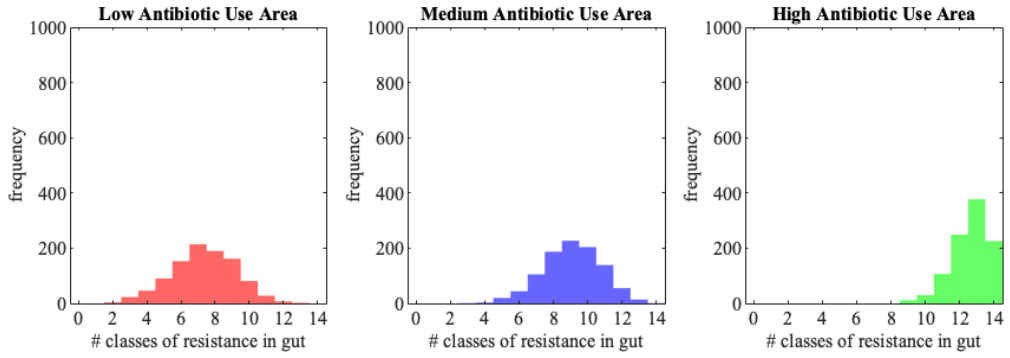

(a) The distribution of the number of ARGs in the resistome for the lifetime resistance model with ARG loss

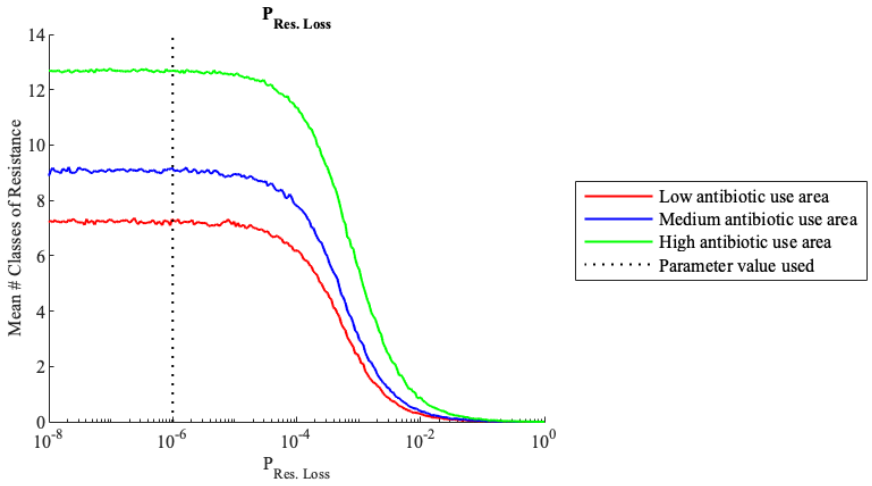

(b) Local sensitivity analysis of the lifetime resistance model with ARG loss to P_{Loss}

Figure 4.7: **(a) Histogram showing the distribution of ARG load in individual's resistomes by age 70 for the lifetime resistance model including ARG washout.** These histograms have been made by simulating the lifetime resistance model for 1000 individuals in each of the three antibiotic usage areas, where at each time step in the model there is a possibility that an individual may lose a resistance with probability $P_{\text{Loss}} = 1 \times 10^{-6}$. The mean and standard deviation, $(\mu,\ \sigma)$, for the low, medium and high antibiotic use areas are $(7.3330,\ 1.8841)$, $(9.0780,\ 1.7131)$ and $(12.6290,\ 1.1012)$ respectively.
(b) Local parameter sensitivity analysis of lifetime resistance model to the probability of resistance gene loss. We vary the value of the probability of an individual losing an acquired resistance, P_{Loss}, across the realistic parameter space (given in table 4.1) and then calculated the mean ARG load at age 70 of 1000 individuals for each of the different parameter values.

We adapted the lifetime model to include the possibility of resistance loss due to ARG washout or other factors. At the end of each time step in the markov chain model, there is a possibility that an acquired

resistance, A_i, may be lost with probability $P_{\text{loss}}(A_i)$. We then simulated the lifetime model with ARG loss (figure 4.7(a)) for 1000 individuals in each of the three antibiotic usage areas using the parameter values given in table 4.1. A comparison of the results of the simulation with ARG loss, figure 4.7(a), and without ARG loss, figure 4.2(b), shows negligible differences between the models for each of the three antibiotic usage scenarios considered.

We then performed a local sensitivity analysis of the lifetime model with ARG loss to the parameter P_{loss} (figure 4.7(b)). Sensitivity analysis showed that the average resistance load was consistent with the standard lifetime model without ARG loss when the probability of resistance loss was less than 10^{-4}, while for P_{loss} greater than 10^{-4}, we see that the chance of ARG loss is high enough that it leads to a significant reduction on the average resistance load. However, it is important to note that this threshold probability of 10^{-4} is much higher than we would expect to see for the probability of ARG washout and the physically relevant parameter space for P_{loss} is expected to be $[10^{-7}, 10^{-5}]$ [43].

4.4 Conclusion

We have shown that the long-term acquisition and retainment of genes providing resistance to different classes of antibiotics can be reduced by at three implementable factors. First, the number of resistance genes acquired by an individual is dependent upon the use of antibiotics over an individual's lifetime. A conservative approach to antibiotic availability and dosing guidelines, as already implemented in many countries, and as advocated in much of literature on antibiotic resistance, would be a practical approach to reducing the long-term number of acquired resistances. Indeed, the converse is true, in that unnecessary antibiotic treatment can lead to long-term harm to the patient being treated, and could be considered unethical; this argument stands in contrast to the more standard argument that the risk of over-use is primarily to patients other than the one being treated. Second, the number of acquired genes can be reduced even further if an individual's intake of resistance genes, carried on both pathogenic and non-pathogenic bacteria, is also reduced. This could be achieved by policy and practice changes in the food supply chain, including agriculture and post-harvest food production. Third, the reduction in intake of resistance genes is particularly effective during periods of antibiotic treatment where selective pressures increase the likelihood of the retainment of genes. We would suggest that dietary advice should be given to those undergoing antibiotic treatment to avoid products at higher risk of carrying ARGs (even on non-pathogens), as well as ensuring that all food consumed during treatment is fully cooked. The level of benefit to be gained from alterations in medical treatment and dietary changes is highly dependent upon the level of antibiotic use, which varies greatly between countries. Whilst our general model shows benefit at all prescribing levels, a differentiated model looking at region- and country-specific practices,

as well as containing specific details of antibiotic classes and associated resistance genes, would be better able to be quantify the potential benefits of such changes. There are several potentially interesting extensions to this model that could be explored in further work. One such avenue may be to explore the impacts of age based dietary and antibiotic treatment patterns - for example we would largely expect an individual to require more antibiotic treatment in early years and in older ages. Another way to extend this model may be to incorporate the probabilistic model presented here into an agent-based model to further explore the heterogeneities of individuals within a wider population (since our model assumes a large amount of homogeneity across the population).

4.A Appendix: Additional Figures

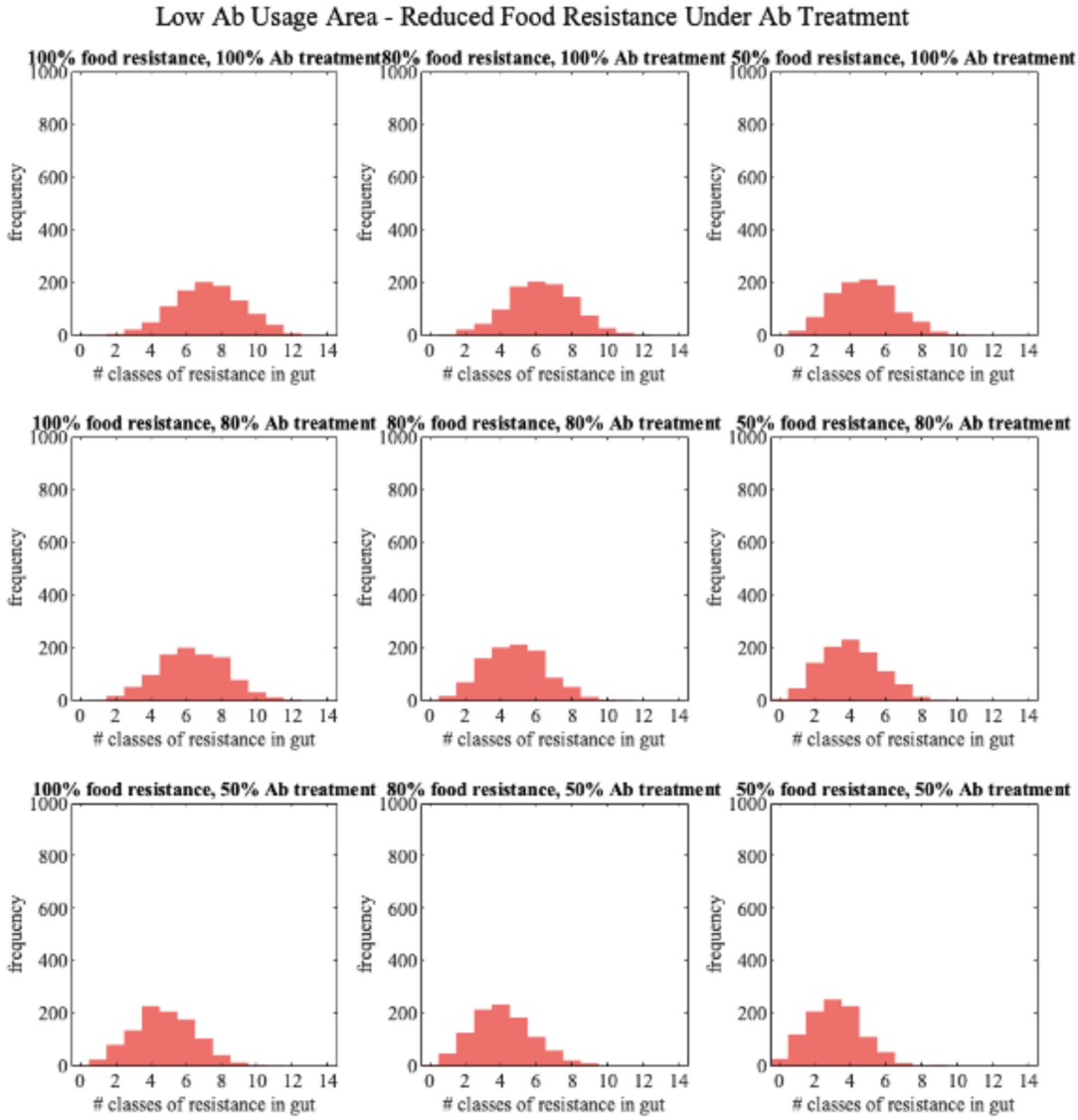

Figure 4.A1: **Distributions of ARG load in resistome for different intervention strategies in low antibiotic usage area.**

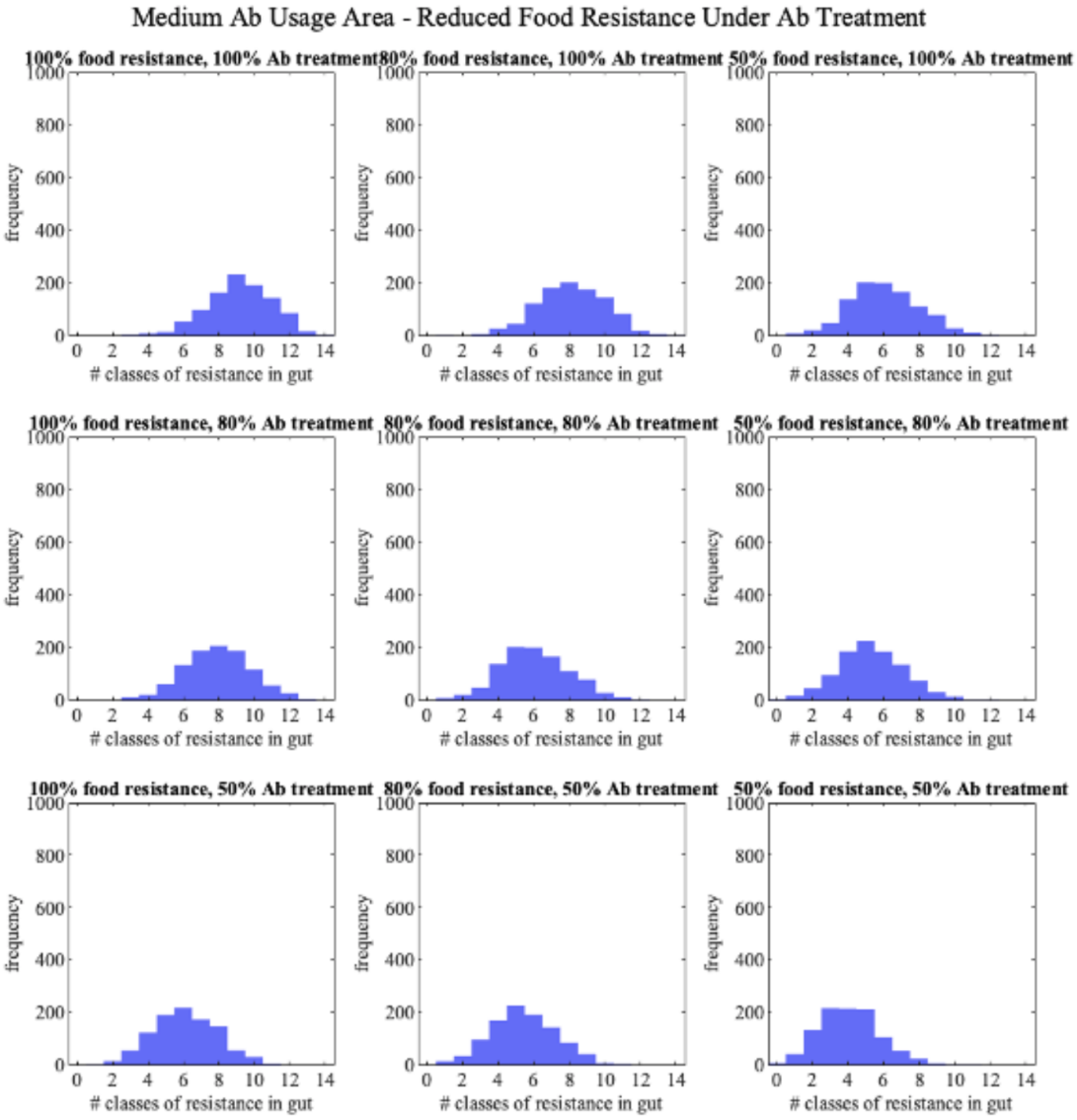

Figure 4.A2: **Distributions of ARG load in resistome for different intervention strategies in medium antibiotic usage area.**

References

[1] Jim O'Neill. Tackling drug resistant infections globally: final report and recommendations. Technical report, The Review on Antimicrobial Resistance, 2016.

[2] J.N. Pendleton, S.P. Gorman, and Gilmore B.F. Clinical relevance of the eskape pathogens. *Expert Rev Anti Infect Ther.*, 11(3):297–308, 2013.

[3] P. Vikesland, E. Garner, S. Gupta, S. Kang, A Maile-Moskowitz, and N. Zhu. Differential drivers of antimicrobial resistance across the world. *Acc Chem Res.*, 52(4):916–924, 2019.

[4] D. Nathwani, D. Varghese, J. Stephens, W. Ansari, S. Martin, and C. Charbonneau. Value of hospital antimicrobial stewardship programs [asps]: a systematic review. *Antimicrob Resist Infect Control.*, 8(35), 2019.

[5] H Bürgmann, D. Frigon, W.H. Gaze, C.M. Manaia, A. Pruden, A.C. Singer, B.F. Smets, and T. Zhang. Water and sanitation: an essential battlefront in the war on antimicrobial resistance. *FEMS Microbiol Ecol.*, 94(9), 2018.

[6] C. Kealey, C.A. Creaven, C.D. Murphy, and C.B. Brady. New approaches to antibiotic discovery. *Biotechnol Lett.*, 39(6):805–817, 2017.

[7] A.L. Flores-Mireles, J.N. Walker, M. Caparon, and S.J. Hultgren. Urinary tract infections: epidemiology, mechanisms of infection and treatment options. *Nat Rev Microbiol.*, 13(5):269–284, 2016.

[8] A. Mazzaril, G. Bazaj, and G. Cornaglia. Multi-drug-resistant gram-negative bacteria causing urinary tract infections: a review. *J. Chemotherapy*, 29(sup1):2–9, 2017.

[9] H. Goossens, M. Ferech, R. Vander Stichele, and M. Elseviers. Outpatient antibiotic use in europe and association with resistance: a cross-national database study. *Lancet*, 365(9459):579–587, 2005.

[10] Y. Hu, X. Yang, J. Qin, N. Lu, G. Cheng, N. Wu, Y. Pan, J. Li, L. Zhu, X. Wang, Z. Meng, F. Zhao, D. Liu, J. Ma, N. Qin, C. Xiang, Y. Xiao, L. Li, H. Yang, J. Wang, R. Yang, GF. Gao, J. Wang, and B. Zhu. Metagenome-wide analysis of antibiotic resistance genes in a large cohort of human gut microbiota. *Nature Communications*, 4, 2013.

[11] P.B. Eckburg, E. M. Bik, C. N. Bernstein, E. Purdom, L. Dethlefsen, M. Sargent, S. R. Gill, K. E. Nelson, and D. A. Relman. Diversity of the human intestinal microbial flora. *Science*, 308(5728):1635–1638, 2005.

[12] N. Kamada, S.U. Seo, G.Y. Chen, and G. Núñez. Role of the gut microbiota in immunity and inflammatory disease. *Nat Rev Immunol.*, 13(5):321–335, 2013.

[13] B. Wang, M. Yao, L. Lv, Z. Ling, and L. Li. The human microbiota in health and disease. *Engineering*, 3(1):71–82, 2017.

[14] R. Khan, F.C. Petersen, and S. Shekhar. Commensal bacteria: An emerging player in defense against respiratory pathogens. *Frontiers in immunology*, 10(1203), 2019.

[15] S. Mazmanian and D. Kasper. The love–hate relationship between bacterial polysaccharides and the host immune system. *Nat Rev Immunol.*, 6:849–858, 2006.

[16] S. Singh, N. Verma, and N. Taneja. The human gut resistome: Current concepts and future prospects. *The Indian journal of medical research*, 150(4):345–358, 2019.

[17] Tarini Shankar Ghosh, Sourav Sen Gupta, Gopinath Balakrish Nair, and Sharmila S. Mande. In silico analysis of antibiotic resistance genes in the gut microflora of individuals from diverse geographies and age-groups. *PLOS ONE*, 8(12):1–15, 12 2014.

[18] B. Robredo, K.V. Singh, F. Baquero, B.E. Murray, and C. Torres. Vancomycin-resistant enterococci isolated from animals and food. *Int J Food Microbiol.*, 54(3):197–204, 2000.

[19] C. Novais, T.M. Coque, M.J. Costa, J.C. Sousa, F. Baquero, and L.V. Peixe. High occurrence and persistence of antibiotic-resistant enterococci in poultry food samples in portugal. *J Antimicrob Chemother*, 56(6):1139–1143, 2005.

[20] A. Lupo, D. Vogt, S.N. Seiffert, A. Endimiani, and V. Perreten. Antibiotic resistance and phylogenetic characterization of acinetobacter baumannii strains isolated from commercial raw meat in switzerland. *J Food Prot*, 77(11):1976–1981, 2014.

[21] V. Dhup, A.M. Kearns, B. Pichon, and H.A. Foster. First report of identification of livestock-associated mrsa st9 in retail meat in england. *Epidemiol Infect*, 143(14):2989–2992, 2015.

[22] Laura Buzón-Durán, Rosa Capita, and Carlos Alonso-Calleja. Microbial loads and antibiotic resistance patterns of staphylococcus aureus in different types of raw poultry-based meat preparations. *Poultry Science*, 96(11):4046–4052, 2017.

[23] H. Guo, L. Pan, L. Li, J. Lu, L. Kwok, B. Menghe, H. Zhang, and W. Zhang. Characterization of antibiotic resistance genes from lactobacillus isolated from traditional dairy products. *J Food Sci*, 82(3):724–730, 2017.

[24] M.A. Herreros, H. Sandoval, L. González, J.M. Castro, J.M. Fresno, and M.E. Tornadijo. Antimicrobial activity and antibiotic resistance of lactic acid bacteria isolated from armada cheese (a spanish goats' milk cheese). *Food Microbiology*, 22(5):455–459, 2005.

[25] S. Mathur and R. Singh. Antibiotic resistance in food lactic acid bacteria–a review. *International Journal of Food Microbiology*, 105(3):281–295, 2005.

[26] M. Jahan, G.G. Zhanel, R. Sparling, and R.A. Holley. Horizontal transfer of antibiotic resistance from enterococcus faecium of fermented meat origin to clinical isolates of e. faecium and enterococcus faecalis. *International journal of food microbiology*, 199:78–85, 2015.

[27] M.J. Fraqueza. Antibiotic resistance of lactic acid bacteria isolated from dry-fermented sausages. *International journal of food microbiology*, 212:76–88, 2015.

[28] X. Hu, Q. Zhou, and Y. Luo. Occurrence and source analysis of typical veterinary antibiotics in manure, soil, vegetables and groundwater from organic vegetable bases, northern china. *Environmental pollution*, 158(9):2992–2998, 2010.

[29] R. Marti, A. Scott, Y. C. Tien, R. Murray, L. Sabourin, Y. Zhang, and E. Topp. Impact of manure fertilization on the abundance of antibiotic-resistant bacteria and frequency of detection of antibiotic resistance genes in soil and on vegetables at harvest. *Applied and environmental microbiology*, 79(18):5701–5709, 2013.

[30] K. Schwaiger, K. Helmke, C. S. Hölzel, and J. Bauer. Antibiotic resistance in bacteria isolated from vegetables with regards to the marketing stage (farm vs. supermarket). *International journal of food microbiology*, 148(3):191–196, 2011.

[31] M.M. Bakri, D.J. Brown, J.P. Butcher, and A.D. Sutherland. Clostridium difficile in ready-to-eat salads, scotland. *Emerging infectious diseases*, 15(5):817–818, 2009.

[32] G. Pesavento, C. Calonico, B. Ducci, A. Magnanini, and A. Lo Nostro. Prevalence and antibiotic resistance of enterococcus spp. isolated from retail cheese, ready-to-eat salads, ham, and raw meat. *Food Microbiology*, 41:1–7, 2014.

[33] G. M. Duran and D. L. Marshall. Ready-to-eat shrimp as an international vehicle of antibiotic-resistant bacteria. *J Food Prot*, 68(11):2395–2401, 2005.

[34] Y. Shen, Y. Liu, Y. Zhang, J. Cripe, W. Conway, J. Meng, G. Hall, and A.A. Bhagwat. Isolation and characterization of listeria monocytogenes isolates from ready-to-eat foods in florida. *Applied and environmental microbiology*, 72(7):5073–5076, 2006.

[35] K. Forslund, S. Sunagawa, J.R. Kultima, D.R. Mende, M. Arumugam, A. Typas, and P. Bork. Country-specific antibiotic use practices impact the human gut resistome. *Genome Research*, 23(7):1163–1169, 2013.

[36] A. Versporten, G. Bolokhovets, L. Ghazaryan, V. Abilova, G. Pyshnik, T. Spasojevic, I. Korinteli, L. Raka, B. Kambaralieva, L. Cizmovic, A. Carp, V. Radonjic, N. Maqsudova, H. D. Celik, M. Payerl-Pal, H. B. Pedersen, N. Sautenkova, H. Goossens, and WHO/Europe-ESAC Project Group. Antibiotic use in eastern europe: a cross-national database study in coordination with the who regional office for europe. *The Lancet*, 14(5):381–387, 2014.

[37] N. Lu, Y. Hu, L. Zhu, Z. Yang, Y. Yin, F Lei, Y. Zhu, Q. Du, X. Wang, Z. Meng, and B. Zhu. Dna microarray analysis reveals that antibiotic resistance-gene diversity in human gut microbiota is age related. *Scientific Reports*, 4(4302), 2014.

[38] Lei Wu, Xinqiang Xie, Ying Li, Tingting Liang, Haojie Zhong, Jun Ma, Lingshuang Yang, Juan Yang, Longyan Li, Yu Xi, Haixin Li, Jumei Zhang, Xuefeng Chen, Yu Ding, and Qingping Wu. Metagenomics-based analysis of the age-related cumulative effect of antibiotic resistance genes in gut microbiota. *Antibiotics*, 10(8), 2021.

[39] A. Mazzariol, G. Bazaj, and G. Cornaglia. Multi-drug-resistant gram-negative bacteria causing urinary tract infections: a review. *J Chemotherapy.*, 29(sup1):2–9, 2017.

[40] T.S.B. Møller, M. Overgaard, S.S. Nielsen, V. Bortolaia, M.O.A Sommer, L Guardabassi, and J.E. Olsen. Relation between tetR and tetA expression in tetracycline resistant Escherichia coli. *BMC Microbiology*, 16, 2016.

[41] A. Pormohammad, M. J. Nasiri, and T. Azimi. Prevalence of antibiotic resistance in escherichia coli strains simultaneously isolated from humans, animals, food, and the environment: a systematic review and meta-analysis. *Infection and Drug Resistance*, 12:1181–1197, 2019.

[42] Y. Sáenz, M. Zarazaga, L. Briñas, M. Lantero, F. Ruiz-Larrea, and C. Torres. Antibiotic resistance in escherichia coli isolates obtained from animals, foods and humans in spain. 18(4):353–358, 2001.

[43] Ternent L., Dyson RJ., Krachler AM., and Jabbari S. Bacterial fitness shapes the population dynamics of antibiotic-resistant and -susceptible bacteria in a model of combined antibiotic and anti-virulence treatment. *J Theor Biol.*, 7(372):1–11, 2015.

[44] Global Action Plan on antimicrobial resistance. Technical report, World Health Organization, Geneva, Switzerland, 2015.